Regulation and Stability of the Intermediates in the B-Cell Signaling

Thesis Submitted for the Award of the Degree of

Doctor of Philosophy

To

Jawaharlal Nehru University

New Delhi, India.

by

Virendra Kumar Chaudhri

Immunology Group

International Centre for Genetic Engineering and Biotechnology

New Delhi, India

2009

Certificate

This is to certify that the research work described in this thesis entitled "Regulation and stability of the intermediates in the B-cell signaling" has been carried out in the Immunology Group, International Centre for Genetic Engineering and Biotechnology, New Delhi, India. This work is original and no part has been submitted for the award of any other degree or diploma to any other university.

Dr. Kanury V. S. Rao
Guide and Head
Immunology Group
ICGEB
New Delhi- 110067
India

Prof. V. S. Chauhan
Director
ICGEB
New Delhi- 110067
India

Declaration

I hereby declare that the research work described in this thesis entitled "Regulation and stability of the intermediates in the B-cell signaling" has been carried out by me under the supervision of Dr. Kanury V. S. Rao at the Immunology Group, International Centre for Genetic Engineering and Biotechnology, New Delhi, India.

Virendra Kumar Chaudhri

Acknowledgements

Contents

Introduction and Review of Literature

Traditionally research in biology has inclination the reductionism approaches, although the nature of biological responses are often complex. The more recent emergence of system level approaches have, however, sought to correct this limitation by considering the larger system as object of study. It is interesting to note that, while biological system are complex, this complexity – nonetheless – elicits from a fundamental simplicity at the root level of its organization (Alon, 2007b). Further, the smallest building block of the organizational complexity of higher organisms is the cell.

From a functional perspective, a cell may be defined to consist of three interacting systems namely *(1) Genetic, (2) Metabolic and (3) Signaling system.* The Genetic system comprises mainly of DNA and RNA, along with the associated polymerases, the splicing apparatus, ribosomes, and posttranslational machinery. The coordinated functioning of these components, however, is dependent upon the metabolic system. The Metabolic system is involved in the production of energy and synthesis, as well as processing and recycling of essential structural units of cellular architecture such as the various types of lipids, amino acids and nucleotides. On the other hand, the Signaling system functions to receive extra cellular cues and relay them across membrane and through the cytoplasm, to eventually induce changes in the genetic and metabolic networks so as to drive an appropriate phenotypic response.

Of these three systems, the last one (Signaling System) is unique in the sense that it is this system that constitutes the central regulator of other functional modules of the cell. The response of a given cell to environmental cues is ensured by the various receptors that are expressed on the cell surface. Extra cellular factors can influence diverse biological processes such as cellular proliferation, differentiation and cell death (apoptosis) through their binding to their specific receptors. The activation of these receptors leads to alteration in gene expression and, consequently, in the biological response. This process of information transfer involves the activation of various signaling intermediates including kinases and phosphatase as well other secondary signaling molecules, some of which may connect signaling to metabolism. A few of these signaling intermediates also translocate to the nucleus and lead, through the activation of transcription factors, to alterations in the gene expression status of the cell.

Various approaches have been used to delineate the mechanisms by which signal is interpreted, during its transmission from the cell membrane to the nucleus. Such studies (Aldridge et al., 2006; Altan-Bonnet and Germain, 2005; Bauman and Scott, 2002; Bhalla and Iyengar, 1999; Binder and Heinrich, 2002; Birtwistle et al., 2007; de Menezes and Barabasi, 2004; Ferrell, 2002; Huang and Ferrell, 1996; Kumar et al., 2008; Kumar et al., 2007; Ma'ayan et al., 2005; Singh et al., 2005) in this direction has shown a promising outcome, yielding important insights into biochemical pathways mediating signal processing. One such mechanism involves the differential stability of the intermediates, which can be explained and defined by the dynamics of the activated versus non-activated or inhibited form of signaling molecules, over time and/or space (Bhalla and Iyengar, 1999; Bhalla et al., 2002; Neves et al., 2008). Different forms of molecules are often represented by covalent modifications (phosphorylation, dephosphorylations), transportation/compartmentalization (e.g. Ca^{++}) or generations of new chemical species by degradation or modifications of biomolecules into secondary messengers (e.g. PIP2, IP3, IP4, DAG). Monitoring such species over relevant time courses and interpreting the changes in dynamics over time and space have provide clues on the information processing system that exists in living cells.

Immunity, Immune system and B lymphocyte Signaling

While single cell organisms deal with pathogenic invasion in a relatively empirical manner, in the case of more complex, multicellular, organisms this requires coordinated communication between cells of various functional categories. Importantly, this communication is facilitated through intracellular signaling events, which then induce the expression of specialized proteins on the cell surface for inter-cellular interactions.

Like cells, the tissues of biological systems are also evolved, but through cooperation and co-ordination of selective cell types and such tissues (e.g. lymphatic tissue) posses' the ability to perform specific functions. The immune system represents one such system, which in turn functionally integrates with the circulatory system in order to perform its primary role of defending against infections.

The immune system has two functional arms namely the innate and the adaptive arms. The innate arm of the immune systems provides the first line of defense and is considered to be antigen non specific. In contrast, adaptive immunity is generated through a complex set-up of diverse cell types, and is specific for either the infection or

antigen. The adaptive immune system mainly consists of different subsets of lymphocytes, each equipped to undertake specific actions against the infinite spectrum of antigens presented by the various pathogens. Purely from a functional point of view, the immune response is defined through the activities of lymphocyte populations existing in one of two phenotypically distinct populations. One of these is the subset of naïve lymphocytes (i.e. lymphocytes that have not yet encountered an antigen), which constitute the population available for the recognition of new antigens. Memory lymphocytes (i.e. an antigen experienced lymphocyte populations), on the other hand are geared for a robust and quick response to re-exposure to a given antigen. Each of these two pools, in turn, can be divided into two populations of cells, the B and the T cells. B cells, both naïve and memory, together constitute the humoral component of an immune response and contribute through the production of specific antibodies against the antigen/pathogen. T cells, on the other hand, contribute in terms of cell mediated immunity and are the main execution arm of the immune system against systemic infections. Both B and T cells are connected via a network of chemokines secreted by these and other cells. In addition, lymphocytes also freely move through the circulatory system and migrate constantly in and out of the spleen and lymph nodes, ready, to mount a response when they encounter either antigens, cytokines, bacterial toxins or any other stimuli (Bishop and Hostager, 2001; DeFranco, 1997; Hasler and Zouali, 2001). This migration of lymphocytes is directed through a co-operative set of chemokines and, survival is promoted by environmental stimuli (Cyster, 1999; Klaus et al., 1997; Rolink et al., 2002). Once a B cell encounters its cognate antigen and receives an additional signal from a T helper cell, it can further differentiate into one of the two types of B cells, either plasma B cells or memory B cells. An absence of such stimulation causes the programmed cell death in B cells (Tarakhovsky, 1997).

B cell receptor signaling

Each B cell expresses a unique receptor protein (B cell antigen receptor, or BCR) on its surface that will bind to one particular antigen. A critical difference between B cells and T cells is how each lymphocyte recognizes its antigen. B cells recognize their cognate antigen in its native form while T cells identify it in a processed form that is presented in association with MHC molecules by antigen presenting cells (APCs) such as macrophages and B cells. The BCR serves the purpose of identifying intact antigens in order to eventually initiate an antibody response. The cytoplasmic tail of the BCR is

associated with immunotyrosine based activation motifs (ITAMs). Although B cell immunoreceptors lack intrinsic catalytic activity, their engagement results in the induction of rapid protein phosphorylation signals (Kurosaki, 2000; Moretta et al., 2001; Tamir and Cambier, 1998; Turner and Kinet, 1999). These signals are essential for the immunoreceptor mediated signaling. The ITAMs are the motifs which consist of sequence **YxxL/I-x(6-8)-YxxL/I** (where Y is tyrosine, L is leucine, I is isoleucine and x is any residue). ITAM function normally involves recruitment of three classes of cytoplasmic protein tyrosine kinases (PTKs), namely the Src Family, the Syk family, and the Btk family (Kurosaki, 2000; Moretta et al., 2001; Tamir and Cambier, 1998; Turner and Kinet, 1999). The Src-related PTKs, which include c-Src, Lyn, are responsible for the initiation of immunoreceptor signaling. In response to immunoreceptor engagement, they become activated and phosphorylate the two tyrosine residues of the ITAMs (Chow and Veillette, 1995; Rolli et al., 2002). This phosphorylation is the key phosphorylation step in the chain of phosphorylation events proximal to immunoreceptors. Autophosphorylation in the activation loop of Lyn (Y416) results in an increase in its catalytic activity. The phosphorylation of ITAMs by Src kinases allows recruitment of the tandem Src homology 2 (SH2) domain containing PTK, Syk (Chan et al., 1994; Latour and Veillette, 2001; van Oers and Weiss, 1995). The enzymatic activity of Syk is also regulated via tyrosine phosphorylation. Phosphorylation of a tyrosine residue in the activation loop of the kinase domain of Syk (Y520) is the key to the enzymatic activation of this molecule. The phosphorylation of this site occurs in a Src kinase dependent manner. In particular a phosphorylated tyrosine in the so called linker domain of Syk (Y317) inhibits the function of Syk family kinases, as a result, increasing its capacity to recruit the negative regulator c-Cbl. When activated, Syk family kinase also phosphorylates downstream adaptor proteins like BLNK.

Activated Syk also phosphorylates ITAM at three more tyrosine sites making it hyper-phosphorylated and thus establishing a positive feedback loop at the BCR (Rolli et al., 2002). In a a parallel pathway, activated Src kinase Lyn also phosphorylate membrane anchored CD22 which, upon phosphorylation, recruits SH2 domain containing protein tyrosine phosphatase 1 (SHP1) to the membrane. The SHP1 along with other potent PTPs (SHP2, HePTP) is a major negative regulator of BCR proximal signaling and act through dephosphoryalting Lyn, Syk, Btk, and the ITAMs (Kurosaki, 1999; Kurosaki, 2002) . This forms a negative feedback loop at the BCR. Interestingly these are not the

only small feedback loops and, as discussed later, there is another strong feedback loop that couples to this negative feedback loop following PLCγ activation.

Adapter molecules also co-operate to with Src family kinases to phosphorylate phospholipase C(PLC) γ and Vav, and the Btk family of PTKs which includes Btk, Tec, and an atypical member termed Rlk/Txk (Lewis et al., 2001; Yang et al., 2000). Typical Btk kinases are recruited to the plasma membrane by a mechanism that requires prior activation of phosphoinositol (PI) 3 kinase by Src and Syk family kinases and also involves membrane anchored CD19 and B Cell Adapter Protein (BCAP) which recruits the different subunits of PI3K active complex (Okada et al., 2000). Activated PI-3-kinase generates membrane bound PI metabolites phosphorylated at 3' position of the inositol ring. One of these, PI(3,4,5)P3 , can bind with high affinity to the pleckstrin homology (PH) domain of Btk kinases and allow their membrane association. After reaching membrane Btk kinases are activated by tyrosine phosphorylation. In the case of Btk it occurs in the activation loop (Y551) and the Src homology 3 (SH3) domain (Y223). It is mediated in part by Src kinases, and in part by autophosphorylation. Despite the fact that Btk family kinases play important role in the BCR signaling, information regarding their substrate is limited. However, it seems that the phosphorylation of PLCγ is particularly dependent on proper Btk function.

Proteins that undergo tyrosine phosphorylation upon BCR stimulation can be subdivided into two categories: enzymatic effectors and adaptors. Here the receptor proximal signaling event leading to the activation of PLCγ cleaves phosphatidylinositol 4.5-bisphosphate (PIP2) to generate IP3 and Di-acyl Glycerol (DAG) as the secondary metabolites. BLNK plays crucial role in both the recruitment of PLCγ to the membrane, and positioning it in proximity with PIP2 (Kurosaki and Tsukada, 2000). The IP3 generated in this process binds to receptors on the endoplasmic reticulum, causing a release of the intracellular stores of Ca^{2+}. The released Ca^{2+} in conjunction with DAG, activates a variety of signaling intermediates including Calcineurin, CaM Kinases as well as various forms of PKCs.

The release of calcium also activates membrane anchored Duox through binding to its EF hand motifs. Activated Duox then generates reactive oxygen species (ROS) which although has very short life still reacts with SHP1's active site and deactivates its phosphatase activity by oxidation. This causes blocking of SHP1 action on the activated

BCR sites and thus effectively leads to an enhanced and sustained tyrosine phosphorylation at BCR and, therefore, sustained PLCγ and Ca^{2+} responses. This creates a strong positive feedback loop of BCR signaling (Singh et al., 2005). This loop has a wider impact on signaling owing to the involvement of the diffusible signaling molecule, Calcium. Calcium diffuses rapidly and therefore, may serve to connect the non-uniformly activated BCR patches of the membranes, thus integrating the response over complete cellular volumes.

An important pathway activated downstream to BCR is the MAP kinase pathway. This pathway, also known as the ERK pathway, can be activated by Ras-mediated activation of MKKKs such as Raf. While the p38 and JNK are among other MAP kinases which are activated by BCR, these are induced through the activation of Rho GTPases such as Rac and Cdc42. Candidate MKKK that are activated by Rho proteins include members of the MEKK and mixed lineage protein kinase (MLK) groups. All these MKKs can be activated by selective/specific activation of the adapter molecules like BLNK, Shc, Grb2 or Vav. Signal transduction through the MAP kinase pathways are facilitated by scaffold proteins like KSR (Veillette et al., 2002). BLNK mediated ERK activation is dependent on classical Grb2 adaptor proteins and SoS as standard GTP exchange factor, but at basal level of signal it also utilizes the recently discovered RasGRP proteins as well. This could likely establish a powerful positive feedback system for robust baseline ppERK levels (Coughlin et al., 2005; Roose et al., 2007).

The MAP kinases are activated by dual phosphorylation at the tripeptide motif Thr-Xaa-Tyr. The sequence of this tripeptide motif is different in each group of MAP kinases: ERK (Thr-Glu-Tyr); p38 (Thr-Gly-Tyr); and JNK (Thr-Pro-Tyr). The dual phosphorylation of Thr and Tyr is mediated by a conserved protein kinase cascade. The ERK MAP kinases are activated by the MAP kinase kinases (MKK) MKK1 and MKK2; the p38 MAP kinases are activated by MKK3, MKK4, and MKK6; and the JNK pathway is activated by MKK4 and MKK7. These MAP kinase kinases are activated, in turn, by several different MAP kinase kinase kinases (MKKK). Different upstream signals can lead to the activation of these MKKK (Dong et al., 2002). The dynamics of phosphorylation of these MAP kinases are in turn regulated by various dual specificity phosphatases as well as many PTPs or Ser/Thr Phosphatases. Therefore, overall signaling event represents a mere interplay between kinases and phosphatases.

6

Network, Patterns and Motifs in Dynamics of Cellular Signaling

Phenotypes and associated underlying cellular functions are well interconnected and these connection patterns remains conserved across functionally and biologically diverse organisms. All biological processes share the various modules (Ravasz et al., 2002) of specific functionalities, and combinatorial exploitation of modules underlies the complexity and efficacy of cellular functional diversity. When it comes to complexity, graphs are best way to represent complex systems. At least most, if not all, biological processes can be represented by graphs, by showing molecules and their biochemical conversions, what we often term biological networks. The biological networks in genetic and metabolic systems are well studied (Albert, 2007; Alon, 2007b; Barabasi and Oltvai, 2004; de Menezes and Barabasi, 2004; Ravasz et al., 2002) and the networks in the cellular signaling shares some of the features described in these studies. Such similarities usually inspire the use of similar protocols for decoding the actual network structure and the corresponding dynamics of the same across different systems.

Identifying the network similarity is attributed to the patterns it forms. A pattern is defined as the part of the graph which is formed when nodes and "vertices connecting nodes" are placed together and has a repetition of the similar arrangements in the same or different graphs. Directionality in the vertices in the graph makes it directed (termed as directed graph). In biological network nodes are usually the molecules, while vertices may be biochemical reactions (binding, catalytic, cytoplasmic shuffling) or the biochemical modifications.

Earlier work (Alon, 2007a; Ma'ayan et al., 2005; Mangan and Alon, 2003; Milo et al., 2002) has shown that various patterns repeatedly occurs in biological networks. These patterns, if occurring at a frequency more than that expected in the similar random networks are termed as "Motifs"; while if these occur at a frequency not significantly different from that expected in similar random networks, they are termed as "Non-motifs". In rare instances, some patterns show a frequency that is lower than that which is expected in the similar random networks. Such is pattern is called "Anti-motif".

Motifs are of key importance in the biological networks for owing to characteristic dynamics associated with each of them (Alon, 2007a; Mangan and Alon, 2003; Milo et al., 2002). A topological feature may provide distinct dynamic properties. Thus investigating topological features is the first step towards system level approaches

in signaling, although alternative approaches also sometimes provide the insights into the intriguing aspects of intracellular signaling (Janes et al., 2005; Krogh, 2008; Kumar et al., 2007; Noble, 2006). But owing to more informative and mechanistic details about network organization, topology based deterministic methods remain widely acceptable.

In most instances, we are interested in topology, not for static information but for the real interplays and the result of the dynamics, offered solely by topology. Dynamics associated with topology usually offers information on modes of regulation by accelerating responses or slowing down the responses while at the same time it can further add the additional characteristic features such as delays in responses (Alon, 2007a; Mangan and Alon, 2003). Thus the patterns formed in biological networks are largely responsible for the dynamics of signal transmission in the network (Ma'ayan et al., 2005).

Mathematical modeling and Cellular networks

A mathematical model uses mathematical language to describe a system. Eykhoff (1974) defined a *mathematical model* as 'a representation of the essential aspects of an existing system (or a system to be constructed) which represents knowledge of that system in usable form'.

Based on the methods a mathematical model can be either of two kinds, 1. Black box model if there is no *a priory* information is available 2. White Box (Glass Box or Clean Box) model if all necessary information is available. Real systems, especially biological systems, lie somewhere between the black box model and white box models.

Generally it is good to have more and more *a priori* information available to make a model more accurate. This is the reason why a white box model is easier and, provided information is used correctly, leads to correct behavior of the system. While if there is no a priori information is available, we use functions as general as possible to cover all different models. In such an approach we try to estimate the functional form of relations between variables and numerical parameters in those functions. Thus this approach is a black box approach and have various difficulties associated with it especially it becomes increasingly difficult when the amount of parameters and different types of functions increases.

A mathematical model defines a system by a set of mathematical equations that defines relationship between variables. Variables in a model can be of different types but

broadly we can divide them into six groups, although it is also quite possible to further divide groups into sub groups. These six types include: decision variables, input variables, state variables, exogenous variables, random variables and output variables. Decision variable can also be defined as independent variables (e.g. Time in some cases). Exogenous variables are sometime called as parameters or sometime constants (in case of models with lumped parameters). Output variable is dependent on the state variables (which include the interdependencies of decision, input, random, and exogenous variables). The variables are generally represented by vectors.

Biological networks are often well described in the way as perceived either entirely by a biologist, or entirely by a mathematician. Thus understanding at the level of creating *in-silico* equivalents is more realistic in models with details of bio-molecular reactions underlying actual mechanisms rather than the models with oversimplifications, like that with a Chemical Master Equations (CME). Although owing to less scope for biologists the latter method has advantage of describing system with simplicity and inviting attention from other related disciplines.

A method is termed as deterministic if it uses realistic/definite sets of variables, whereas it is called as stochastic if it uses largely probabilities and/or random numbers. Earlier work on biological networks has used ODE based models (Bhalla and Iyengar, 1999; Bhalla et al., 2002; Birtwistle et al., 2007), Flux Balance Analysis (FBA)(Segre et al., 2002), Boolean networks (Kachalo et al., 2008; Thakar et al., 2007), Stochastic models (Locasale et al., 2007) and combinations of these. Most of time the models in biology ascertains certain properties which are the result of nothing but the modulation of signaling and metabolic intermediates over time. This introduces important attributes of biological networks which include ultra sensitivity (Huang and Ferrell, 1996), bistability (Bhalla et al., 2002), and delays (Alon, 2007a; Angeli et al., 2004; Mangan and Alon, 2003) like behaviors which may be exploited by cellular networks to isolate signals from noise, or adapting cells itself for a threshold of signal. Although the same network may behave differently to the signals depending on the concentrations of species, often referred to as weightage (Jain and Krishna, 2001) of the nodes. Thus the population dynamics of these networks play important roles in determining the way network behaves in different conditions (Jain and Krishna, 2001).

Our recent understanding on the cellular networks has been quite improved by using mathematical modeling to describe them. Earlier biological maps of interaction are

merely representation of the interaction maps of cells at a fixed time, i.e. static maps. Describing models of networks in terms of mathematics has helped the investigators to think beyond the structural modularity. Mathematics has helped to think and expand towards time and space variations versions of earlier static maps/networks. Such developments have spurred the emergence of a new discipline that is more commonly referred to as "Systems biology" (Csete and Doyle, 2002; Davidson et al., 2002; Kitano, 2002).

Signaling through MAP kinase: models and signal processing

There are certain pathways that are evolutionary conserved and these include kinase modules that link extra-cellular signals to the machinery that controls fundamental cellular processes. Mitogen activated protein kinase (MAPK) pathways are such kinase modules which are highly conserved (Lewis et al., 1998; Widmann et al., 1999). MAPK pathways are composed of three tier kinase modules in which a MAPK is activated upon phosphorylation by a Mitogen activated protein kinase kinase (MAPKK). This in turn is activated upon phosphorylation by a MAPKKK. To date six distinct groups of MAPKs have been characterized in mammals; Extracellular signal regulated Kinase (ERK)1/2, ERK3/4, ERK5, ERK7/8, Jun N-terminal kinase(JNK)1/2/3 and p38 isoforms (Dhillon et al., 2007). Out of these B cells express three major MAPK including ERK1/2, p38 and JNK (Kurosaki, 1999; Kurosaki, 2000; Kurosaki, 2002).

Among all these, the ERK pathway is the best studied of the mammalian MAPK pathways. ERK is activated by MEK, which in turn is activated by Raf. Raf and MEK are negatively regulated by the PP2A and ERK is negatively regulated by Mitogen Activated Protein kinase phosphatases (MKP) 1,2 &3. MKP1 is stabilized by ERK itself through phosphorylations which protects it against ubiquitnation (Brondello et al., 1999). This stabilization of MKP1 creates a negative auto regulation (NAR) on ERK. The ERK activation also induces transcriptional up-regulation of mkp1 transcript. A potential positive feedback of ERK on PKC, the activator of the Raf, is absent since cytoplasmic phospholipase A2 (cPLA2) a target of ERK and responsible for activating PKC at low calcium levels is not expressed in the B cells (Gilbert et al., 1996). Activated ERK also hyper-phosphorylate Raf and results in inhibition of Raf population. The activation of Raf then primarily depends on Protein phosphatase 1(PP1) through the reversal of this hyper-phosphorylation (Ueki et al., 1994). Another negative regulation of Raf is mediated

10

through Akt-dependent phosphorylation at ser259, which then requires PP2A for dephosphorylation (Birtwistle et al., 2007; Dougherty et al., 2005; Hatakeyama et al., 2003). Other phosphatases include MKP2 and 3 of which MKP3 has recently drawn lot of attention owing to fact that this phosphatase has different levels of expression in different cell types and also expression levels changes with the developmental stages of the cells (Dickinson et al., 2002; Dickinson and Keyse, 2006; Echevarria et al., 2005; Kawakami et al., 2003). MKP3 might also regulate the developmental outcome of FGF signaling by setting appropriate level of activated ERK (Echevarria et al., 2005; Kawakami et al., 2003). In addition, MKP3 has been recently identified in setting the threshold for thymocyte positive selection (Bettini and Kersh, 2007) which suggest its importance in tuning physiological responses via signaling. However, the mechanisms associated with MKP3 are probably varied since MKP3 is also phosphorylated like MKP1, although unlike in the case of MKP1, ERK mediated phosphorylation renders MKP3 prone to degradation. Further, MKP3 is also a substrate for phosphorylation by Casein kinase2α (CK2α) although the outcome of this process remains unclear (Castelli et al., 2004).

Activation of ERK is known to regulate various cellular processes depending upon its mode of activation. Transient versus sustained ERK activation regulates growth versus differentiation processes in neuronal cell lines such PC12 (Sasagawa et al., 2005). The difference in the activation mode of ERK is attributed to the activation of different GTPases with the each receptor. Thus differential activity of the ERK in response to the different stimuli, Epidermal Growth Factor (EGF) and Nerve Growth Factor (NGF) induce transient and transient and sustained ERK activation respectively. These ERK dynamics depends on Ras and Rap1 dynamics, the inactivation process of which are growth factor dependent and independent respectively. Ras activates c-Raf and B-Raf while Rap1 activates only B-Raf which explains that this dynamics is a result of two different ways of input on the same signaling module. Here the role of network topology as we have discussed before becomes clear in separating signals of different kinds and developing them into unique dynamics.

The manner in which a given stimulus activates ERK has also been suggested to depend on the phenotypic context of the cells, leading to unique response patterns following variation in strength of the stimulus. However, studies in this direction have remained limited. Previous work has shown that MAPK (ERK) exhibits ultra sensitivity

and that this feature enables the system to discriminate between signal and noise (Altan-Bonnet and Germain, 2005; Huang and Ferrell, 1996). In addition to this, it has also been shown that the ERK response to signal may lie in either of two stable states of low and high activity, a feature termed as bistability. A bistable response system provides robustness to the activation of ERK, wherein the response can either be ultrasensitive or proportional, depending on the concentration of the Mitogen activated protein kinase phosphatase 1 (MKP1) (Bhalla et al., 2002). This phosphatase acts as a regulator of MAP kinase, wherein high concentration of MKP1 ensure a proportional response system, whereas low concentrations of MKP1 facilitate the ultrasensitive response mode that functions as an all or none switch. Thus the phosphatase MKP1 can control the way MAPK system responds to the signal. Therefore, it becomes obvious that phosphatases can play significant roles in defining the way a system responds to the stimulus. The effect of concentration-dependent effects also emphasizes the importance of nodal weightages in the network as a parameter that contribute in defining the flow of the signal, wherein network behavior can be altered through modulations in nodal weightage. Many computational models of MAPK signaling also inferred oscillations depending on the feedbacks (Kholodenko, 2000) or on certain set of parameters, sequestration effects, or relative phosphatase strengths, (Bluthgen et al., 2006; Qiao et al., 2007). All of these directly relate to the relative weightage of nodes in the network. Although the role of phosphatases has been shown in regulating the response in signaling (Heinrich et al., 2002), an active role for phosphatase dynamics was first shown by Bhalla (Bhalla et al., 2002). Scaffold and sequestration effect also define the dynamics of MAPK signaling. However, these studies have concluded that the shape of response falls into regimes which may again controlled by the strength of phosphatase activities (Bluthgen et al., 2006; Locasale et al., 2007).

Bistability is a feature that is often described as switches in biological systems. Recent mathematical models have, however, provided insights into the new dimensions offered by bistability in terms of regulating the flow of signal through large cellular volumes through bistability dependent phosphoprotein waves (Markevich et al., 2006). In this connection the proportional response configuration of MAPK has also revealed the possibility that regulation by modulating duration of signal can shift the range of dose for which a proportional response can be obtained (Behar et al., 2008). Thus the emergence of modulation in proportional response systems offers versatile modes of fine-tuning the input-output relationships. Such a system also offers modules allowing tuning of various

dimensions of signals, an exact mechanism for which may be extended from receptors to MAPKinase in various modules.

From the above discussion of the phosphatase-mediated regulation of system behavior, it becomes obvious that local modules may exploit such mechanisms to integrate/interpret spatial patterns into the signal (Neves et al., 2008). In other words signaling module can significantly use modulation of negative regulators in order to describe the allowed regimes of responses. Incorporation of strength of signal, dynamic assembly/formation of network and modulations of nodal weightage may also contribute towards expansion of ranges of such regulations in multiple dimensions. As discussed in this thesis, this feature emerges as a powerful operating principle for information processing.

Rationale of Study

Binding of Extracellular messengers ("ligand" in a wider perspective) to the receptor cause relay of signal across the membrane, up to the nucleus. In nucleus it may cause the alteration of gene expression. Interestingly this effecter mechanism needs to be carefully interpreted and regulated before it reaches nucleus. In addition to this the interpretation should also integrate the "net sum of earlier signals" so that the interpretation can be more context specific and responses will be unique. A good way to achieve the same may be the regulation of signal processing by means of those changes which are the result of earlier "relevant" signals faced by cells. Mechanism like these becomes more obvious when it comes to highly conserved signaling modules, which are involved in regulating wide variety of cellular functions/processes.

Signal processing in artificial systems i.e. electronic circuit, is achieved by the combinatorial use of modules. Even different kinds of modules can be built by the combinatorial use of components. At the crude level of function and architecture the human built high tech devices resembles the biological systems (Csete and Doyle, 2002). Cellular signal processing can also be viewed like this and the combinatorial modules as described already, could be the part of the signaling network, having topology associated with the characteristic dynamics, better called patterns or motifs, making functional modules. Combination of the motif can provide the unique function(s). So unit of signaling can be the very unique components (signaling molecules) while the unit of signal processing can be signaling modules/motifs. Of these the similar modules/motifs can be formed by different and unique components, adding specificity and co-ordination in signaling machinery.

Network motifs as suggested by earlier works, are able to filter signal, out of noise and can set/regulate the timing of output as well (Alon, 2007a; Mangan and Alon, 2003; Milo et al., 2002). An earlier study has shown that the different aspects of any specific component's activity/kinetic features are responsible for the context specific response of the cell and fate is determined only upon the certain aspects of the components only (Kumar et al., 2007). It refers to the existence of specific motifs/modules operational on these components which function to shape only that specific feature which in turn shapes the net output of the response. A detailed dissection

of such small networks and extraction of the new topological features responsible for the very unique context specific responses becomes essential.

An attractive system for this kind of study is the MAPK cascade, which is highly conserved (Lewis et al., 1998) and known to regulate vast variety of cellular responses from activity and localization of individual proteins, transcriptional status of the cell, cell cycle entry, to cellular proliferation, differentiation, development, cell motility and other sequenced programs for animal development (Gille et al., 1995; Khoo et al., 2003; Levenson et al., 2004; Lewis et al., 1998; Maekawa et al., 2005). Plenty of work has suggested the roles of MAPK malfunction in various diseases like cancer (Mansour et al., 1994; Roberts and Der, 2007; Ward et al., 2001; White et al., 1995; Zebisch et al., 2007; Zuber et al., 2000), diabetes (Arnette et al., 2003; Benes et al., 1998; Frodin et al., 1995; Gibson et al., 2006; Khoo and Cobb, 1997; Lawrence et al., 2007; Lawrence et al., 2005; Malecki, 2005; Oyadomari et al., 2002; Sumara et al., 2009) and recently cardiac hypertrophy (Lorenz et al., 2009). Mutations and abnormalities in MAPK kinase tier and upstream activator like Ras, are associated with most of cancers. This strengthens the idea of looking at it for potential drug target in such disorders. ERK pathway, the best studied of the mammalian MAPK pathways, alone, is deregulated in approximately one third of all human cancers. ERK pathway responds to variety of stimuli of which the pathways activating ERK in response to growth factors and mitogens are of particular relevance of cancers. Mode of activation of ERK pathway for different stimulus in many cases depends on what kind of Ras or other GTPase activated (Sasagawa et al., 2005). Further it is subjected to network wide fluctuations which may incorporate the changes at the level of three-tier cascade of MAPK. Interestingly the MAPK specific phosphatases like MKPs known to be regulated via phosphorylations. Phosphatases are known to regulate the dynamics of kinases (Bhalla et al., 2002; Heinrich et al., 2002; Kumar et al., 2008) and they show wider range of substrate choices as compared to kinases. Hypothetically we can say that in this scenario phosphatase may contribute to buffer/influence local versus global changes in signaling networks, though may be indirectly. Adding to this the phosphatases regulation itself may depend on kinases and this kind of mutual regulations are worth to study when it comes to signal processing. Cross regulation of phosphatases is another dimension which could be the another layer of "signal processing unit" hierarchy since the kinase mediated phosphatase regulation cannot be shaped alone until another/same phosphatase negatively regulate this "process". Such kind of propositions can be studied on the MAPK cascade since it is

highly conserved across biological diversity and has its functional significance in variety of cellular functions. This may help in elucidating the signal processing mechanism which may contribute to the processing and simultaneous interpretation during signal relay across cell.

Our earlier studies (Kumar et al., 2008; Kumar et al., 2007) has provided robust sets of data which has explained the modes of signal transmission as a function of discrete features of nodal contributions regulating the cell fate, while this contribution can be processive by phosphatases, enhancing the response spectrum, yet keeping system still under tight check. However, a mechanistic explanation to this remains unclear. Interestingly the data also examine the various effect of phosphatases perturbation on the MAPK tier. Enhanced understanding of the operating principles of this cascade can help to understand the fundamental signaling and its evolutionary basis, besides its conservancy. Keeping the aspects discussed so far we aimed at building mathematical model of BCR induced activation of MAPK (ERK) with special focus on the known phosphatases associated with this cascade. The study involves the extraction of new topological features of network around ERK (MAPK) cascade and creating a mathematical model fitting to original data, followed by the intensive analysis of the model and testing it on the new predictions that can be validated experimentally.

A Mathematical Model for BCR-Dependent Activation of the MAPK Pathway

The BCR is composed of heavy and light chains and the associated immuno-tyrosine activation motifs (ITAMs). ITAMs get phosphorylated in response to BCR engagement by antigen, which then leads to cross linking of the BCR molecules. The BCR dependent phosphorylation of ITAMs is sustained through Syk dependent phosphorylation on three additional sites on the ITAMs. For simplicity, however, we have defined all stages of this multiple phosphorylated states as the doubly phosphorylated BCR (which represents-ITAM + Immunoglobulin part of the BCR). Both singly and doubly phosphorylated BCR activates the src kinase Lyn. Syk, which is immediately downstream to Lyn, is then phosphorylated in a Lyn-dependent manner. This establishes a positive feedback loop at the BCR (Rolli et al., 2002). Antigen-bound BCR also undergoes internalization, although internalized receptors do not contribute towards further signaling (Hou et al., 2006). Lyn also phosphorylates CD22, a membrane anchored intermediate of B cell signaling. This, in turn, recruits the protein tyrosine phosphatase SHP1 to the membrane. Since SHP1 is a negative regulator of a majority of protein tyrosine kinases including Lyn and Syk, a negative feedback loop is established. Thus a negative and a positive feedback loop are both established in the immediate vicinity of the BCR. Both Lyn and Syk also activate Brutons' tyrosine kinase (Btk). Btk in turn phosphorylates PLCg when the latter is bound to the Syk-phopshorylated BLNK, a major scaffold protein that connects BCR initiated signaling to downstream events (Jumaa et al., 2005; Kurosaki, 1999). Lyn via CD19, and Syk via BCAP (B Cell Adopter Protein), activate PI3-Kinase signaling with the consequent generation of PIP3. This leads to recruitment of cytoplasmic Akt and PDK to the membrane, where PDK then phosphorylates Akt (Jumaa et al., 2005).

Syk mediated activation of BLNK also leads to the formation of a BLNK-Grb2-SoS complex, which functions as the RasGDP-GTP exchanger in B cells. The GAP and GEF are modeled according to the scheme as described by Bhalla et. al.(Bhalla and Iyengar, 1999; Bhalla et al., 2002). We have summarized the activation of all PKC isoforms by DAG mediated PKC recruitment to the membrane. RasGTP binds to Raf and resulting complex of Raf-RasGTP is then phosphorylated by PKC. Phosphorylated Raf activates the classical Raf-MEK-ERK pathway. Although lymphocyte signaling also involves RasGRPs in activation of RasGTPs via SOS (Coughlin et al., 2005; Oh-hora et

al., 2003), the effect of RasGRPs are better characterized in terms of maintaining the basal levels of RasGTP activity (Coughlin et al., 2005). The stimulus induced effect of RasGRPs on RasGTP kinetics is still unclear. Therefore, we kept our model at the level of RasGTP simple and invoked only the classical activation pathway of RasGTP via SoS as the standard GEF. The predicted ligand dose response yielded a good match with the experimental results and more importantly the simplification of the activation pathway of RasGTP did not affect the performance of our model. ERK negatively regulates Raf by hyper phosphorylating it (Bhalla et al., 2002; Ueki et al., 1994). In addition Raf is also negatively regulated through phosphorylation at Ser259 by activated Akt (Hatakeyama et al., 2003). This process has been modeled accordingly. Dephosphorylation of activated Raf is mediated through PP2A whereas the inactivated form represented by hyperphsophorylation or Ser259 phosphorylation, is dephosphorylated by both PP1 and PP2A.

Several reports in the literature have indicated that phosphorylation of ERK1/2 is also regulated by phosphatases (Bhalla et al., 2002). In more recent experiments we have demonstrated that the BCR dependent phosphorylation profiles of all the three constituents of the MAPK module (i.e. Raf, MEK1/2 and ERK1/2) were profoundly influenced when cells were depleted of a range of cellular phosphatases by siRNA. Interestingly, depending upon the phosphatases that were depleted, both negative and positive effects were noted suggesting the existence of diverse modes of regulation (Kumar et al., 2008). Therefore to explore this further, we also incorporated these earlier results for five phosphatases. These were PP1, PP2A, MKP1, MKP2 and MKP3. We started by linking core MAPK module recursively with the phosphatases in a manner that satisfied the experimental data. The phosphorylation profile of ERK was used as eventual output, although the simulated profiles of Raf and MEK1/2 were also compared with the experimental data for the purpose of model validation.

Whereas PP1 (or, Calcineurin) was treated as an unregulated pool, the dual specificity phosphatases MKP1 and MKP3 were modeled as previously described (Bhalla et al., 2002), but with the modification that phosphorylation of MKP1 was modeled as a single step process. An interesting aspect of our earlier experimental results was the finding that depletion of MKP3 by siRNA resulted in contrasting effects on the BCR-stimulated phosphorylation profiles of MEK and ERK. Whereas phosphorylation of MEK-1/2 was markedly enhanced, the sensitivity of ERK-1/2 to BCR stimulation was

18

attenuated (Kumar et al., 2008). This observation could be rationalized by invoking the related finding of (Castelli et al., 2004), that the PKC substrate Casein kinase2α both interacts with and phosphorylate MKP3. Thus, although MKP3 is known to negatively regulate ERK1/2 activation, the simultaneous over-expression of CK2α – however reversed this effect. This attenuating effect of CK2α on MKP3 involves phosphorylation of the latter (Castelli et al., 2004). In our present system we found that MKP3 expression was up regulated upon BCR stimulation (Fig1B) and our model depicts that the interaction of CK2α with this phosphatase modulates the MKP3-mediated co-ordination of the negative feedback loop influencing ERK-1/2 phosphorylation. Importantly our earlier results also implicated MKP1, which is positively regulated by ERK-1/2 as a direct target of MKP3. While modeling the MAPK pathway, however, the possibility that the MKP3 acted simultaneously on both ERK-1/2 and MKP1 seemed unlikely since such a proposition failed to explain the previously described experimental results. We therefore, considered the possibility that the ERK-1/2 and MKP1 may represent alternate substrate for MKP3, with substrate specificity being determined by the phosphorylation state of MKP3. Whereas the non phosphorylated MKP3 functioned as a negative regulator of ERK-1/2 activation, its phosphorylation by CK2α alters its substrate preference in favor of MKP1, with the consequent attenuation of its activity. This postulates yielded a satisfactory solution after a few optimization and simulation exercises.

Our earlier findings that the depletion of MKP3 from cells by si-RNA resulted in a marked enhancement in the BCR-dependent phosphorylation of MEK-1/2 (Kumar et al., 2008) also prompted us to link phosphorylated MKP3 as a negative regulator of MEK-1/2. Consequently, while phospho-MKP3 would not be expected to directly inhibit ERK-1/2 activation this would nonetheless, be compensated by the inhibitory effect of MKP3 on the upstream kinase MEK-1/2. Further, PP2A has been described as a regulator of the phosphorylation of MEK-1/2 (Bhalla and Iyengar, 1999; Bhalla et al., 2002; Kolch, 2000). In addition, a marked increase in ERK-1/2 phosphorylation was also observed under these conditions. We accounted for these unexpected findings by considering the possibility that phosphorylation of MKP3 could be reversed by the direct action of PP2A. Thus in addition to de-phosphorylating Raf and MEK-1/2, PP2A is also likely to function in regulating the balance between the phosphorylated and non-phosphorylated pools of MKP3. The resulting model for the MAPK module yielded a

A. Simulated profile of restimulation following 6hrs after first stimulus

ppERK (a.u.)

ppErk
Erk

0   5   10   20   30

ppErk
Erk

360   365   370   380   390

0   10   20   30   360   370   380   390

First Stimulus   *Second Stimulus*

Time (Minutes)

B. MKP3 Expression Following BCR activation

MKP3
(GAPDH) Loading Control

Time (hours)   0   2   4   6   8   10   12
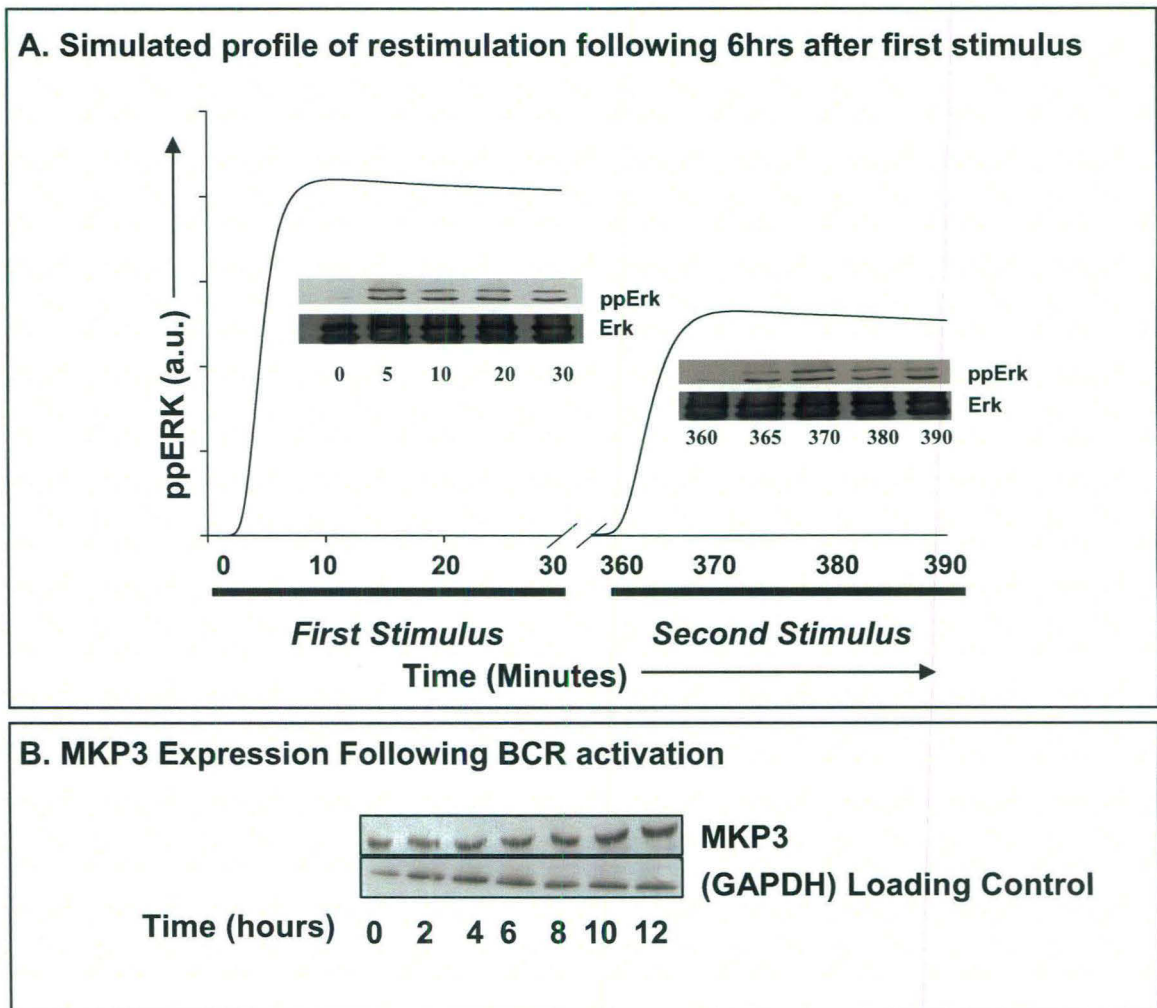
Figure 1 Top panel shows here the simulation profile of ERK phosphorylation (ppERK) following a first stimulus of thirty minutes and a second stimulus 6 hours after the first stimulus. Inset in the top panel shows the Western blot from the similar experiment on A20 cells. Both Western blot and *in silico* prediction showing the excellent match. Lower Panel shows the MKP3 expression level over 12 hours following BCR stimulation. Both panels are validating the model proposed.

prediction for the time dependent phosphorylation of ERK-1/2 that was in excellent agreement with the experimentally obtained results.

The above results thus identify a cascade of phosphatases (PP2A-MKP3-MKP1) that is aligned in parallel with the MAPK cascade (Raf-MEK-ERK). ERK activation also leads to transcriptional up-regulation of MKP1 and MKP3. We have achieved the same through a reaction scheme similar to as proposed by (Bhalla et al., 2002), although the rates are scaled according to the present concentration of these two phosphatases. The concentrations of c-Raf, MEK, ERK, PP2A, MKP1, RasGDP-GTP total, Akt were determined by Western blot titrations that compared against corresponding levels present in NIH3T3 and CHO cells (Data not shown here). Concentrations of the remaining molecules were estimated.

Complete scheme of biochemical interactions described above is converted into a system of coupled differential equations (see Annexure for details) to generate the model. Model is implemented and optimized in Simbiology 2.2 (MATLAB) (www.mathworks.com).

Assumptions and criteria for implementation of the model

Few important considerations have been taken while implementing model in mathematical form which are as follows:

1. Since a detailed description of the early signaling events at the BCR signalosome is currently unavailable, the steps were minimized and unnecessary complexity was avoided. For this, the parameters were constrained to the extent possible for describing the kinetics of these events without affecting the known outputs, and keeping the system simple. For example, phosphorylation of BLNK at multiple sites was represented by a single step. Further, the four different (1+ 3) events of phosphorylation at the ITAMs (BCR in the model) by BCR activation and Syk mediated feedback were simplified in two steps (1 by BCR engagement + 1 by Syk) keeping the positive feedback effect of Lyn-Syk-ITAM feedback loop intact.

2. Activated to unactivated ratios were maintained for different molecules in accordance with their cytoplasmic locations and mode of activation. Compartmentalization was not considered in our analysis.

3. In the case of regulation by multiple phosphatases, the experimental results obtained by Western blot analyses cannot be directly correlated to exact relative levels of activated molecules since quantitation by this technique is not linear over a large range. Thus a true regression scheme cannot be employed for phosphatase-mediated perturbations involving large variations in phosphorylation levels. Further, shifts in baseline phosphorylation levels also cause problems, which are not usually encountered in the traditional model building exercises where maximum phosphorylation levels of substrates following on receptor activation are considered as 100% and regression is then applied for a comparatively smaller range of modulations in phospholevels. However post implementation techniques were employed for assessing regression stability of the parameters. These were Multi Parametric Sensitivity Analysis (MPSA) and Partial Rank Correlation Coefficients (PRCC), as described later in sensitivity analysis and robustness scores.

21

4. Parameters describing the kinetics of molecules on the network periphery were grouped together to define the representative kinetic behavior relevant to the present MAPK module.

Sensitivity of the Model

Having constructed the model, we performed an exhaustive sensitivity analysis for identifying the key regulatory features of BCR induced MAPK (ERK). Table 1 shows selected sensitivities and their corresponding parameters with their reaction scopes. Sensitivity analysis was done using four different methods using SBML_SAT (Zi et al., 2008) a MATLAB toolbox for sensitivity analysis of systems biology models which is based on SBML. SBML_SAT is free and available at (http://sysbio.molgen.mpg.de/SBML-SAT/).

We used four different methods of sensitivity analysis on integrated response of model output variables. All these methods of analysis identified BLNK-mediated activation of the BLNK/Grb2/SOS complex, which functions as the RasGTP-GDP exchanger upon BCR stimulation. BLNK has a key role in B cell receptor induced signaling. It serves as a scaffold for SoS and, therefore, couples Syk with downstream signaling events of BCR signalososme (Ishiai et al., 2000; Ishiai et al., 1999; Pappu et al., 1999). Global sensitivity analysis methods use multiple parameter variations. The scores identify the Multi-parametric Sensitivity analysis and give Kolmogorov-Smirnov (K-S) statistics values for the distance between frequencies of the acceptable and unacceptable parameter sets generated through random perturbations. That is, MPSA reveals the uncertainty of the parameter space used. Thus the K-S value here specifically revealed that kcat_123 (the enzymatic action of ppMEK on ERK) and kf_124 (binding of pERK to the ppMEK), had a significant effect on the ppERK response. This has also been reported earlier, and the consistency of these parameters found in all the methods employed suggests that this two-step phosphorylation is an important step in shaping the both integrated responses and the maximal responses of ppERK. Interestingly, the two-step phosphorylation of ppMEK does not actually give high K-S value or local sensitivity coefficient for the enzymatic action of pRaf on MEK (kcat_104), and this remains consistent on both the integrated and maximum response of ppMEK. The detailed Sensitivities of ppMEK and ppERK are provided in the accompanying CD.

Table 1: List of Sensitive parameters for ppERK response, identified by multiple sensitive analysis methods.
(Highlighted values are chosen by low cut-off of the scores in each method. Both negative and positive values are selected in cases wherever required.)

Parameter no.	Name	Scope (Reaction)	Value	INTEGRATED RESPONSE ppERK				MAXIMUM RESPONSE ppERK	
				LSA	MPSA	PRCC	WALS	LSA	PRCC
3	kf_2	[L:BCR] -> [L:BCRp]	0.99	0.029204	0.043819	0.070292	2.2845	0.020365	0.081712
4	kon_3	[L:BCRp] + Lyn <-> [L:BCRp:Lyn]	0.8857	0.037552	0.065934	0.10865	2.4007	0.037694	0.097706
6	kcat_4	[L:BCRp:Lyn] -> [L:BCRp] + Lynp	0.515	0.028499	0.046031	0.096054	2.3485	0.032711	0.058961
7	kon_5	Lynp + SHP1 <-> [Lynp:SHP1]	7	-0.02222	0.029844	-0.11401	-0.15307	-0.01859	-0.10919
8	koff_5	Lynp + SHP1 <-> [Lynp:SHP1]	7.9716	0.017748	0.049554	0.084544	0.96652	0.01486	0.063383
9	kcat_6	[Lynp:SHP1] -> Lyn + SHP1	2	-0.01922	0.038369	-0.07513	-1.6353	-0.01607	-0.06662
10	km_7	Lynp + CD22 -> Lynp + CD22p	1.933	0.01182	0.02282	0.05168	0.61933	0.02376	0.10261
11	vm_7	Lynp + CD22 -> Lynp + CD22p	5.4291	-0.01237	0.028449	-0.10304	-0.54861	-0.02388	-0.0735
12	kf_8	CD22p + SHP1c <-> [CD22p:SHP1c]	0.7532	-0.01929	0.066175	-0.12033	-1.611	-0.02785	-0.10627
13	kb_8	CD22p + SHP1c <-> [CD22p:SHP1c]	1.201	0.014022	0.051081	0.054348	-1.7142	0.012024	0.068158
14	kcat_9	[CD22p:SHP1c] -> CD22p + SHP1	0.9426	-0.01476	0.060674	-0.06679	-1.0386	-0.01242	-0.05681
15	kf_10	SHP1 -> SHP1c	0.01	0.012677	0.069115	0.086093	1.0282	0.010086	0.12424
16	kf_11	CD22p -> CD22	0.0943	0.011214	0.02936	0.08423	2.8871	0.010491	0.023539
18	kf_12	Lynp + Syk <-> [Lynp:Syk]	0.448	0.053245	0.061226	0.24421	4.0278	0.057128	0.19438
19	kcat_13	[Lynp:Syk] -> Lynp + Sykp	21.56515	0.016662	0.044864	0.0879	1.4256	0.026035	0.10032
20	kf_14	Sykp + SHP1 <-> [Sykp:SHP1]	20	-0.03165	0.085495	-0.17647	-2.7199	-0.02746	-0.17125
21	kb_14	Sykp + SHP1 <-> [Sykp:SHP1]	3.6	0.02689	0.045941	0.12013	1.31	0.023202	0.12074
31	kon_22	2 [L:BCR1] <-> [L:BCR]	10	0.016718	0.022684	0.027805	-1.5481	-0.01006	-0.01625
82	kf_55	Sykp + BLNK <-> [Sykp:BLNK]	2.4	0.07698	0.055654	0.19513	4.4512	0.05042	0.19611
83	kb_55	Sykp + BLNK <-> [Sykp:BLNK]	4	-0.06144	0.038016	-0.1235	-1.8585	-0.03912	-0.13691
84	kcat_56	[Sykp:BLNK] -> Sykp + BLNKp	1	0.065816	0.057549	0.14234	5.0224	0.041205	0.14063
87	kf_58	BLNKp + Grb2 <-> [BLNKp:Grb2]	1	0.053132	0.051447	0.15254	3.236	0.037963	0.12557
88	kb_58	BLNKp + Grb2 <-> [BLNKp:Grb2]	0.05	-0.0494	0.062139	-0.11943	-3.2013	-0.03794	-0.10347
89	kf_59	BLNKp + Pase2 <-> [BLNKp:Pase2]	222	-0.04783	0.053274	-0.14956	-3.2291	-0.03444	-0.13002
90	kb_59	BLNKp + Pase2 <-> [BLNKp:Pase2]	3.68	0.038179	0.018583	0.075944	1.5954	0.027512	0.094075
91	kcat_60	[BLNKp:Pase2] -> BLNK + Pase2	0.926	-0.0586	0.081336	-0.13187	-2.1264	-0.04382	-0.12428
92	kf_61	[BLNKp:Grb2] + SoS <-> [BLNKp:Grb2:SoS]	0.05	0.14803	0.10632	0.27137	5.1205	0.10744	0.25726
93	kb_61	[BLNKp:Grb2] + SoS <-> [BLNKp:Grb2:SoS]	1	-0.14749	0.12379	-0.26859	-5.224	-0.10744	-0.28619
97	kf_64	PLCgp + Pase3 <-> [PLCgp:Pase3]	52	5.99E-05	0.035205	-0.13772	0.46904	-0.02243	-0.09551
98	kb_64	PLCgp + Pase3 <-> [PLCgp:Pase3]	0.54	0.000371	0.05392	0.016948	2.9354	0.000139	0.034664
108	kf_71	RasGTP -> RasGDP	0.25	-0.14	0.10863	-0.32322	-5.8548	-0.10986	-0.29429
109	kf_72	GEFp + RasGDP <-> [GEFp:RasGDP]	0.08	0.002824	0.021912	0.10295	1.2201	0.001874	0.075113
120	kf_80	PKCm + Sykp <-> [PKCm:Sykp]	0.25	-0.02158	0.044368	-0.03314	-1.6908	-0.01976	-0.05608
127	kf_85	Raf + RasGTP <-> [Raf:RasGTP]	100	0.15104	0.14929	0.34641	6.2859	0.11765	0.34396
128	kb_85	Raf + RasGTP <-> [Raf:RasGTP]	2	-0.03933	0.072863	-0.20153	-2.3882	-0.02812	-0.1836
129	kf_86	[Raf:RasGTP] + PKCm <-> [Raf:RasGTP:PKCm]	8	0.054611	0.086794	0.25403	3.0138	0.059179	0.24523
149	kf_99	Sykp + PLCg <-> [Sykp:PLCg]	10	-0.00864	0.036119	0.13652	1.5703	-0.00194	0.13414
151	kcat_100	[Sykp:PLCg] -> Sykp + PLCgp	4	-0.00205	0.047205	0.12754	1.3759	0.03828	0.098158
152	kf_101	Rafp + PP1 <-> [Rafp:PP1]	3	-0.2553	0.21149	-0.48536	-8.2838	-0.1968	-0.45958
153	kb_101	Rafp + PP1 <-> [Rafp:PP1]	4	0.12761	0.12365	0.21967	4.2975	0.098391	0.25047
154	kcat_102	[Rafp:PP1] -> Raf + PP1	4	-0.12192	0.080181	-0.22685	-4.2892	-0.09364	-0.22694
155	kf_103	Rafp + MEK <-> [Rafp:MEK]	6.8	0.078856	0.10069	0.26756	4.0473	0.044245	0.26303
156	kb_103	Rafp + MEK <-> [Rafp:MEK]	9.62	-0.06309	0.061531	-0.2007	-3.2638	-0.0354	-0.18786
157	kcat_104	[Rafp:MEK] -> Rafp + MEKp	2.405	0.063937	0.059647	0.19725	3.2865	0.035856	0.20891
158	kf_105	Rafp + MEKp <-> [Rafp:MEKp]	6.8	0.21811	0.18623	0.32331	4.805	0.18673	0.30276
159	kb_105	Rafp + MEKp <-> [Rafp:MEKp]	9.62	-0.17448	0.093219	-0.23512	-3.8752	-0.14939	-0.24828
160	kcat_106	[Rafp:MEKp] -> Rafp + MEKpp	2.405	0.17634	0.099473	0.22414	3.8703	0.15091	0.21605

| 161 | kf_107 | PKCm + CK2alpha <-> [PKCm:CK2alpha] | 2 | 0.00215 | 0.039536 | -0.03877 | 3.6096 | 0.002523 | -0.04317 |
162	kb_107	PKCm + CK2alpha <-> [PKCm:CK2alpha]	8	-0.00161	0.028508	0.024229	1.2526	-0.00189	0.032473
163	kcat_108	[PKCm:CK2alpha] -> PKCm + CK2alphap	2.667	0.001957	0.043663	0.003555	3.9474	0.002263	-0.00634
164	kf_109	CK2alphap -> CK2alpha	0.333	-0.00263	0.029098	0.01183	1.4589	-0.00289	0.044563
165	kf_110	CK2alphap + MKP3 <-> [CK2alphap:MKP3]	1	0.062408	0.033284	-0.04216	-1.3307	0.067634	-0.07989
167	kcat_111	[CK2alphap:MKP3] -> CK2alphap + MKP3p	1.16	0.050177	0.026022	-0.00492	-0.94637	0.054468	-0.04071
168	kf_112	MKP3p + PP2A <-> [MKP3p:PP2A]	15	-0.06344	0.030185	0.051785	1.399	-0.06806	0.058377
169	kb_112	MKP3p + PP2A <-> [MKP3p:PP2A]	16	0.050754	0.026687	-0.01522	-0.95654	0.054448	-0.02305
171	kf_114	MEKpp + PP2A <-> [MEKpp:PP2A]	1.31	-0.05791	0.03069	-0.10188	-0.97887	-0.05763	-0.10585
174	kf_116	MEKp + PP2A <-> [MEKp:PP2A]	1.31	-0.01488	0.049138	0.085984	1.254	-0.01278	0.092898
175	kb_116	MEKp + PP2A <-> [MEKp:PP2A]	4	0.0119	0.051496	-0.13872	-2.6973	0.010226	-0.15639
176	kcat_117	[MEKp:PP2A] -> MEK + PP2A	1	-0.0121	0.046098	-0.07203	-1.4551	-0.01047	-0.08579
177	kf_118	MEKpp + MKP3p <-> [MEKpp:MKP3p]	26	-0.12597	0.069778	-0.08032	-2.4753	-0.12682	-0.11419
178	kb_118	MEKpp + MKP3p <-> [MEKpp:MKP3p]	64	0.10078	0.057211	0.090769	1.0251	0.10146	0.06711
179	kcat_119	[MEKpp:MKP3p] -> MEKp + MKP3p	16	-0.10037	0.039735	-0.03907	-1.0278	-0.10101	-0.07616
183	kf_122	ERK + MEKpp <-> [ERK:MEKpp]	1.6	0.25499	0.067188	0.17925	2.1096	0.23681	0.18892
184	kb_122	ERK + MEKpp <-> [ERK:MEKpp]	1	-0.20391	0.062512	-0.1526	-1.4375	-0.18915	-0.13563
185	kcat_123	[ERK:MEKpp] -> ERKp + MEKpp	0.25	0.34169	0.12394	0.24024	2.6227	0.30825	0.22344
186	kf_124	ERKp + MEKpp <-> [ERKp:MEKpp]	1.6	0.47591	0.12742	0.23206	2.8028	0.47353	0.23443
187	kb_124	ERKp + MEKpp <-> [ERKp:MEKpp]	1	-0.38052	0.089974	-0.17524	-2.0164	-0.37883	-0.18166
188	kcat_125	[ERKp:MEKpp] -> ERKpp + MEKpp	0.25	0.52203	0.084564	0.21452	2.3409	0.51628	0.23496
195	kf_130	ERKpp + MKP1 <-> [ERKpp:MKP1]	0.30101	-0.24219	0.047866	-0.06191	-0.15167	-0.24239	-0.02741
196	kb_130	ERKpp + MKP1 <-> [ERKpp:MKP1]	4.44	0.16201	0.038562	0.015221	0.074303	0.16317	0.039771
197	kcat_131	[ERKpp:MKP1] -> ERKpp + MKP1p	2.2	-0.16438	0.040929	-0.00984	-0.10902	-0.16571	-0.00138
198	kb_132	MKP1p + MKP3p <-> [MKP1p:MKP3p]	108	-0.18802	0.019547	0.002995	-0.06317	-0.19406	-0.01
199	kf_132	MKP1p + MKP3p <-> [MKP1p:MKP3p]	141	0.2349	0.064807	0.020359	0.065316	0.2409	0.00806
200	kcat_133	[MKP1p:MKP3p] -> MKP1 + MKP3p	27	0.18783	0.017308	0.003829	0.055951	0.19385	-0.01054
201	kf_134	ERKpp + MKP2 <-> [ERKpp:MKP2]	76	-0.05673	0.05477	-0.12398	-1.7391	-0.03585	-0.14203
202	kb_134	ERKpp + MKP2 <-> [ERKpp:MKP2]	4	0.042128	0.045962	0.06242	1.0312	0.036957	0.088384
203	kcat_135	[ERKpp:MKP2] -> ERKp + MKP2	1	-0.18257	0.068503	-0.12992	-1.1808	-0.18475	-0.11008
204	kf_136	ERKp + MKP2 <-> [ERKp:MKP2]	76	0.009324	0.065293	-0.10452	-1.4809	0.014826	-0.12148
205	kb_136	ERKp + MKP2 <-> [ERKp:MKP2]	4	-0.00785	0.036169	0.048345	0.92584	-0.0131	0.074341
206	kcat_137	[ERKp:MKP2] -> ERK + MKP2	1	-0.12558	0.081798	-0.16248	-1.7516	-0.11475	-0.13575
221	kf_148	[Rafp:RasGTP] -> Rafp + RasGTP	1	0.071143	0.06721	0.097229	1.3666	0.054611	0.074144
222	kf_149	[L:BCR1] + BCR <-> [L:BCR]	10	0.008757	0.031247	0.042901	-2.7834	0.033819	0.029415
223	kb_149	[L:BCR1] + BCR <-> [L:BCR]	2	0.00016	0.027101	-0.02317	4.2148	0.004053	-0.00312
224	kf_150	[L:BCRp] + SHP1 <-> [L:BCRp:SHP1]	83	-0.00764	0.039382	-0.01822	-1.8154	-0.00518	-0.06862
230	km_154	[BLNKp:Grb2:SoS] + RasGDP -> [BLNKp:Grb2:SoS] + RasGTP	0.050505	-0.0953	0.088828	-0.15972	-3.1803	-0.07055	-0.18217
231	vm_154	[BLNKp:Grb2:SoS] + RasGDP -> [BLNKp:Grb2:SoS] + RasGTP	22	0.14926	0.095559	0.28961	5.1958	0.10841	0.27124
232	kf_155	ERKpp + MKP1p <-> [ERKpp:MKP1p]	450	-0.3104	0.038073	-0.01653	-0.3368	-0.32582	-0.05521
233	kb_155	ERKpp + MKP1p <-> [ERKpp:MKP1p]	600	0.24832	0.030035	0.007364	0.28074	0.26066	0.036606
234	kcat_156	[ERKpp:MKP1p] -> ERKp + MKP1p	150	-0.27853	0.038234	-0.04164	-0.54174	-0.2936	-0.02657
235	kf_157	ERKp + MKP1p <-> [ERKp:MKP1p]	450	-0.17439	0.042172	-0.02909	-0.15417	-0.18474	-0.05329
236	kb_157	ERKp + MKP1p <-> [ERKp:MKP1p]	600	0.13698	0.06439	0.002892	0.083899	0.14117	0.011061
237	kcat_158	[ERKp:MKP1p] -> ERK + MKP1p	150	-0.16366	0.059964	-0.01193	-0.12975	-0.16943	-0.0273

Weighted average of local sensitivity (WALS) which uses the weighted average of local sensitivity indices on parameters space and calculate the least square errors of reference simulation and perturbations. The scores of WALS here primarily identified the component important for the dose response components of present network including the main phosphatases of the model and the BCR-LYN-SYK positive feedback loop. The popular Global Sensitivity Analysis (GSA) method of regression-based rank transformation method Partial Rank Correlation Coefficient (PRCC) uniquely isolates the vm_7 (Vmax of CD22 phosphorylation) which is the part of Negative auto-regulatory loop at BCR dependent Lyn activation, and responsible for the membrane recruitment of SHP1 which negatively regulate and shapes the activity of BCR signalosome. PRCC also uniquely identified the binding of MEKpp to PP2A, the negative regulator of both MEK and Raf activity, both in the Integrated and maximum response of ppERK. This identifies that the first step of ppMEK binding to PP2A competes along with pMKP3, which is another negative regulator of MEK activity in the phosphatase cascade. In all cases of ppERK and ppMEK, the integrated response was invariably affected by the action of PP1 on pRaf, which we found to be true experimentally as well (Kumar et al., 2008). PRCC also revealed the role of the initial conditions on various model output variables and is shown in figure 2.

Figure 3 to 8 shows the various output variables and their sensitivities for integrated and maximum responses by the different methods of LSA and GSA. The sensitivity of time dependent responses were also measured (data not shown), and this was consistent with the present results and model behavior. The model was also tested for various perturbations and combinations of the initial concentrations of Raf-MEK-ERK and we found that the solution for the SAM converged to the same response spectrum. Although we identified parameters which were sensitive to perturbations, the sensitivity of these parameters did not affect model output significantly since the cut off for the highlighted results chosen was as low as 10% of the maximum possible sensitivity in each case. Thus model was robust with respect to variations in parameters and initial conditions.
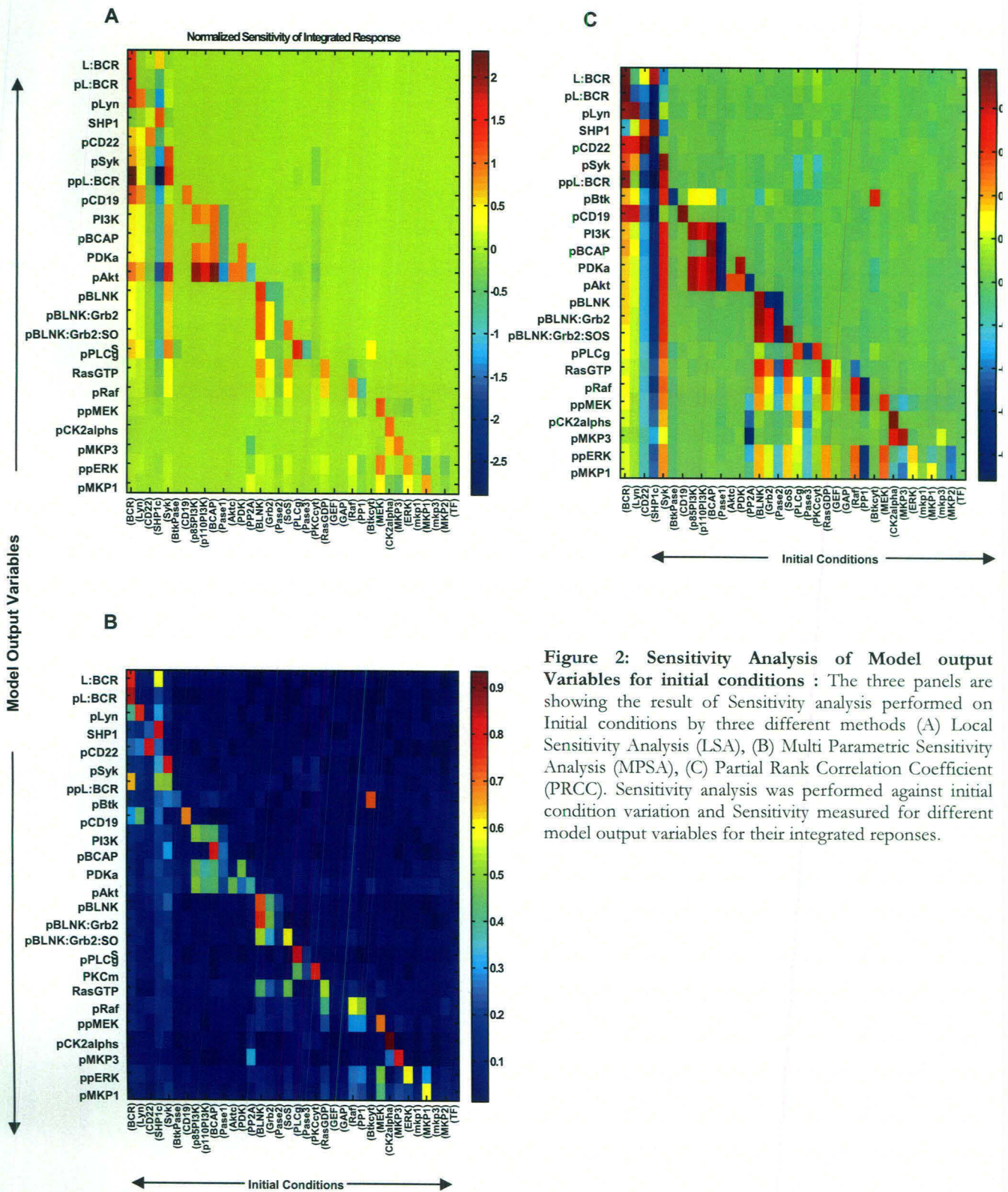
Figure 2: Sensitivity Analysis of Model output Variables for initial conditions : The three panels are showing the result of Sensitivity analysis performed on Initial conditions by three different methods (A) Local Sensitivity Analysis (LSA), (B) Multi Parametric Sensitivity Analysis (MPSA), (C) Partial Rank Correlation Coefficient (PRCC). Sensitivity analysis was performed against initial condition variation and Sensitivity measured for different model output variables for their integrated reponses.

Integrated Sensitivity of ppERK response
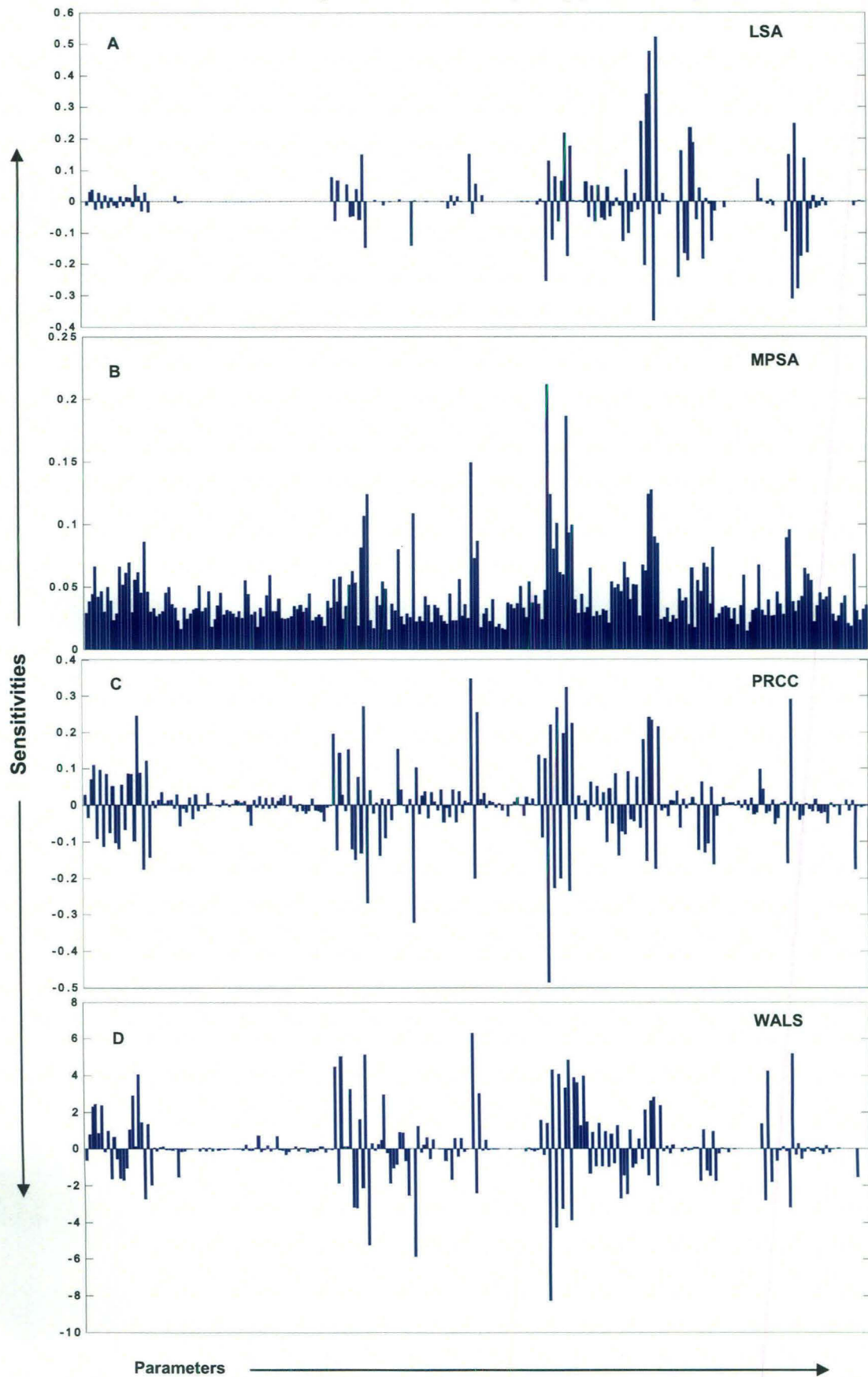
Figure 3: Sensitivities of Integrated response of ppERK to Parameters variations as measured by four different methods of local and global sensitivity analysis. (A) Local Sensitivity Analysis (LSA) (B) Multi Parametric Sensitivity Analysis (MPSA) (C) Partial Rank Correlation Coefficient (PRCC), and (D) Weighted Average of Local Sensitivities (WALS)
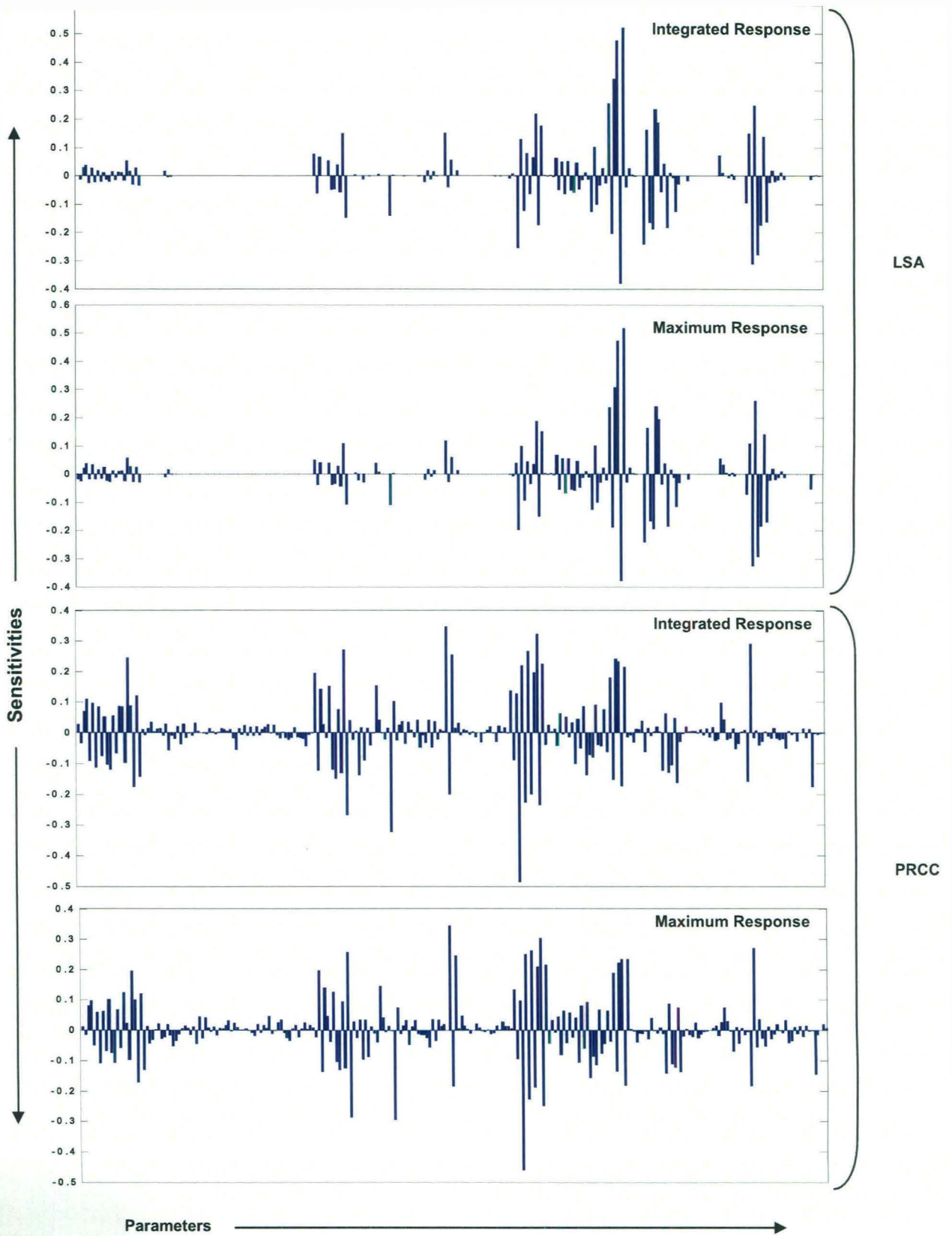
Figure 4: Comparison of sensitivities of integrated response and sensitivities of maximum response of ppERK to Parameter variations as measured by local and global sensitivity analysis. Fully Normalized Sensitivities from Local Sensitivity Analysis (LSA) and Global Sensitivity Analysis by Partial Rank Correlation Coefficients (PRCC).

Integrated ppMEK response
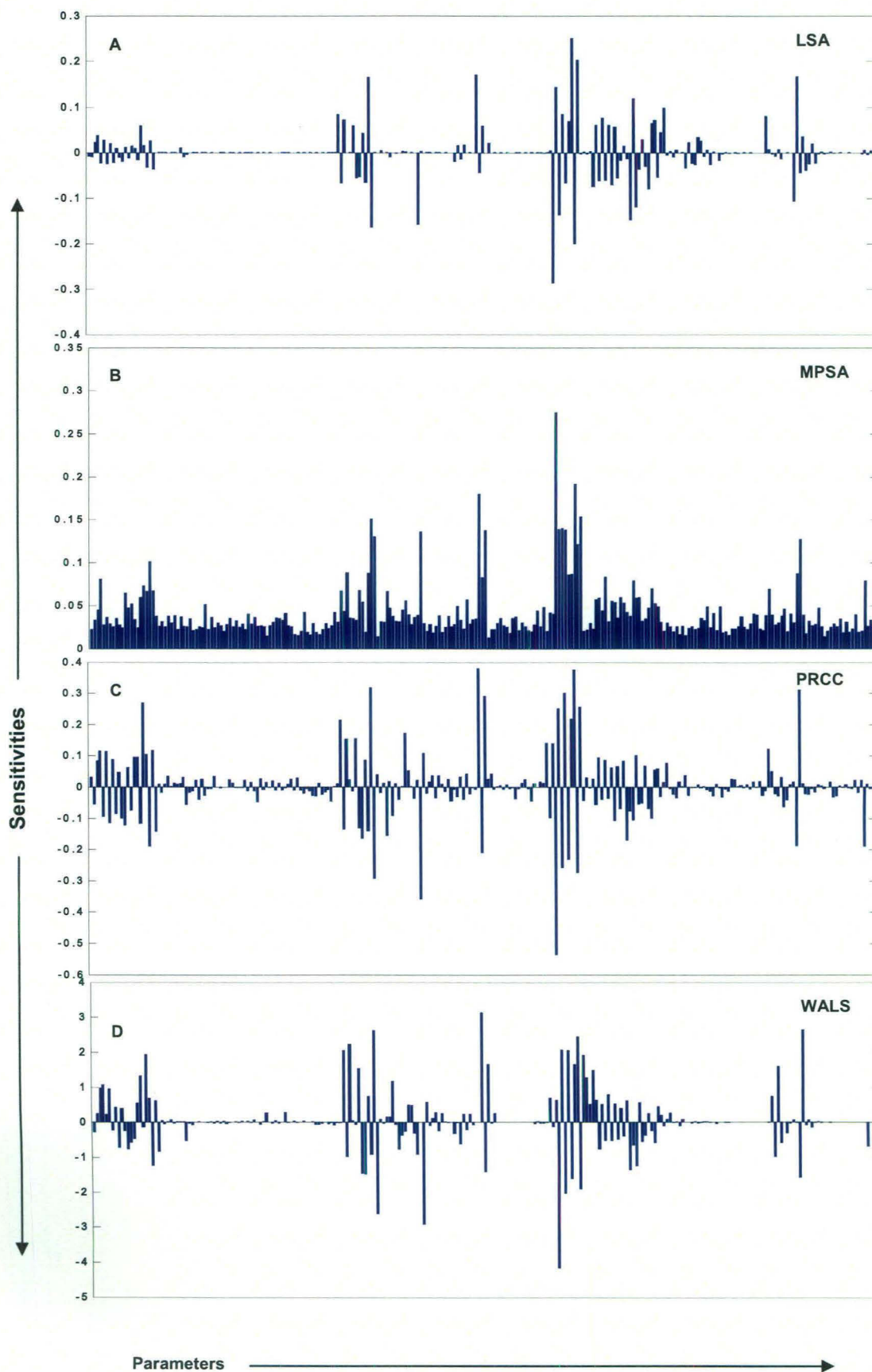
Figure 5: Sensitivities of Integrated response of ppMEK to Parameter variations as measured by four different methods of local and global sensitivity analysis. (A) Local Sensitivity Analysis (LSA) (B) Multi Parametric Sensitivity Analysis (MPSA) (C) Partial Rank Correlation Coefficient (PRCC), and (D) Weighted Average of Local Sensitivities (WALS)
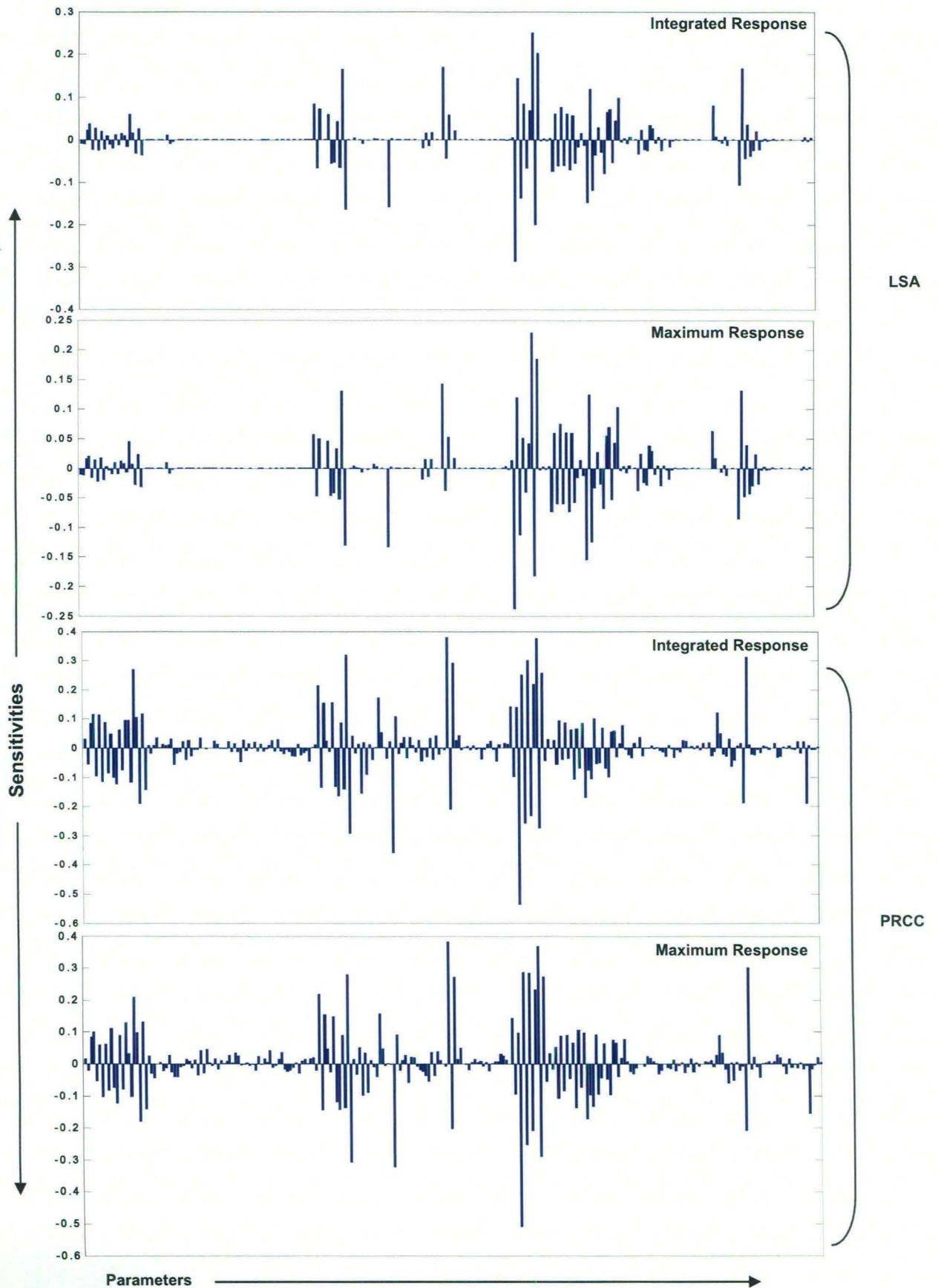
Figure 6: Comparison of sensitivities of integrated response and sensitivities of maximum response of ppMEK to Parameter variations as measured by local and global sensitivity analysis. Fully normalized sensitivities from Local Sensitivity Analysis (LSA) and Global Sensitivity Analysis by Partial Rank Correlation Coefficients (PRCC) .
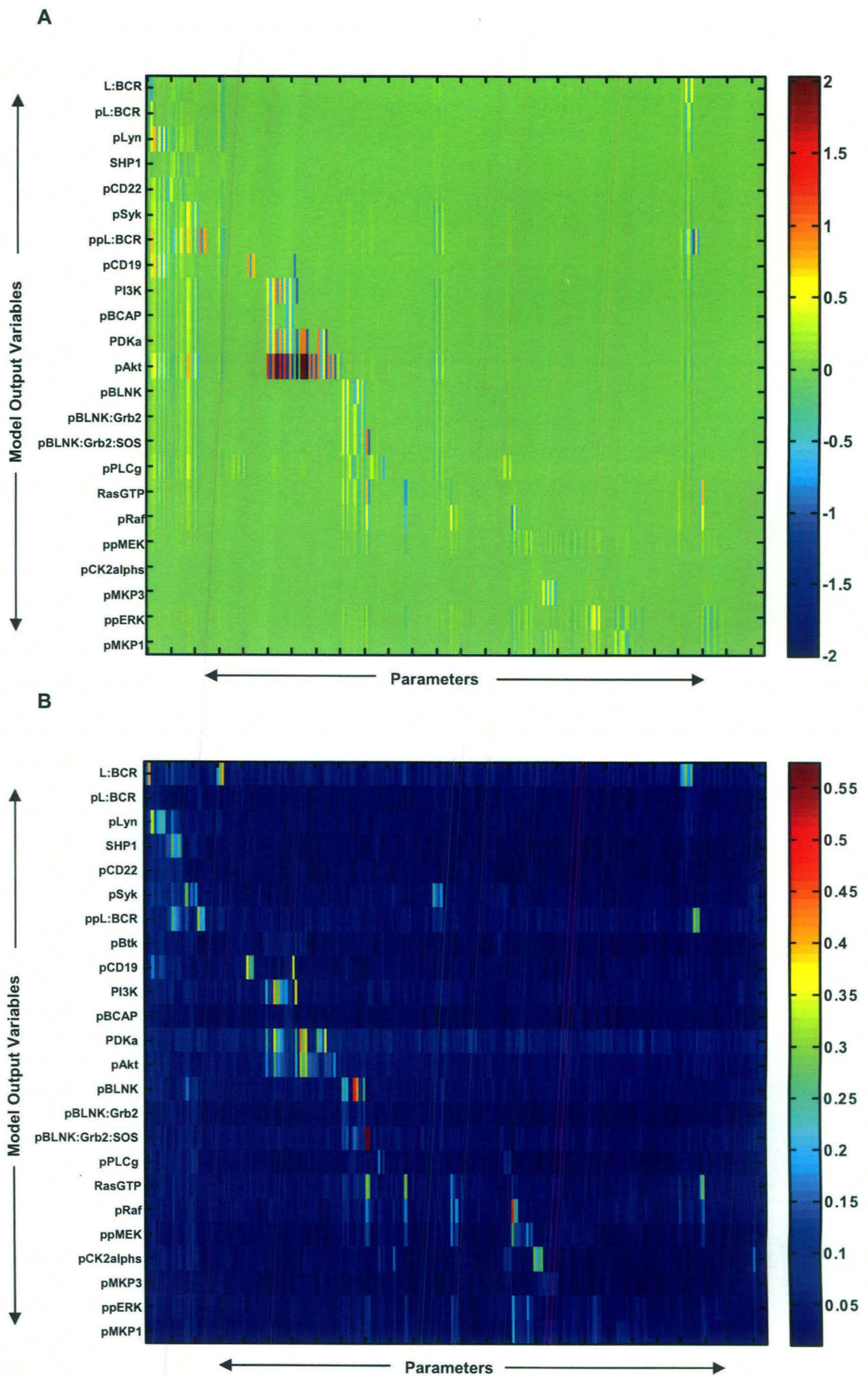
Figure 7: Comparison of sensitivities of integrated response of different model output variables for Parameter variations as measured by local and global sensitivity analysis. (A) Local Sensitivity Analysis (LSA) and (B) Global Sensitivity Analysis by Multi-Parametric Sensitivity analysis .
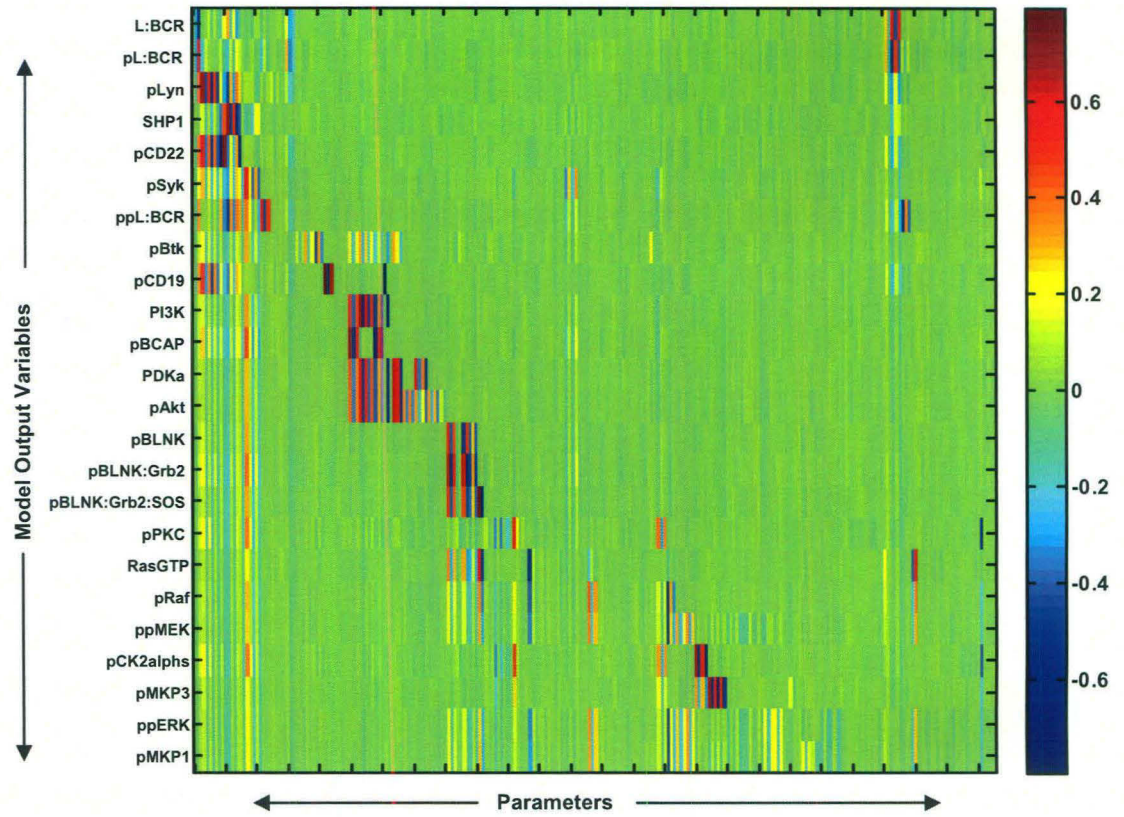
Figure 8: Sensitivities of integrated response of different model output variables for Parameter variations as measured by global sensitivity analysis by Partial Rank Correlation Coefficients (PRCC) Method .

Robustness of the Model

Our present model was unique in that it also modeled active regulation by phosphatases. It included active regulation of phosphatase by the kinase components of the network, which in turn was negatively regulated by these active phosphatases. Thus it became important to test the model for its robustness to the parameter variations, at least to the extent that it compared well with existing models. Robustness is a fundamental property of biological systems, which allows the systems to maintain its behavior against random perturbations (Kitano, 2007; Stelling et al., 2004). We preformed the Robustness analysis by SBML_SAT (Zi et al., 2008), a free software and is available at (http://sysbio.molgen.mpg.de/SBML-SAT/). Robustness analysis was performed as described (Barkai and Leibler, 1997; Bluthgen and Herzel, 2003), and Robustness scores measured as Total Parameter Variations (TPV) by randomly generated parameters by Latin Hypercube Sampling (LHS) method.

The R scores (Robustness scores) of a biological model assumes a negative value. The closer it is to zero, the more robust the model. Here we compared some of the most of models for the MAPK pathways in the literature with our present model. The corresponding R scores of MAPK components of those models, calculated under identical conditions of perturbations, are given in Table 2. As is evident here, the robustness score of our model compares well with that of the others, particularly with those that take phoshatases into consideration. Our model shows a particularly good agreement with that of (Bhalla et al., 2002), the only other model that incorporates active regulation of the phosphatase MKP1.

Table 2: Comparison of the robust scores of various Models of MAPK:

Model Name	Receptor/ Activator	RasGTP	pMAPKKK	ppMAPKK	pMAPK	Phosphatase Regulation
Huang Ferrell	-0.00543320	-------	-0.662038	-0.961861	-1.23605	No
Kholodenko 2000	-------	-------	-0.537109	-1.00071	-1.25602	No
Levchenko With scaffold	-------	-------	-0.344902	-0.67925	-1.11045	No
Levcheno No Scaffold	-------	-------	-0.561329	-1.3463	-2.80383	No
Hatakeyama 2003	-0.58779	-1.53691	-1.59975	-1.78692	-3.52799	Phosphatases Buffered
Sasagawa	-0.472733	-0.79791	-0.875844 (cRaf) -0.980000 (BRaf)	-1.2053	-1.99484	Phosphatases Buffered
Bhalla 2002	-1.44197e-034	-0.158336	-0.88649	-3.01403	-5.13613	MKP1 Regulation by MAPK
Present Study	-0.386837	-0.980019	-1.34911	-2.27352	-4.98263	Active phosphatase cascade.

Experimental Validation of the Model

Modeling BCR-dependent activation of the MAPK network

Our previous experimental studies of the plasticity of the BCR signaling network, and its response to specific perturbations (Kumar et al., 2008; Kumar et al., 2007; Singh et al., 2005), provided us with an internally normalized dataset for modeling salient features of the signaling network. We, therefore, combined these results with data from the literature to develop a block diagram for the BCR-activated MAPK signaling network. Here we specifically included the results from our most recent experiments probing the consequences of siRNA-mediated depletion of various cellular phosphatases, on BCR-dependent phosphorylation of the constituents of the MAPK pathway (Kumar et al., 2008). Data generated from the depletion of five of the tested phosphatases were taken for this study, and these five phosphatases were: PP1, PP2A, MKP1, MKP2, and MKP3. The selection of these phosphatases was guided by the fact that MKPs are known regulators of phoshorylation of the intermediates in the MAPK pathway (Bhalla et al., 2002; Brondello et al., 1999; Dickinson and Keyse, 2006). Further Raf, MEK, MKP1 and MKP3 are all regulated through phosphorylation at Ser/Thr residues (Brondello et al., 1999; Castelli et al., 2004), thereby implicating a possible role for PP1 and PP2A.

Modeling of BCR mediated signal transduction involved the basic reaction scheme from the receptor, to the intermediate molecules leading to the MAPK pathway and, eventually, to the regulation of ERK (Fig 9A). This process involved several rounds of iterations before the model could completely reproduce the experimental dataset, which involved upstream kinases and phosphatases apart from the core MAP kinase module. Model parameters such as initial concentrations, Km and Kd values, and other rate parameters were either taken from literature or, when not available, were optimized for producing the best experimental fit. The model incorporated generic rate laws such as mass action and Michaelis-Menten reaction schemes to represent the interactions among the species. The system was taken as appropriately modeled when it could fit the experimental phenotypic data (e.g. the previous results of our siRNA experiments, Fig 11), which included both the upstream and the MAPK intermediates. Apart from the general schematic (Fig 9A) of BCR signal transduction leading to ERK, the core MAPK module regulated by cellular phosphatases (Fig 9B) was of our interest for analysis. Care was taken to incorporate these phosphatases in the network in a manner that was
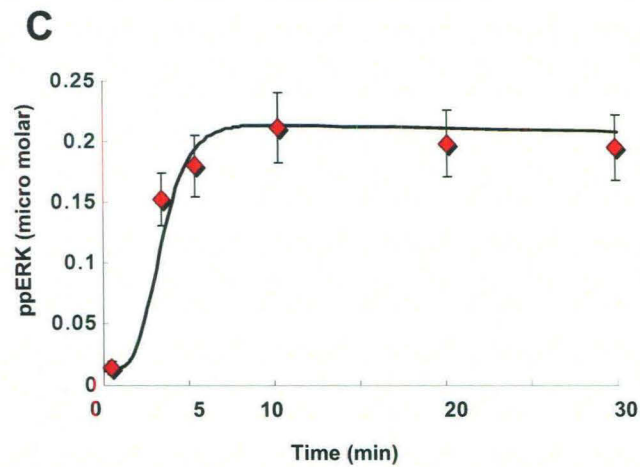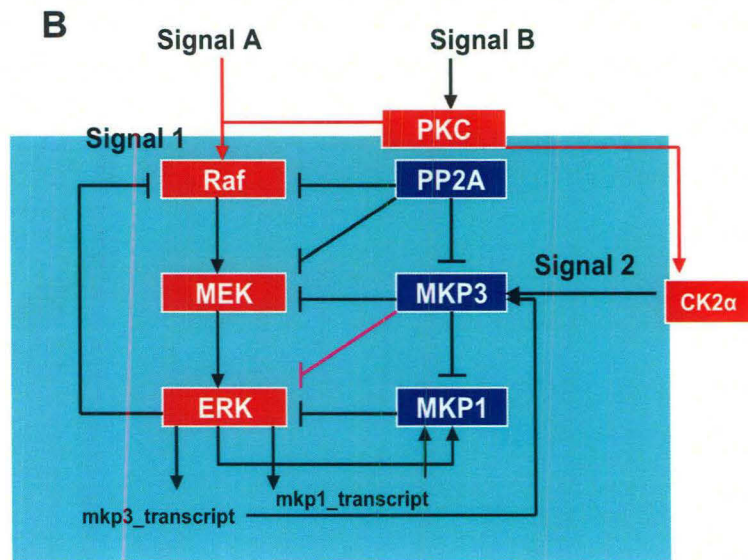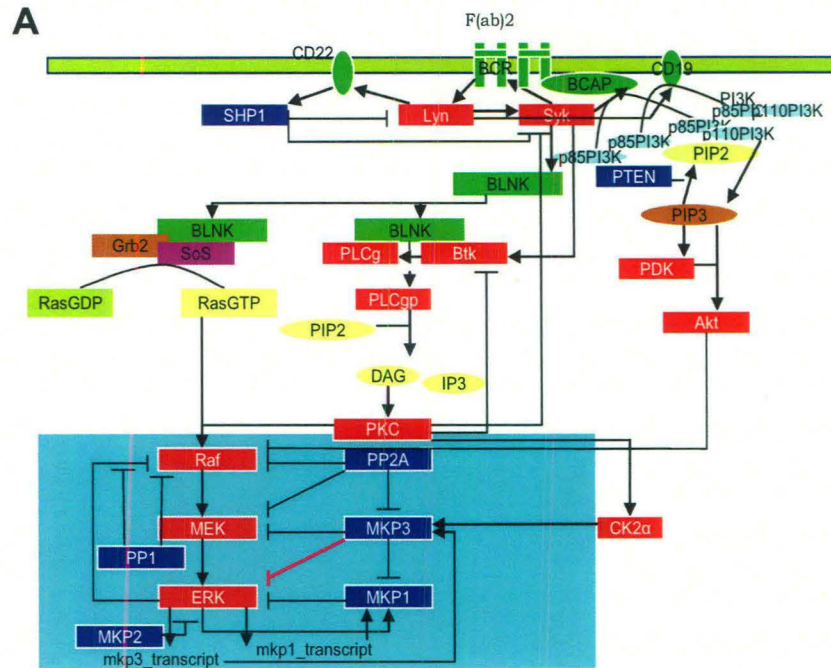
Figure 9: Signaling through the Lymphocyte receptor induces a novel regulatory motif for MAP kinase activation.

A schematic overview of the reactions for BCR dependent activation of MAP kinase ERK-1/2 is shown in panel A. The highlighted area represents the novel signaling motif identified and this is expanded in panel B. Panel C shows the concordance obtained between experiment (red diamonds, values as mean ±S.D., n=3) and simulation (black line) examining the time course of ERK phosphorylation obtained upon stimulation of A20 cells with a saturating (25 μg/ml) concentration of anti-IgG.

consistent with the known literature information and, in cases where adequate information was not available; assumptions were made based on our own experimental data to fit the phosphatases. Overall, the model consisted of 158 variables representing different pools of molecules, 172 biochemical reactions, and 256 total parameters (Annexure S1).

The resulting model was fairly complex, encompassing the span of regulatory events emanating from the receptor and terminating at ERK (Fig. 9A, B). To test the model, we performed Local and Global Sensitivity analyses using several independent methods to evaluate the parameters for their robustness against fluctuations that are inherent to noisy biological conditions. We found that parameters that were most sensitive were those that are already known to be critical for shaping the BCR-specific signaling response (see previous section for details). In other words, our model indeed reflected the true kinetic properties of BCR-dependent signaling. Parameters specific for the MAPK-phosphatase module (Fig 9B) were robust in terms of the output behavior, and could tolerate a broad range of perturbations against the ERK activation response. Further, we also verified that the robustness of our model compared well with that of other prominent models described for the MAPK pathway (Table 2). At the experimental level, the model also successfully recapitulated results available in the literature, which included our own earlier experimental data on BCR-dependent signaling in A20 cells (Fig 10 and Fig 11). Further, as shown in Figures 9C and D, the time-dependent phosphorylation profile of ERK predicted by our model was in agreement with the experimentally obtained results.

Analysis of the model

The model described in Figure 9A exhibited several intriguing topological and dynamical features. This is especially evident from Figure 9B, which highlights the co-alignment of a phosphatase cascade alongside the MAPK pathway, leading to several cross-regulatory interactions between the two. Notably, these interactions also included two novel links for MKP3. That is, in addition to ERK, our model described MKP3 to also interact with – and negatively regulate - MEK and MKP1 (Fig. 9B). Further, another related prediction by the model was that MKP3-dependent regulation was tightly controlled through a modulation of its substrate bias. In other words, while phosphorylated MKP3 was described to exhibit a preference for MEK and MKP1, its non-phosphorylated form was
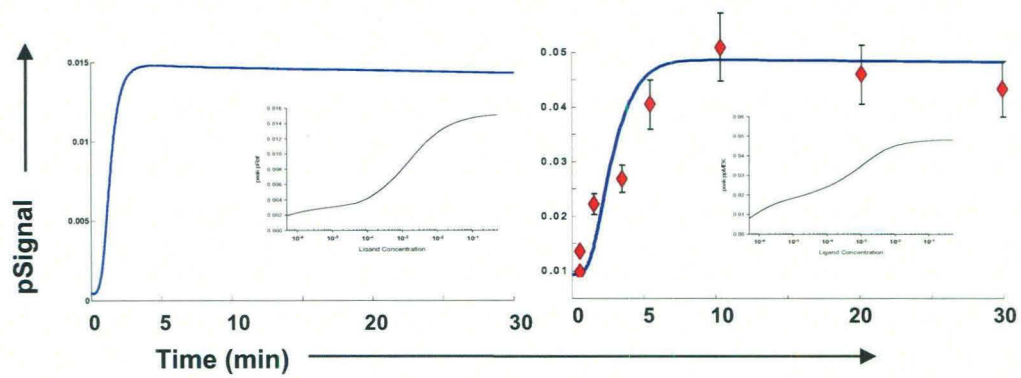
Figure 10. Shown here is a simulation of the time course of phosphorylation Raf (pRaf) and MEK (ppMEK) in cells stimulated with a saturating concentration of ligand. The inset in each panel gives the peak level of phosphorylation obtained over a wide range of ligand concentrations. These profiles are consistent with the experimental results derived in our earlier studies(Kumar et. al., 2007, 2008) The concordance between the experimental (red diamonds, values are mean $\pm$ S.D. of three experiments) and the simulated profiles is shown for ppMEK.
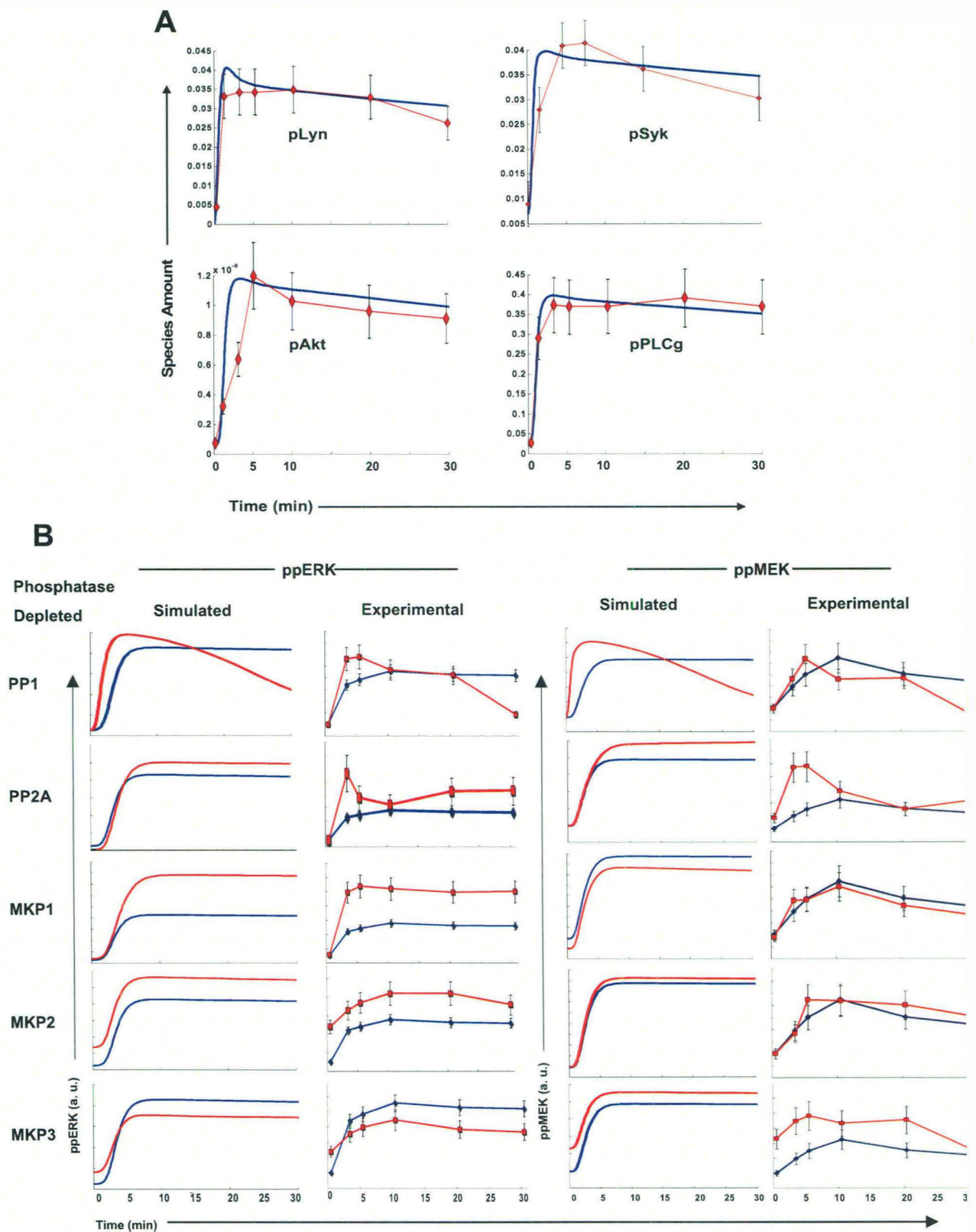
Figure 11. Panel A show simulation of the time course of phosphorylation of the indicated molecules in cells stimulated with a saturating concentration of the ligand. For the purposes of comparison, the experimentally derived values at the various time points are also included (red diamonds, values mean ± S.D. of three experiments). These values are from our earlier study (Kumar et. al., 2007, 2008). For the *in silico* profiles simulations were first run for 3000 seconds to achieve the steady baseline levels of phosphorylations prior to stimulation. This explains the baseline levels of phospho-species seen in these profiles. Panel B compares the experimentally derived (Experimental) and *in silico* (Simulated) profiles of ERK and MEK phosphorylation following depletion of cells with the indicated phosphatases. The values for the experimental group were taken from Kumar et. al. (2008). In all cases the X-axes start from zero although the units are arbitrary. In all the panels the profiles obtained in mock (i.e. GFP-siRNA) treated cells are shown in blue whereas those for phosphatase-specific siRNA treated cells are in red. For the *in silico* profiles simulations were first run for 3000 seconds to achieve the steady baseline levels of ERK phosphorylations prior to stimulation. This explains the minor lag period seen in these profiles.

predicted to be more selective for ERK. As a result, shifts in the distribution of MKP3 between the phosphorylated and non-phosphorylated pools potentially served as a mechanism for diversifying the influence of MKP3 on MAPK signaling.

An *in silico* analysis of ERK phosphorylation in response to varying ligand concentrations yielded an incremental dose-response profile (Fig. 12A). This prediction of a graded ERK output could be experimentally confirmed by stimulating A20 cells with increasing concentrations of anti-IgG (Fig 13C). Importantly, ERK response to ligand dose was found to be graded regardless of whether it was monitored at the level of the cell population by Western blot analysis (Fig 12B), or at the level of single cells through intracellular staining for phospho-ERK and detection by flow cytometry (Fig 12C).

Experimental verification of the model

We have already noted earlier that our completed model for the BCR-dependent activation of ERK retained its ability to describe the activation profiles of the intermediates in a manner that was consistent with the experimental data. Further, predictions on both the kinetics of ERK phosphorylation, and on the graded nature of the ERK response could also be subsequently borne out by experiment. Collectively these results would seem to support the veracity of our model, as well its sensitivity to perturbations in a context dependant manner. Nonetheless, it was also necessary to additionally confirm some of the topological features of the model, and their contribution to the systems properties of the MAPK module.

As shown in Figure 9B, a significant aspect of our model was the description of MKP3 as an important regulator of MAPK signaling through its ability to regulate MEK, ERK, and MKP1. While the interactions between MKP3 and ERK are well known (Maillet et al., 2008; Zhao and Zhang, 2001), the MKP3-MEK and MKP3-MKP1 interactions represent novel links identified here. We, therefore, sought to verify the existence of these latter links by performing co-immunoprecipitation experiments from lysates of A20 cells, using antibodies specific either for MEK, MKP1, or MKP3. As shown in Figure 14A, immunoprecipitation of either MEK or MKP1 also led to the simultaneous enrichment of MKP3, whereas immunoprecipitates of MKP3 were enriched for both MEK and MKP1. Although immunoprecipitation results do not permit quantification they, nonetheless, support at least the existence of MKP3 in a simultaneous complex with MKP1 and MEK, thereby confirming the interactions
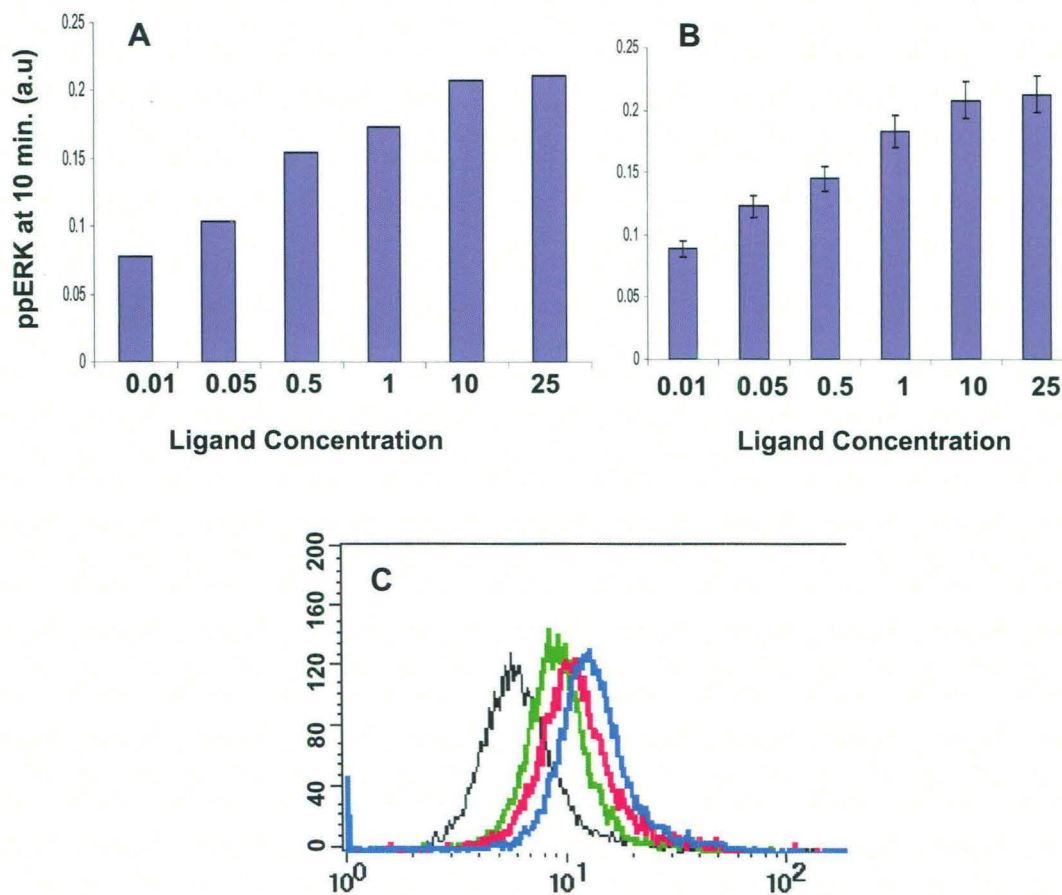
Figure 12: The ERK phosphorylation response is proportional to the stimulus strength.
Panel A shows the results of an *in silico* analysis estimating the magnitude of ERK phosphorylation obtained after stimulation of cells with varying anti-IgG concentrations. Panel B gives the corresponding results of an experiment where A20 cells were stimulated for 15 min, with the indicated doses of anti-IgG. ERK phosphorylation was then determined in lysates by Western blot analysis (Figure 13C). Values are the mean (±S.D.) of three independent experiments. Stimulated cells were also subjected to staining for intracellular phospho-ERK using specific antibodies followed by FITC-labeled secondary antibodies. Stained cells were then analyzed by flow cytometry and the results are shown in panel C. Depicted here are the profiles obtained for cells stimulated with either 0.1 (black line), 0.5 (green line), 5 (pink line), or 25 μg/ml (blue line) of anti-IgG. The profile for unstimulated cells overlapped with that for cells stimulated with 0.1 μg/ml of ligand. For the negative control, cells were stained with rabbit IgG instead of the anti-phospho-ERK antibody.

A

Effect of MKP3 knock down by siRNA on MKP1 expression level

WB

Normal

MKP1

PLCg

0   15   30   60   120

MKP3 siRNA

MKP1

PLCg

0   15   30   60   120

Stimulation Time (min)
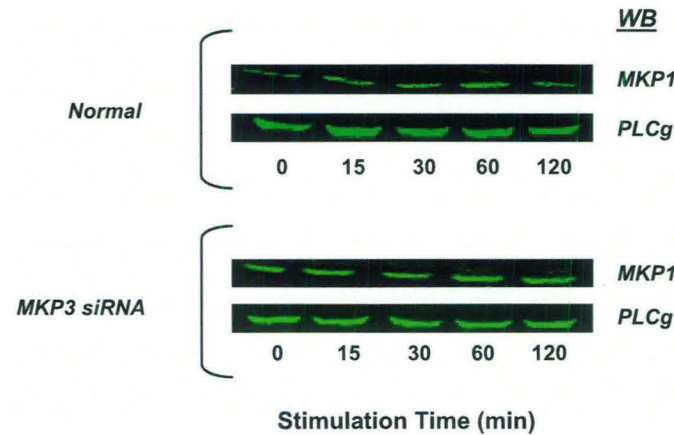
B

Activation profiles in the presence of DRB (CK2 inhibitor)

Normal   **DRB added**

ppERK

Ctrl

Stimulation Time 0 1 3 5 10 20 30   0 1 3 5 10 20 30
(Min)
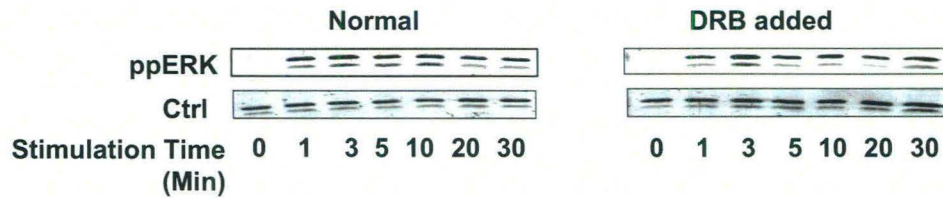
C

Graded ERK response for various concentrations of Ligand (F(ab)₂)

Stimulation Time (min) 0   1   3   5   10   0   1   3   5   10

0.01

0.05

0.5

1

10

25

Ligand Conc.   ppERK   GAPDH
(µg/ml)
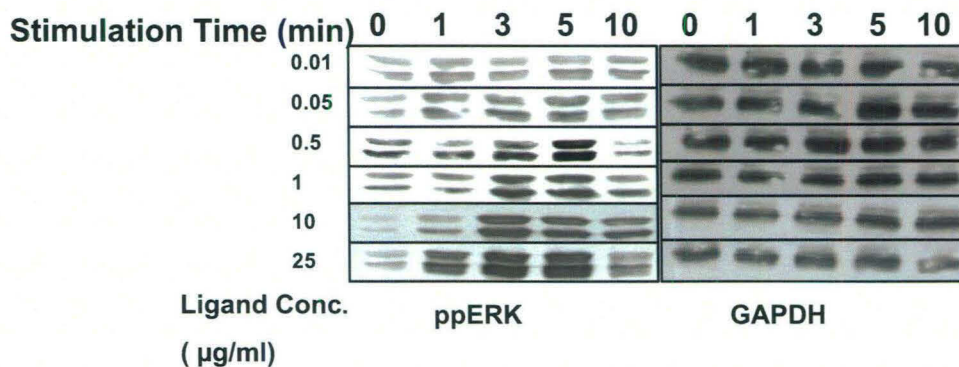
Figure 13. Panel A shows the Western blot profile of MEK in A20 cells treated either with non-silencing (GFP) siRNA (labeled Normal), or with MKP3-specific siRNA. In both cases the cells were stimulated with the F(ab)₂ fragment of anti-mouse IgG for the indicated times. For quantification band intensities were normalized against that obtained for PLCg, which was used as loading control. **Panel B** shows the stimulation time-dependent phosphorylation profiles of ERK (ppERK) in either treated cells, or in cells pre-treated with DRB. GAPDH (Ctrl) served as the loading control for band intensity normalization in these experiments. Shown in **Panel C** are the time dependent phosphorylation profiles of ERK (ppERK) at the indicated concentrations of ligand. Here again, GAPDH was used for the loading control and for normalization of band intensities.
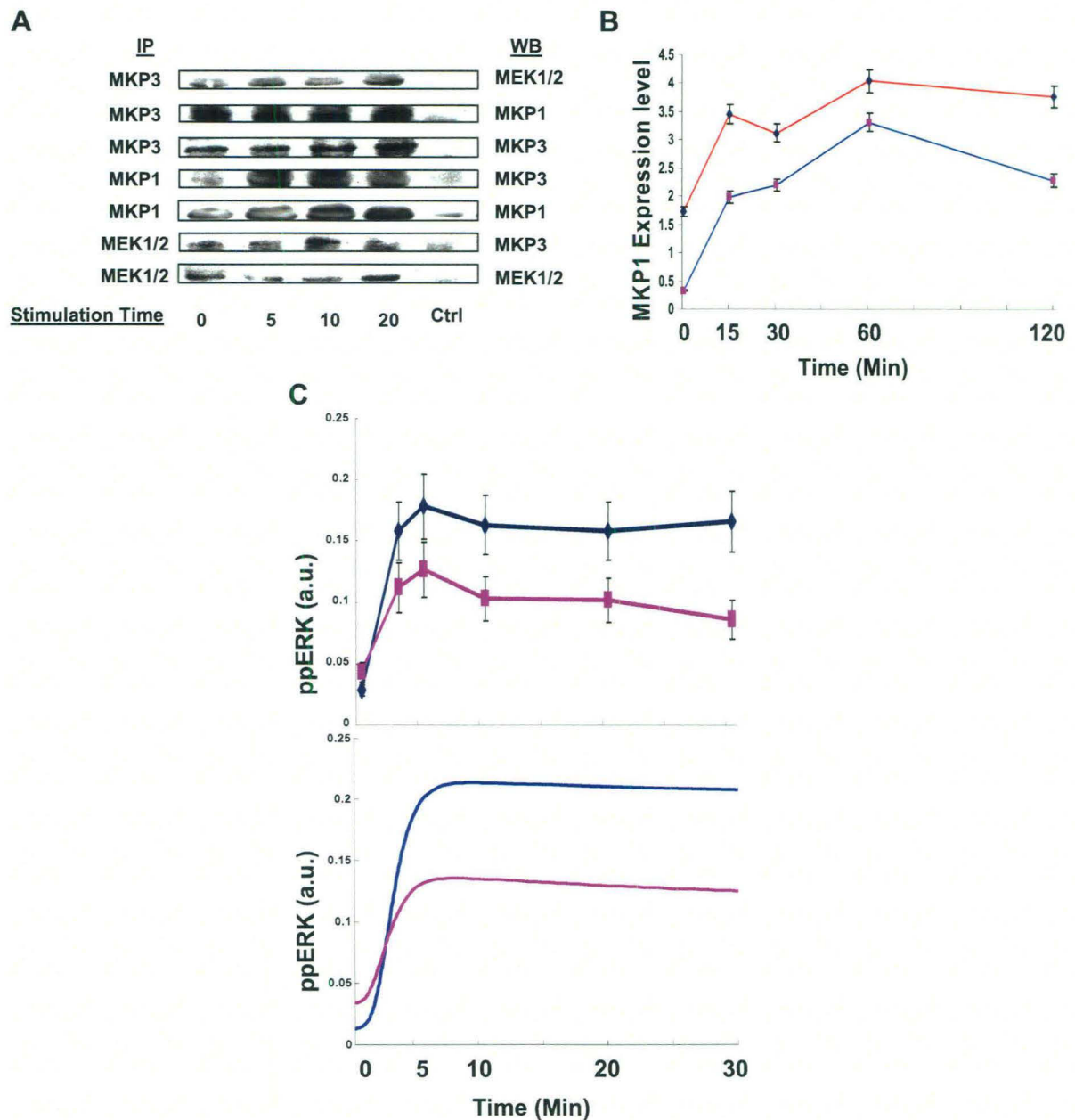
Figure 14: Verification of novel interactions incorporated in the model

In panel A, lysates from stimulated or unstimulated A20 cells were immunoprecipitated with antibodies specific either for MKP3, MEK, or MKP1 (Materials and Methods) (left column, IP). Immunoprecipitates were then subjected to a Western blot analysis using the antibodies indicated in the right column (WB). As a negative control (ctrl), parallel immunoprecipitates with rabbit IgG were also probed with the corresponding antibodies.

Panel B shows the results of Western blot analyses for MKP1 in A20 cells treated either with MKP3-specific siRNA (red line), or with non-silencing (i.e. GFP-specific) siRNA (blue line). Stimulation times with anti-IgG (25 µg/ml) are indicated, and values are the mean ± S.D. of three separate experiments. We have previously demonstrated that siRNA-mediated silencing of MKP3 results in a >70% reduction of this phosphatase protein in A20 cells(Kumar et. al., 2008).

In Panel C the top panel shows the effect of DRB (30µM) on the anti-IgG dependent phosphorylation of ERK. The lower panel shows the corresponding profiles obtained from an *in-silico* analysis. The blue color identifies the profiles obtained in the absence of any inhibitor, whereas the pink color denotes the profiles obtained in the presence of DRB.

depicted in Figure 9B. In subsequent experiments we observed that the siRNA-mediated depletion of MKP3 resulted in a significant (~ 4-fold) increase in the basal levels of MKP1 (Fig. 13A and 14B). These levels were further increased upon stimulation of cells through the BCR (Fig. 14B). The stability of intracellular MKP1 is dictated by its phosphorylation status. While the non-phosphorylated form exhibits a short half-life, phosphorylation enhances its stability (Brondello et al., 1999). Thus the observed inverse relationship between MKP3 and MKP1 levels in Figure 14B provides additional support for the functional nature of the link between these two phosphatases.

To verify whether the phosphorylation status of MKP3 indeed modulated its substrate-specificity, we also examined anti-IgG-mediated stimulation of A20 cells in the presence of the CK2 inhibitor, DRB (Zandomeni et al., 1986). As shown in Figure 9B, MKP3 is primarily phosphorylated by CK2α. Inhibition of this kinase, therefore, leads to a concomitant inhibition of MKP3 phosphorylation (Castelli et al., 2004). According to our model then, this should then also result in an increased efficiency of MKP3-mediated dephosphorylation of ERK. As expected, stimulation of DRB-treated cells led to inhibition of BCR-dependent phosphorylation of ERK (Fig. 13 and 14C). These results are also consistent with previous findings that CK2α dependent phosphorylation of MKP3 attenuates its inhibitory effect on ERK phosphorylation (Castelli et al., 2004).

Collectively then, both the consistency between predicted and experimentally obtained phosphorylation profiles of the various signaling intermediates described above, as well as the experimental confirmation of the new MKP3-dependent regulatory links proposed, provide experimental support for the model depicted in Figure 9A.

Integration of the Phosphatase Cascade with the MAPK Pathway Leads to a Novel Signal Processing Function

Integration of the Phosphatase Cascade with the MAPK Pathway leads to a Novel Signal Processing Function

Signal-dependent assembly of the MAPK cascade into a unique regulatory module

According to the model in Figure 9B, each intermediate in the MAPK pathway was under the regulatory control of both the co-aligned, and its immediately upstream, phosphatase. Thus, MEK was regulated by both PP2A and MKP3, whereas ERK was regulated by MKP3 and MKP1 (Fig. 9B). The entire model consisted of links that collectively belonged to all of the four possible categories; activation of activator (PKC to Raf, and Raf to MEK), inhibition of activator (PP2A to Raf, and MKP3 to MEK), activation of inhibitor (PKC to MKP3, and ERK to MKP1), and inhibition of inhibitor (PP2A to MKP3 and MKP3 to MKP1, 2) (Fig. 9A, B).

A particularly striking aspect here was that co-alignment of the two cascades resulted in the generation of a novel regulatory motif that was composed of a contiguous set of two square units. The first of these consisted of Raf, MEK, PP2A, and MKP3 as the vertices, whereas the second unit involved MEK, ERK, MKP3, and MKP1 (Fig. 9B). Further, the linkage relationships between the corresponding vertices were also replicated (Fig. 9B). Interestingly, a closer inspection of this motif revealed that it was in fact composed of four smaller regulatory units (each triangle in the motif) that represented alternately placed type-2 coherent and incoherent feedforward loops (FFLs, defined as in (Alon, 2007a)). A more detailed analysis of these sub-structures, and their individual contributions to the overall properties of the parent motif is currently under way as a separate study. Here we focused solely on the role of the larger motif, in regulating signal processing by the MAPK cascade.

Assembly of this regulatory motif required two separate input signals originating from the BCR. The first of these was a PKC- and RasGTP-dependent AND gate that mediated Raf activation in a signal-dependent manner (Bhalla et al., 2002; Kolch, 2000). The second input signal was defined by the CK2α -dependent phosphorylation of MKP3 (Fig. 9B). It has previously been demonstrated that MKP3 and CK2α form a protein complex wherein CK2α specifically phosphorylates MKP3, with the corresponding

increase in ERK-2 phosphorylation (Castelli et al., 2004). As discussed later, the regulation of MKP3 between its phosphorylated and non-phosphorylated states has significant implications for signal processing by the MAPK pathway. Finally, phosphorylation of MKP1 by ERK was also a prerequisite for the assembly of this motif, signifying the importance of crosstalk between these two cascades in this process.

Phosphatase-mediated regulation of the ERK response

We first examined how the connected network of phosphatases influenced signal output from the MAPK module. This was achieved through *in silico* experiments examining the ligand dose-dependency of ERK phosphorylation, under conditions where the individual phosphatases were depleted one at a time. Figure 4 shows the results of these experiments where panel A depicts the profile obtained in the unperturbed condition. It is evident that, with the exception of PP1, no other phosphatase depletion had any significant effect on the proportional nature of ERK activation (Fig. 15), The observed effect of PP1 depletion is consistent with our earlier experimental findings involving depletion of this enzyme by siRNA. In these experiments, a marked decrease in the magnitude of ERK activation was obtained at the later time points (Kumar et al., 2008). Thus these results indicate that PP1 may play an important role in buffering the inactive pool of hyper-phosphorylated Raf, which is generated by activated ERK through a positive feedback loop, and Akt (Bhalla et al., 2002; Hatakeyama et al., 2003; Ueki et al., 1994).

Depletion of any of the remaining phosphatases resulted only in a modulation of the amplitude of ERK phosphorylation, with MKP1 depletion yielding the most pronounced effect (Fig. 15). Notable, however, were the qualitatively distinct effects seen upon depletion of the individual, MAPK-associated, phosphatases. Suppression of PP2A expression yielded a marginal effect on the shape of the dose response curve (Fig. 15), whereas that of MKP3 resulted in a diminished activation window for ERK due to a simultaneous increase in sensitivity to lower ligand concentrations, and a decrease in the peak level that was achieved (Fig. 15). In contrast, removal of MKP2 induced a comparable increase in both the upper and lower bounds of ERK activity (Fig. 15). Thus, selective depletion of each of the phosphatases exerted its own individual effect on the ligand-dependent dose-response profile of ERK activation.
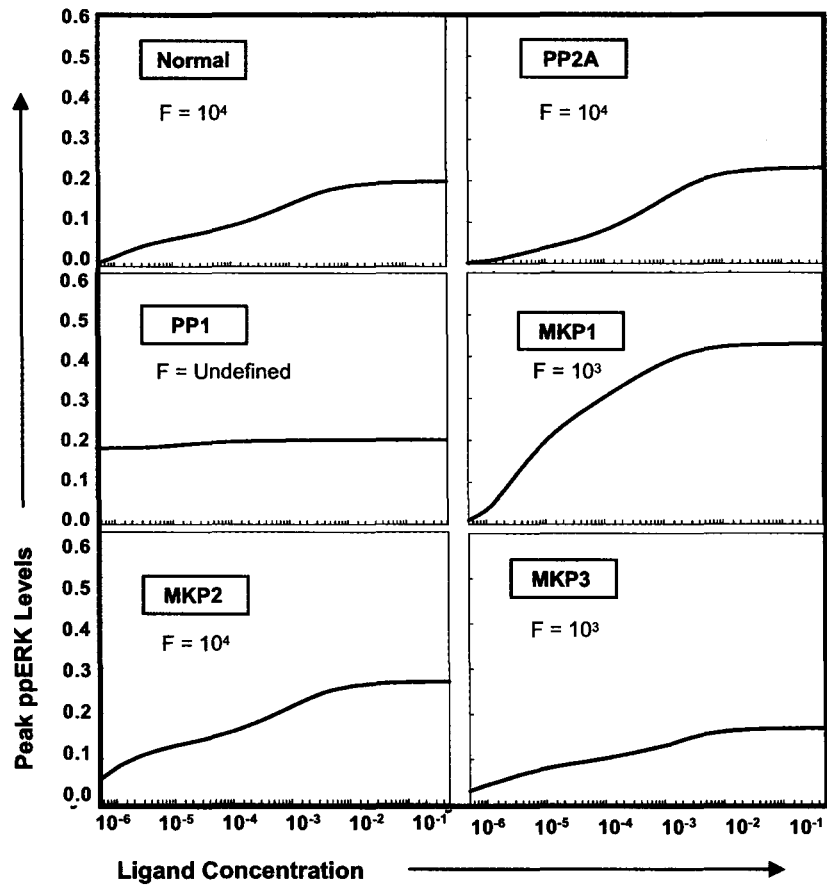
Figure 15: Phosphatase-mediated regulation of the MAPK signaling response.

The influence of individual phosphatases in sensitizing the ERK output was monitored *in-silico* by analyzing ligand dose versus peak phospho-ERK levels within the first 30 min of activation. This analysis was performed either in normal cells (Normal), or in cells where the indicated phosphatase was depleted from the system. In each panel, the fold change in ligand concentration required to increase ERK phosphorylation from 10% to 90% of its maximal value is also given (F). These values confirm that the ERK response remains proportional under all of these conditions.

Perturbation in phosphatase concentrations modulates the MAPK response

The output of a signaling network is primarily determined by the topology of the network, and the concentrations of its nodal constituents. As shown in Figure 15, the topological allocation clearly had a significant bearing in terms of defining the extent of regulation that each phosphatase exerted on the MAPK signaling pathway. We, therefore, next examined how variations in the concentration of these phosphatases would impact on BCR-initiated MAPK signaling. This involved *in silico* experiments in which the concentration of the individual phosphatase was varied from one that was ten-fold lower, to one that was ten-fold higher than its constitutive level in A20 cells. The phosphorylation of both MEK-1/2 and ERK were examined under these conditions.

While such experiments were also carried out for PP1 and MKP2 (Fig. 17), only the results obtained for the three phosphatases that are incorporated in the 'two-square' structural motif are shown in Figure 16. The figure describes the effect of varying the concentration of these individual phosphatases, on the peak levels of MEK and ERK phosphorylation. Of particular note here was the fact that changing PP2A concentrations exerted dissimilar effects on MEK and ERK. A bimodal effect was observed for MEK and this feature was retained at all strengths of signal (i.e. ligand doses) employed (Fig. 16). Contrary to this, ERK yielded a PP2A-dependent bimodal profile only at low ligand concentrations while the response to this phosphatase became linear as the signal strength was increased (Fig. 16). Thus, PP2A-mediated regulation imparted non-identical effects on these two – consecutively positioned - signaling intermediates of the MAPK pathway. Further, the extent of deviation in behavior between these two intermediates was also dependent upon the strength of the stimulus at the BCR. Increasing PP2A concentrations also led to a progressive reduction in the amplitude of both MEK and ERK responses although the effect on the latter molecule was more pronounced (Fig. 16). This aspect could be experimentally verified by stimulating A20 cells in the presence of the PP2A inhibitor okadaic acid (OA). Although OA is a known inhibitor of both PP2A and PP1, the 100-fold lower IC_{50} value for PP2A allowed us to use a concentration range that was specific for PP2A.

As shown in Figure 18, while inhibition of PP2A activity led to an increase in ERK phosphorylation, that of MEK was significantly inhibited. The sensitivity of ERK

31
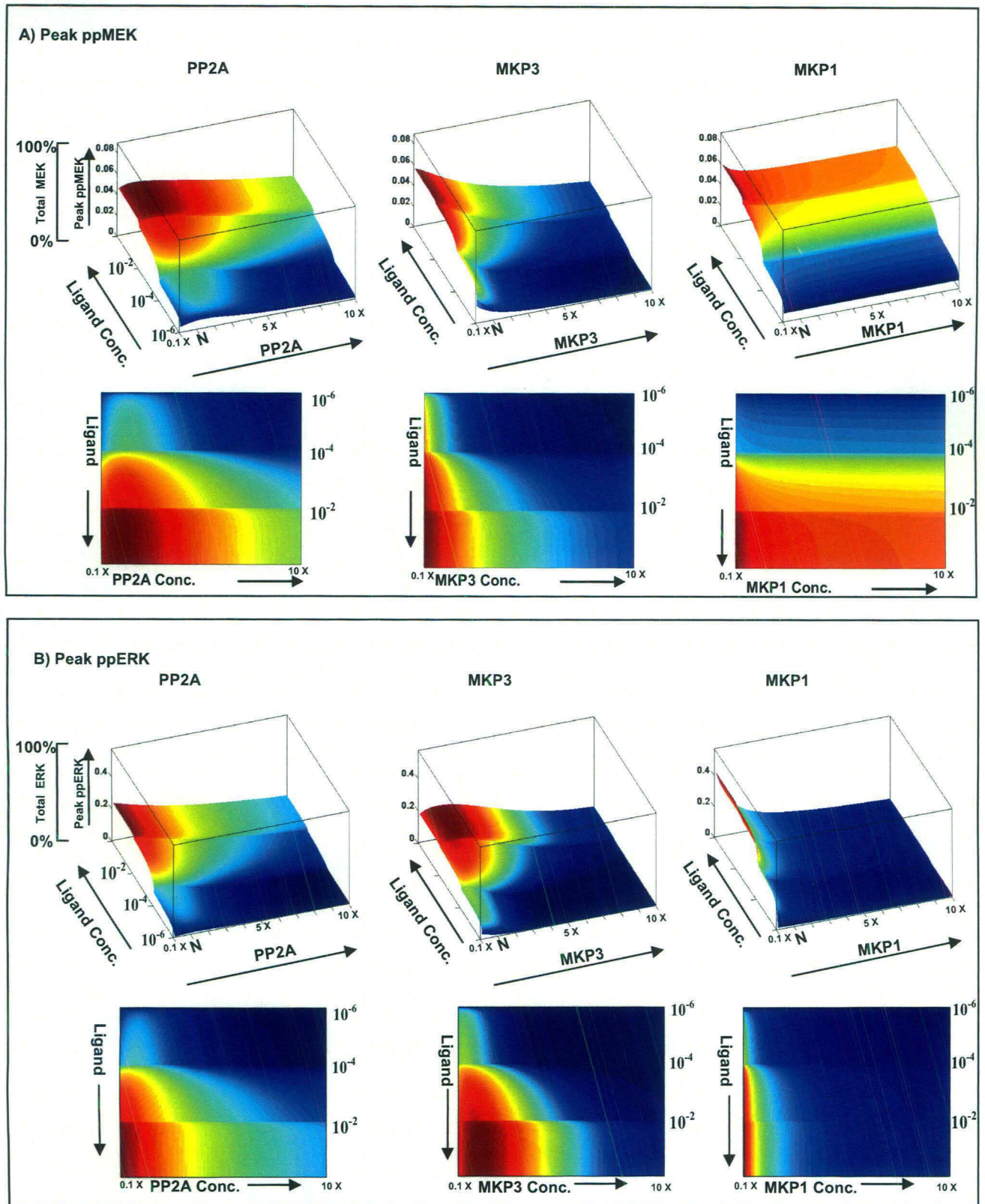
Figure 16: Modulation in phosphatase concentrations further shape ligand-sensitivity of the MAPK pathway.

Peak phosphorylation of ERK (ppERK) and MEK (ppMEK) was monitored in response to variations in both ligand and individual phosphatase concentrations. Three separate sets of simulation, within a defined concentration window, were used to reduce the computing time. For each phosphatase, 100 different concentrations of phosphatase were used, varying from 10 times lower to 10 times higher than its constituent concentration level in A20 cells. The combined data is plotted here. Panel A profiles peak phospho-MEK levels as a combined function of both varying ligand doses (Conc. in μM), and varying concentrations of each of the three phosphatases. Here, the top panel shows the 3-dimensional plot, while the lower panel depicts the same results in the form of a heat map. Similarly, panel B shows peak phospho-ERK levels as a combined function of both ligand dose and varying concentrations of the three phosphatases.
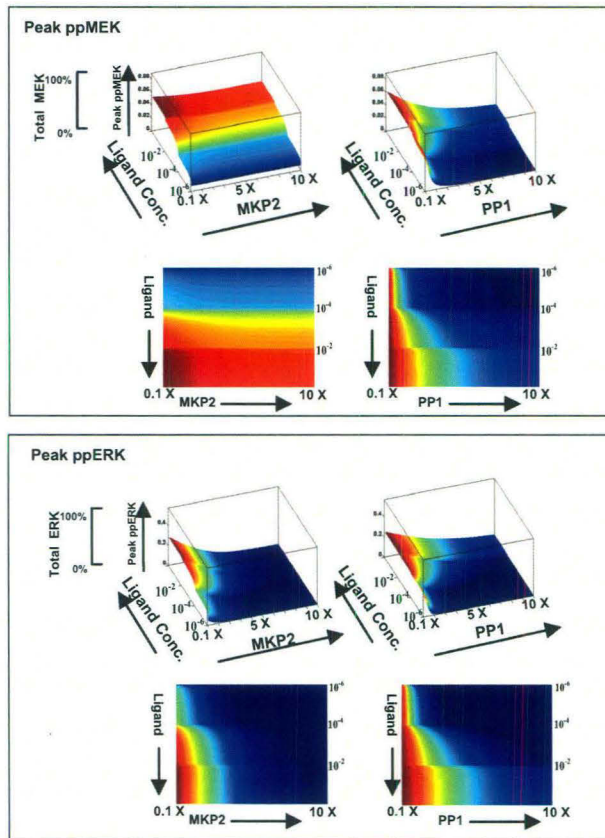
Figure 17: The peak phosphorylation of MEK (ppMEK, top subpanel) and ERK (ppERK, bottom subpanel) was determined in response to variations in concentrations of both ligand and either PP1 or MKP2. The remaining details are identical to that described for Figure16.
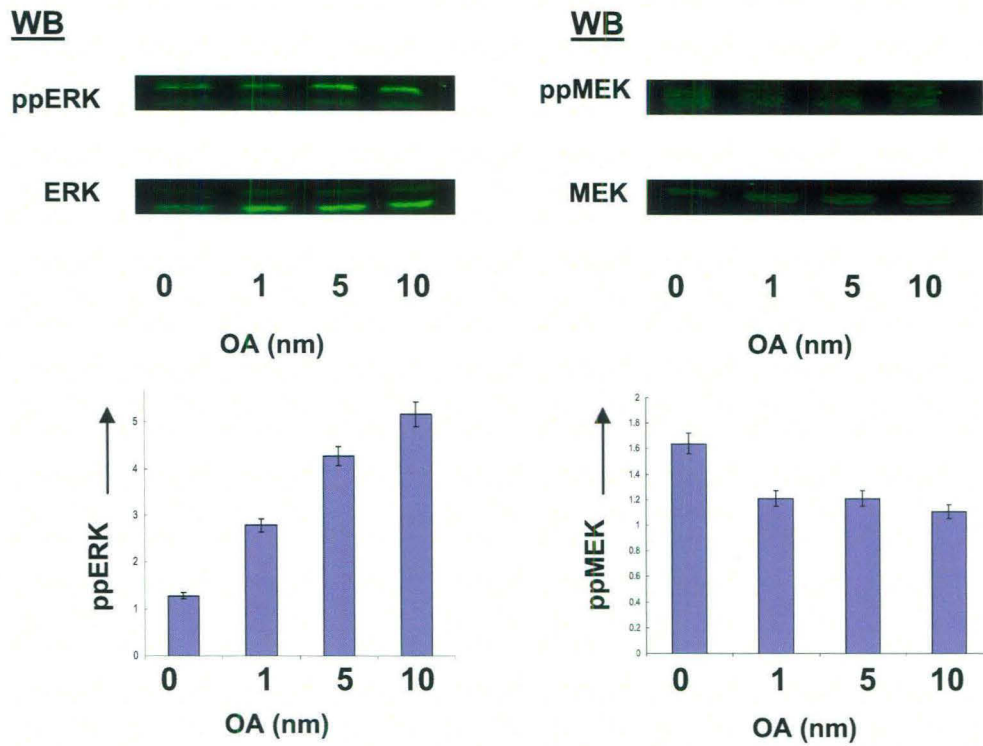
Figure 18: Shown here are the Western blots for phospho-ERK (ppERK) and phospho-MEK in cells treated with the indicated concentrations of Okadaic acid (OA). The bar plots show the quantitative variations, at 30 minutes after stimulation, obtained after normalization of each phospho-protein blot against that for the corresponding protein (i.e. ERK and MEK).

to PP2A activity likely derives from the concomitant decrease in the size of the pool of non-phosphorylated MKP3, as a result of decreasing PP2A levels. As discussed earlier, this would decrease the efficiency of MKP3-dependent dephosphorylation of ERK. In addition to this, however, a diminished pool of phospho-MKP3 would also imply a consequent reduction in the negative regulation of MKPI and, thereby, an increase in the MKP1-dependent inactivation of ERK.

In similar experiments where MKP3 concentrations were varied, we observed an inverse relationship between the amplitude of MEK phosphorylation and MKP3 concentrations. In contrast to this, ERK activation displayed a bell-shaped profile (Fig. 16). The curvature of the bell was, however, more pronounced at higher ligand concentrations supporting that ERK activation remained responsive to the strength of the stimulus. The bimodal effect of MKP3 on ERK activation again probably reflects the consequence of concentration-dependent shifts in the distribution of MKP3 between its phosphorylated and non-phosphorylated states. At low concentrations, the non-phosphorylated form of MKP3 would predominate due to the dominant action of PP2A. The increased specificity of this form for ERK can then explain the reduced levels of peak ERK phosphorylation. As MKP3 levels increase, however, the proportion of its phosphorylated form is also expected to increase. The consequences of this on ERK activation would then be defined by the balance of the effects of MKP3 on ERK, and that of phospho-MKP3 on MEK and MKP1 respectively. Thus, MKP3 negatively regulates ERK activity by ensuring its dephosphorylation. In contrast, phospho-MKP3 preferentially targets MEK and MKP1 but with opposing consequences. While MEK inactivation also inhibits transmission of signal to ERK, the dephosphorylation and consequent destabilization of MKP1 diminishes the negative regulation of ERK by this enzyme. It is the quantitative shifts in balance between these distinct activities that would then shape the ERK response to variations in MKP3 concentrations.

Consistent with expectations, increasing MKP1 levels led to a steep decline in peak levels of ERK phosphorylation whereas the effect on MEK was only marginal (Fig. 16). Thus the cumulative results in Figure 16 emphasize that signal-dependent formation of the "two-square" motif enables tight regulation of the MAPK signaling by the associated phosphatases. Importantly, both quantitative and qualitative aspects of signal transmission between two consecutive nodes were selectively influenced, thereby,

providing a mechanism by which signal transmission at the MEK/ERK interface could be further calibrated.

The phosphatase axis orients signal processing by the MAPK module

Concentrations of phosphatases frequently vary from one cell type to another. Further, even within a given cell type, either differences in environmental conditions (histories of stimulus) and/or developmental stages can lead to significant changes in intracellular phosphatase concentrations (Dickinson et al., 2002; Dickinson and Keyse, 2006; Echevarria et al., 2005). This is particularly true for MKP's in lymphocytes, where changes either in the activation or differentiation state of the cell can lead to marked alteration in the relative levels of this class of phosphatases (Dickinson and Keyse, 2006). Thus, given the high connectivity between the MAPK and the phosphatase cascade, it was reasonable to suspect that variations in the relative concentration or activity of the MAPK-associated phosphatases would have a significant impact on signal processing. To explore this we examined the consequences of simultaneously varying the concentration of any two of the three MAPK-associated phosphatases, while keeping the third at its constitutive level. The effects on the magnitude of peak phosphorylation of both MEK and ERK, at a fixed ligand dose, were monitored. All the three possible phosphatase combinations were tested, over a range of 10,000 different pairs – in a 100 x 100 matrix – of their respective concentrations. The range of phosphatase concentrations employed here was identical to that described for Figure 16.

Figure 19A depicts the results of such an exercise in which PP2A and MKP3 concentrations were varied, while keeping MKP1 at a fixed level. As shown, MEK activity yields a bell-shaped curve in the direction of increasing PP2A levels, although this profile tends to progressively 'flatten' as MKP3 concentrations also increase. While the inhibitory effect of MKP3 on MEK activation was monotonic it was, nonetheless, buffered at high PP2A concentrations (Fig. 19A). In other words, the relative concentrations of PP2A and MKP3 have a significant role to play in defining the sensitivity of MEK phosphorylation, to ligand-induced stimulation of cells. This was also true in the case of ERK although, here, a bimodal activation profile was obtained in the directions of both increasing PP2A and MKP3 concentrations. This latter observation suggests the existence of compensatory effects between these two phosphatases, whereby

Figure 19: Inter-phosphatase crosstalk regulates signal transmission through the MAPK pathway.
The effects of simultaneous variations in the concentration SAM-associated phosphatases on peak phospho-MEK (ppMEK) and peak phospho-ERK (ppERK) levels within a 30-minute activation window are shown here. A total of 100 different concentrations were employed for each phosphatase. These varied from 10 times lower, to 10 times higher than the constituent concentration in A20 cells. The three combinations shown here are MKP3-PP2A (A), MKP3-MKP1 (B) and PP2A-MKP1 (C). In each case the top panel shows peak phospho-MEK levels, while the lower panel shows peak phospho-ERK responses. The left and the right panels depict the 3-dimensional landscape, and the corresponding heat-map representation respectively. The corresponding profiles for the remaining components of the module that are also regulated by phosphorylation (i.e. Raf, MKP1, and MKP3) are shown in Figure 20.

Figure 20: This Figure represents a part of the experiment performed in Figure 19. Shown here are the effect of variation in concentrations of the indicated phosphatase pairs on peak phosphorylation levels of Raf (pRaf), MKP1 (pMKP1), and MKP3(pMKP3). It is notable that, as per our expectations from the model in Figure 1A, the amplitude of Raf phosphorylation is only weakly sensitive to changes in concentration of PP2A. According to our model, the effect of altered PP2A levels is buffered by the excess of available PP1.(In all cases arrows showing minimum to maximum conc. of the corresponding enzymes)

multiple combinations of their respective concentrations yield the same level of peak ERK activity.

Figure 19B shows the results of a similar experiment where the concentrations of MKP3 and MKP1 were varied, under conditions where PP2A levels were kept constant. As may be expected, variations in MKP1 concentrations exerted little or no effect on peak MEK activity and the resulting landscape was heavily biased in favor of the concentration-dependent inhibitory effects of MKP3. In contrast, a bimodal activation curve was again observed for ERK along the MKP3 axis. The curvature of this profile, however, was stringently controlled by MKP1, with ERK activation being completely inhibited even at moderately higher concentrations of this phosphatase (Fig. 19B).

Similar to the results in Figure 19A, varying combinations of PP2A and MKP1 also yielded a bimodal MEK profile in the direction of PP2A, but with a significant reduction in the phosphatase concentration window where at least detectable MEK activation was allowed (Fig. 19C). With the exception of attenuating the amplitude of MEK activation, varying MKP1 levels had little effect on the profile. Qualitatively similar effects were also noted for ERK where increasing MKP1 levels served to further exacerbate the inhibition of ERK activation that was observed as a function of increasing PP2A levels. However, here the inhibitory effect of MKP1 was far more pronounced (Fig. 19C). Thus, although the MAPK module functions as a proportional response system, these results emphasize that the net output is further specified by the relative concentrations of the individual MAPK-associated phosphatases that are present. In this connection, the assembly of these phosphatases into a regulatory axis is particularly relevant. As a result, variations in the concentration gradient along this axis exercise a combinatorial influence on signal processing by the MAPK pathway.

Finally, yet another intriguing feature revealed from a cursory examination of Figure 19 is the fact that the range of allowed concentration regimens of phosphatases was significantly more restricted for ERK than it was for MEK. This was generally true for all the three pairs of phosphatase combinations studied where the activation landscape for MEK was always larger in area than that obtained for ERK (Fig. 19). These observations suggest that the control exerted by the co-aligned phosphatase axis is further accentuated during transmission of signal from MEK to ERK, the effector molecule of the MAPK pathway.

Experimental support for a regulatory phosphatase axis

To confirm the above findings we examined - as a representative case - the consequences of experimentally modulating MKP3 levels, in conjunction with variations in the concentration of active PP2A. MKP3 levels in A20 cells were altered either through the use of specific siRNA, which reduces the amount of the protein by >70% (Kumar et al., 2007), or by stably over-expressing it in these cells to achieve a net two-fold increase in its concentration (Materials and Methods, Annexure S2). To modulate the concentration of active PP2A, we again employed its inhibitor OA. Thus, cells expressing either constitutive, reduced (through siRNA), or increased (through over-expression) levels of MKP3 were individually treated with varying OA concentrations, and each of these groups were then stimulated with a range of ligand (i.e. anti-IgG) doses. Peak phosphorylation levels of ERK were determined in each case, and the results obtained are presented in Figure 21 and 22.

We first compared these results with the predicted effects - on peak ERK phosphorylation - of varying levels of the individual phosphatases shown in Figure 16B. The panel 'a' in Figure 24A shows an expanded region of these predicted profiles obtained at the higher range of ligand doses, and over the estimated range of either MKP3 concentrations or PP2A activities employed in the present set of experiments (Figure 23). Panel 'b' of Figure 24A depicts the experimentally obtained results under these conditions. A high degree of correspondence between the simulated and the experimentally derived profiles is clearly evident here. This was equally true when peak ERK phosphorylation profiles in cells stimulated with sub-optimal doses of the ligand were compared (Fig. 24B). In addition to this, the data obtained in Figure 21 also served to substantiate the results of our *in silico* experiments describing the effects of simultaneously varying MKP3 and PP2A levels, on the magnitude of ERK phosphorylation (Fig. 19A). A comparison of results from the two approaches is shown in Figure 24C and D. Here, panel 'a' shows the results of our *in silico* analysis performed by employing either a high (Fig. 24C), or a suboptimal (Fig. 24D) concentration of ligand for cell stimulation. The corresponding profiles derived from our experimental data (Figure 21) are shown in panels 'b' of these figures. Again, a good correlation between results from the two approaches is clearly evident here.
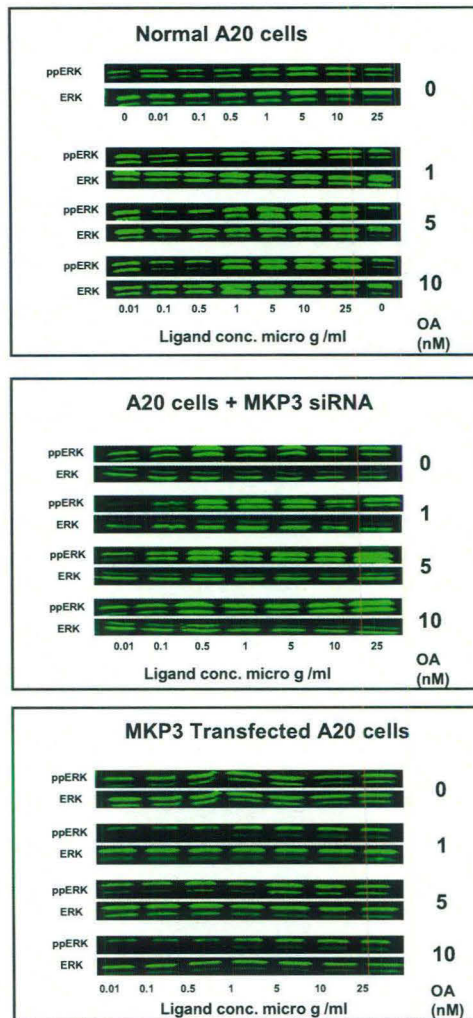
Figure 21:Ligand dose response of ERK phosphorylation to variations in levels of phosphatase activity. Shown here are the Western blot profiles for both the ERK protein, and its phosphorylated form in either normalA20 cells, in cells treated with MKP3 specific siRNA, or in cells transfected with an MKP3 bearing plasmid (see Experimental Procedures). For each group and condition, cells were stimulated with the indicated concentration of ligand, and the level of phosphorylation monitored 10 min later.
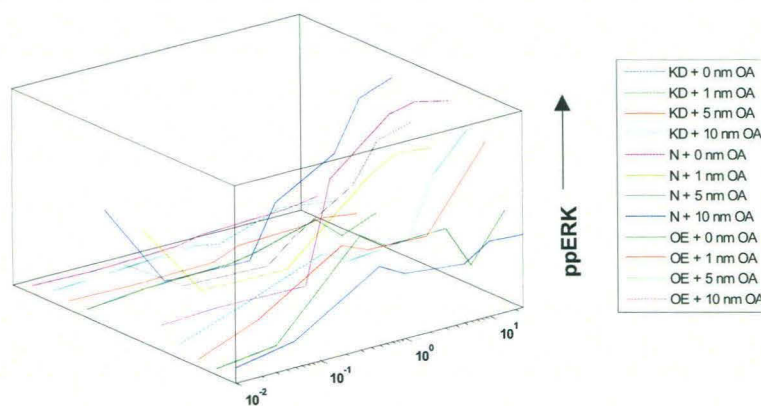
Figure 22: Modulation of dose response by varying phosphatase concentrations: Western Blots in Figure 21 were normalized and quantified using our toolbox (Gel-norm) as described earlier (Kumar et. al., 2007). The plot of these values are shown here.
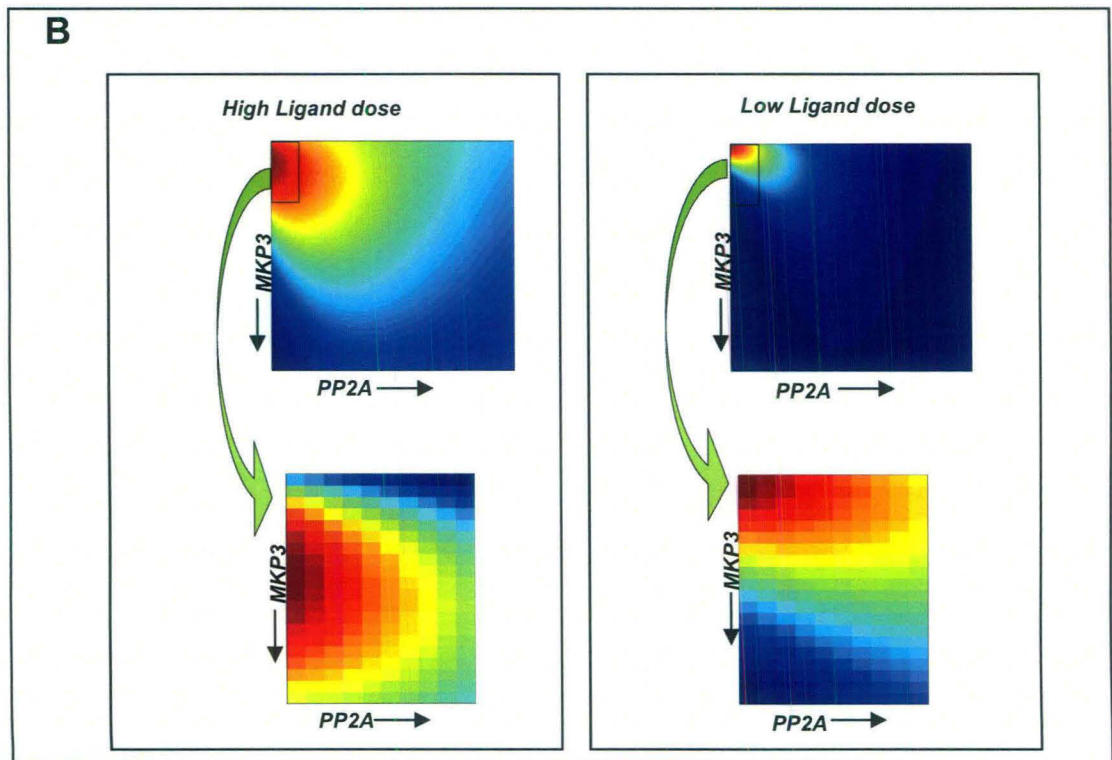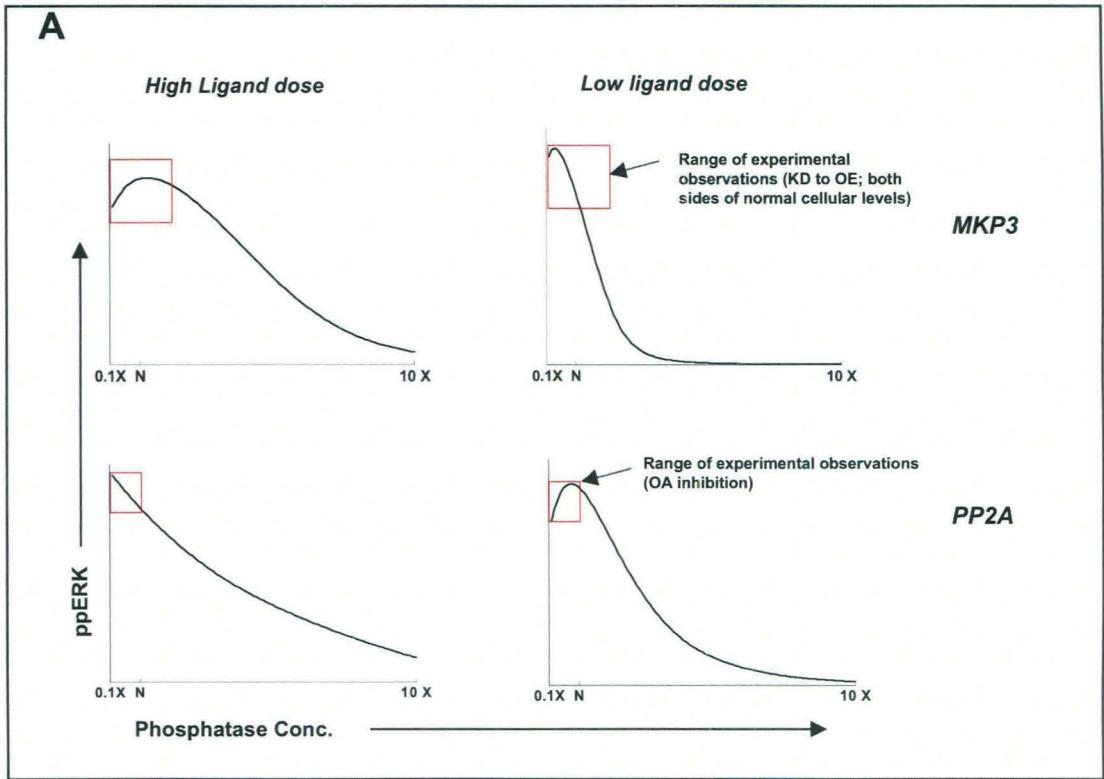
Figure 23. Panel A of this figure gives the simulated profile of peak phospho-ERK (ppERK) levels under conditions where concentrations of either MKP3 or PP2A ranged from 10-fold lower, to 10-fold higher than their respective levels in A20 cells. ERK phosphorylation responses at both high and low ligand doses are shown here. In each profile the boxed region indicates the concentration (for MKP3), or activity (for PP2A) range that was taken for the experiments described in Figure 24A and B.

Panel B shows the results of a simulation experiment where peak phospho-ERK responses were monitored under conditions where the concentrations/activities of both phosphatases were derived from the same range as described for Panel A. Here again, results obtained at high and low ligand doses are shown. The top part of this panel gives the results obtained over all the combinations of PP2A and MKP3 concentrations tested, and the boxed region identifies the range represented by the experiments in Figure 24C and D. The lower part of this panel shows a magnification of this boxed region.
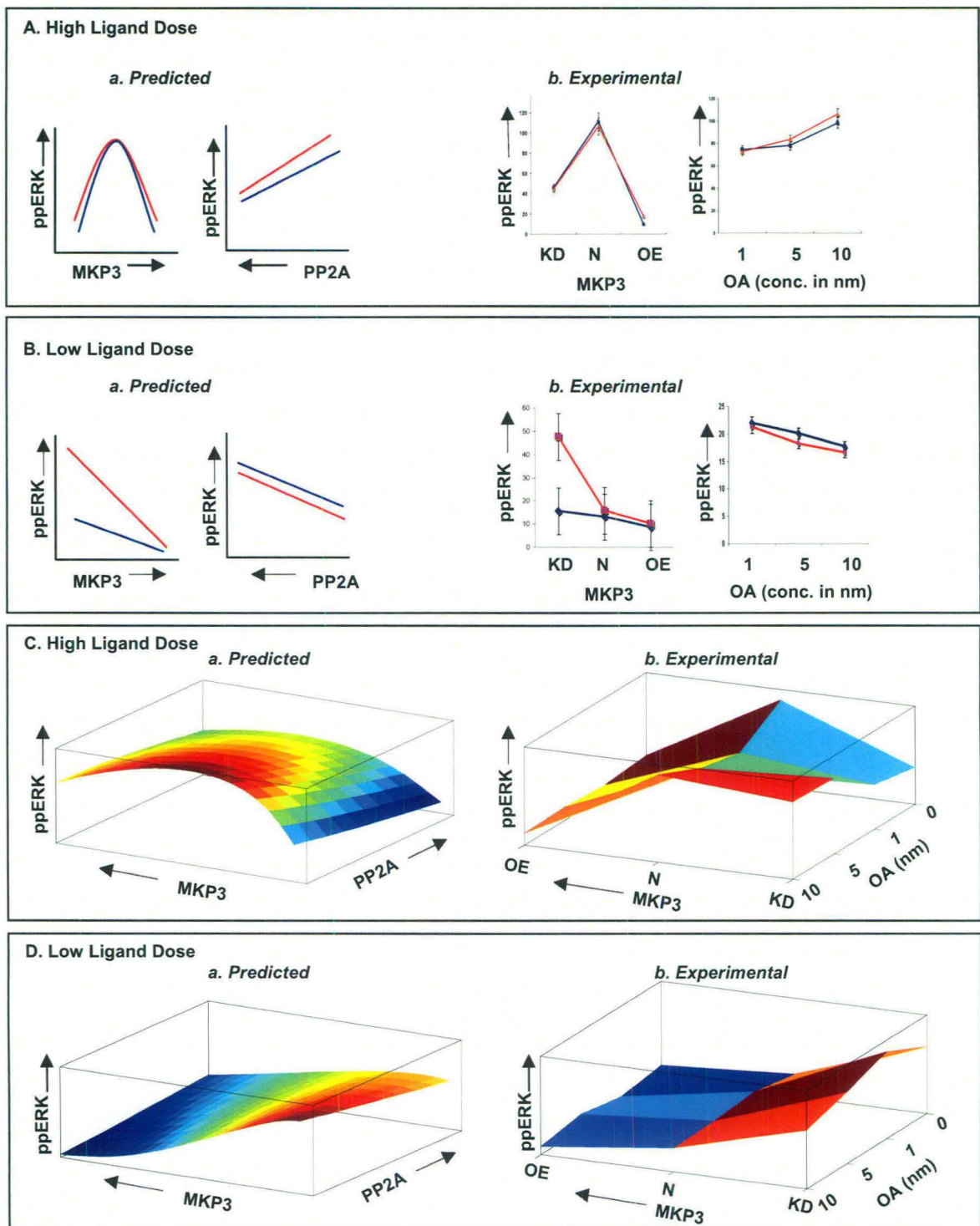
Figure 24: Experimental confirmation of the systems properties of the MAPK-associated regulatory module.

Panels A and B depict ERK phosphorylation levels obtained as a function of changes either in MKP3 or PP2A concentrations as described in the text. For the profiles obtained *in silico* (Predicted), the concentration ranges utilized is described in Figure 23, whereas the extent of variation in phosphatase concentration/activity obtained experimentally (Experimental) is described in the text. The anti-IgG concentrations employed for the experiment in panel A were 10 (red line) and 25 (blue line) µg/ml; whereas for panel B it was 0.05 (blue line) and 0.5 (red line) µg/ml.

Panels C and D describe the effects of combined variations in levels/activities of both MKP3 and PP2A, on the magnitude of ERK phosphorylation. Here again a comparison between the *in silico* (Predicted), and the experimentally (Experimental) obtained results is shown. Although a similarity in profiles between the two groups is clearly evident, the absence of a higher degree of concordance was primarily due to the limited number of data points in the experimental group. As described in the text, MKP3 levels were varied in the Experimental sets either through specific depletion by siRNA (KD), or by over-expression (OE).

Thus by verifying the accuracy of the resulting predictions, the data in Figure 24 support the fidelity of the model described in Figure 9A. In addition, these findings also firmly establish the role played by the co-associated phosphatase axis, in terms of further calibrating the stimulus-dependent responsiveness of the MAPK pathway.

Discussion

The prototypic Mitogen Activated Protein Kinase (MAPK) pathway consists of a three-tiered module composed of a MAPK (ERK-1/2), which is activated via phosphorylation by a MAPKK (MEK-1/2), which in turn is phosphorylated by a MAPKKK (Raf). This pathway exists in all eukaryotic organisms and controls fundamental cellular processes such as proliferation, differentiation, migration, survival, and apoptosis (Chang and Karin, 2001; Cobb, 1999; Widmann et al., 1999). Importantly, the cascade arrangement of this module permits integration of a wide range of conserved cellular process, thereby enabling a precise control of the amplitude, kinetics, and duration of ERK-1/2 (ERK) activation. Several studies have documented that it is the ability to modulate these individual parameters of ERK activation that confers signaling specificity to this pathway, in terms of regulating the cellular response (Ebisuya et al., 2005; Friedman and Perrimon, 2006; Kolch et al., 2005; Tan and Kim, 1999).

The contrast between the apparent biochemical simplicity of this pathway, and the range of complex cellular functions that it controls, has prompted extensive investigations on the structure and regulation of this pathway. One approach towards this goal has been through computational modeling of this pathway. The earliest model by Huang and Ferrell demonstrated that ERK activation exhibited ultrasensitivity, and that this was primarily due to the distributive mechanism involved in the dual phosphorylation of ERK (Ferrell and Bhatt, 1997; Huang and Ferrell, 1996). Subsequent to these pioneering findings, an increasing number of models that have gained both in size and complexity have been developed over the years. The various aspects examined by these models include feedback cooperativity and inhibition, hysteresis, oscillations, Ras activation, scaffolding proteins, signal specificity and robustness among others (Das et al., 2009; Eungdamrong and Iyengar, 2007; Orton et al., 2005; Qiao et al., 2007). From the standpoint of input/output relationships, these models have provided important new insights on feedback, sequestration, and scaffolding influences on the ERK response (Bluthgen et al., 2006; Kholodenko, 2000; Levchenko et al., 2000; Locasale et al., 2007).

A less explored aspect of MAPK regulation, however, has been the role of phosphatases in regulating signal specificity (Raman et al., 2007). An earlier study by Bhalla and co-workers identified MAPK phosphatase (MKP) as the locus of flexibility

that regulated between monostable and bistable regimes of operation (Bhalla et al., 2002). More recently, the protein tyrosine phosphates (PTP) SHP-1 was shown to be critical for defining the ligand discrimination threshold of the ERK response in T lymphocytes (Altan-Bonnet and Germain, 2005). Nonetheless, in view of the multiple phosphatases known to be associated with components of the MAPK pathway, a more integrated view of how such phosphatases regulate input/output relationships is presently lacking.

Our earlier study in murine B lymphoma A20 cells had demonstrated that the B cell antigen receptor (BCR)-dependent phosphorylation profiles of all the three constituents of the MAPK module (i.e. Raf. MEK-1/2 and ERK-1/2) were profoundly influenced when cells were depleted of a range of cellular phosphatases by siRNA (Kumar et al., 2008). Interestingly, depending upon the phosphatase depleted, these effects were either positive or negative suggesting diverse modes of regulation. Therefore, in the present study, we integrated this experimental data with existing literature to generate a mathematical model for ERK phosphorylation. The resulting model revealed an additional level of regulation of the MAPK pathway, which was enforced through the parallel alignment of a cascade of phosphatases. Importantly, the crosstalk between the MAPK and the phosphatases cascade led to the assembly of a novel regulatory motif that enabled independent calibration of signal at each successive node. As a result signal transmission through the MAPK pathway was non-linear, leading to a combinatorial expansion of the landscape of potential output responses. Significantly, in addition to parameters such as signal strength and duration, the bounds of this landscape also incorporated variations in the relative levels (or, activities) of the associated phosphatases. Thus, our studies identify a novel processing principle as a result of which the signal output represents an integrated expression of the properties of the stimulus, and the phenotypic status of the cell.

The remarkable versatility of the MAPK module is evident from the fact that ERK activation can display a wide range of activity profiles depending on the interfaces that regulate signal transmission through this module. Thus depending on the cell type, ERK activation can be ultrasensitive, converting graded inputs into a digital output response (Orton et al., 2005).Embedding this pathway within a positive feedback loop can lead to a dramatic amplification of signal, and also endow it with both bistability and hysteresis (Bhalla et al., 2002). In contrast, a negative feedback loop combined with intrinsic ultrasensitivity brings about sustained oscillations in ERK phosphorylation

37

(Kholodenko, 2000; Qiao et al., 2007). The sensitivity of the MAPK pathway to the cellular milieu is further underscored by the fact that, under certain conditions, it can also function as a monostable system yielding a proportional output response at the level of ERK phosphorylation (Birtwistle et al., 2007; Santos et al., 2007). At least some of the determinants of the nature of input/output relationships identified so far are the concentration of MKPs (Bhalla et al., 2002) the concentration of the scaffolding proteins involved (Levchenko et al., 2000), and the extent of sequestration of ERK in a complex with its kinase, MEK (Bluthgen et al., 2006). In addition to defining the threshold between a switch-like versus a proportional response, these parameters also play a critical role in modulating the amplitude and kinetics of the output signal.

In the present case, the proportional nature of the input/output relationship – despite incorporating a distributive mechanism for the dual phosphorylation of ERK - appears to be combinatorially defined through the relative concentrations/activities of the MAPK pathway-associated phosphatases. Thus, *in silico* exercises involving select modulations in phosphatase concentrations yielded an enhanced slope for ERK activation under conditions where either PP1 or MKP3 levels were significantly increased (Figure 25). Alterations in levels of the MAPK pathway components had no such effect. Consistent with this is our experimental demonstration that siRNA mediated silencing of these individual phosphatases had a significant effect on the amplitude, the stability, the kinetics, and the baseline levels of ERK phosphorylation. A role for filtering spurious noise by MAPK-associated phosphatases has also been recently discussed (Locasale et al., 2007).

Our finding that phosphatase-dependent regulation of the MAPK pathway involves organization of the phosphatases into a co-aligned cascade was especially interesting. Traditionally, negative regulation of intracellular signal transduction is conceived to occur as a discrete set of localized interactions between a phosphatase and its target molecule, and a cascade organization for phosphatases has not been considered so far (Dickinson and Keyse, 2006; Keyse, 2000). Importantly, this co-alignment resulted in the formation of a novel regulatory module that was composed of a contiguous set of two square units with the MAPK constituents and the phosphatases PP2A, MKP3, and MKP1 constituting the vertices of these units. We have termed this novel signaling motif, induced upon BCR-dependent stimulation of cells, as the 'Signal Activated Motif' (SAM).

A

0.1 X
N
2X
3X
5X

PP1

PP2A

MKP1

MKP2

MKP3

Peak ppERK

Ligand Concentration ⟶

B

Peak ppERK

0.35
0.3
0.25
0.2
0.15
0.1
0.05
0

10^{-5} 10^{-4} 10^{-3}

Ligand Concentration ⟶
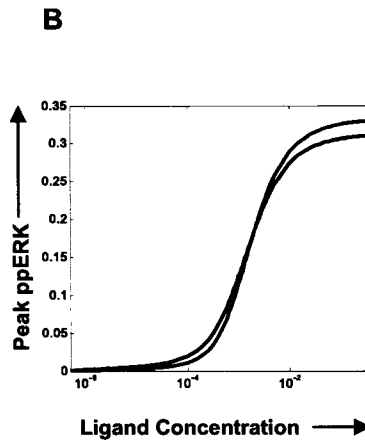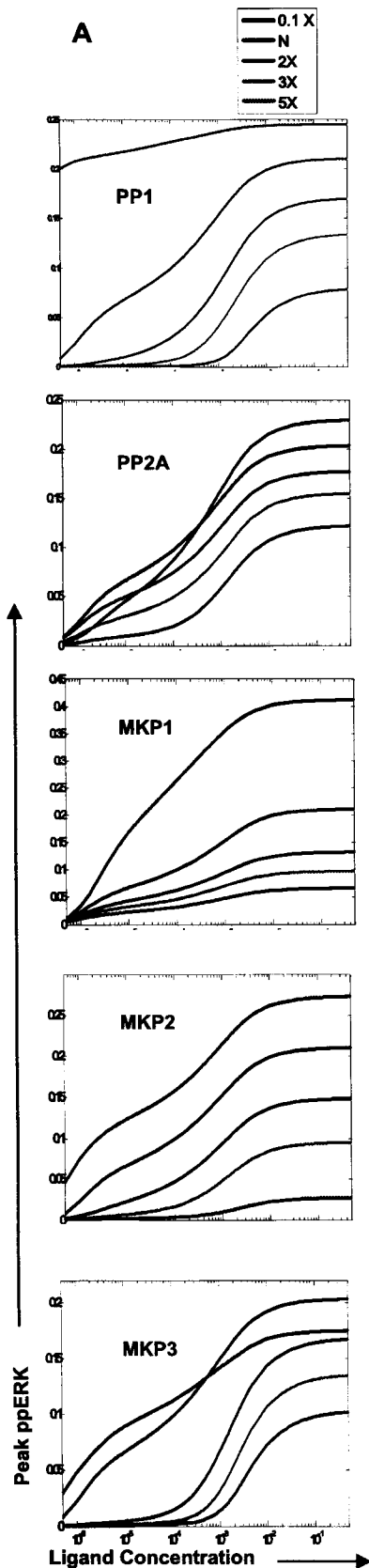
Figure 25. Panel A of this figure shows the effect of varying phosphatase concentrations on the ligand dose sensitivity of ERK phosphorylation. Here ERK phosphorylation was measured at 30 minutes of stimulation. Both the ligand dose (Conc. in μM) employed and the phosphatase concentrations tested, are indicated. A marked effect of phosphatase concentration on the dose response profile is clearly evident in all the cases. However only an increase in either PP1 or MKP3 levels led to sharp increase in the slope for ERK activation. Contrary to the findings for another cell line (Bhalla et. al., 2002), modulation of MKP1 concentrations did not yield an ultrasensitive response. This is probably because of the absence of the previously described feedback loop since cPLA2 is not expressed in mature lymphocytes. Finally, no trend towards ultrasensitivity could be detected upon varying the concentrations of the MAPK pathway constituents Raf, MEK, ERK.

Panel B shows the dose response profile for ERK phosphorylation obtained following a 3- fold increase in the concentration of either PP1 (blue line) or MKP3 (Green line) under conditions where the MKP1 levels was reduced by tenfold relative to the experimentally determined values in A20 cells. Thus the shape of the ERK output response to BCR stimulation clearly reflects a combinatorial outcome of the relative concentrations of the individual MAPK pathway-associated phosphatases

Assembly of the SAM involved two distinct input signals that, in turn, separately activated the functionally distinct components of the module. The first of these involved the combined action of PKC and RasGTP to activate Raf, thereby initiating signal flow through the MAPK cascade. The second signal, on the other hand, involved the CK2α - dependent phosphorylation of MKP3. This event was critical to the regulatory function of the phosphatase axis. Thus, while BCR activation activated signal flow through the MAPK pathway on the one hand, it also simultaneously embedded this pathway within a regulatory module so that the net signal output could be carefully regulated.

Central to the functioning of the SAM was the distribution of MKP3 between its phosphorylated and non-phosphorylated states where the balance between these two forms was defined by the reciprocal actions of the constitutively active PP2A, and the signal- activated CK2α. This segregation of input signals to activate both the positive and negative regulatory components of the SAM motif provided the mechanism by which filtration and appropriate calibration of the signal output could be achieved. Key to this was the differential substrate bias displayed by phosphorylated and non-phosphorylated MKP3, with the relative proportion of these two subsets being governed by the extent to which the input signal (i.e. activated CK2α) could buffer the action of PP2A. The conditional shifts in the equilibrium between these two pools played a critical role in defining the signal output in terms of the ERK activation profile. In other words, this ability to modulate substrate preferences enabled MKP3 to function as an additional response element for signal discrimination whereby both signal amplitude and sensitivity to ligand concentration could be further tuned.

Our subsequent analysis of how output responses were shaped by alterations in phosphatase concentrations also provided interesting new insights into the properties of the SAM. While MKP3 levels were important in defining the amplitude of ERK activation, it was the MKP1 concentrations that strictly defined the window of ERK activation. That output regulation involved the coordinated action of associated phosphatases was also emphasized in our studies examining the effect of simultaneously varying concentration of two phosphatases. For example, the available levels of the remaining two phosphatases further modulated the effects of varying MKP3 concentrations. This was equally true for PP2A and MKP1, thereby reaffirming the signal-dependent assembly of these phosphatases into a functional axis that intimately regulates signal processing.

The net outcome of the coordinated action of phosphatases was that information flow through the MAPK pathway did not occur in a linear fashion. Rather, signal was differentially processed at each intermediate in the pathway. Consequently, in addition to strength of the stimulus, transmission of signal between successive nodes was also rendered sensitive to the relative concentrations of the associated phosphatases. Thus, for example, conditions yielding a potent activation of MEK did not necessarily translate into a similar profile for ERK. Instead, signal transmission from MEK to ERK was additionally regulated by the activity and/or concentration of the two remaining phosphatase components of the SAM. The resultant combinatorial effects then ranged from a marked amplification, to a complete suppression, of ERK activation. Indeed even the limited investigations performed here reveal how the intricate coupling of a kinase with a phosphatase axis can provide for flexible regimes of regulation where the activity and/or concentrations of the participating phosphatases make key contributions to calibration of the signal output. A direct consequence of this was an expanded landscape of potential ERK responses where a given output characterized not only the strength of activating stimulus, but also the phenotypic state of the cell – at least when characterized in terms of the MAPK-associated phosphatase milieu.

Differences in the tissue-specific origin of cells are also often reflected at the level of differences in concentration of the individual MKPs. Similarly, variable MKP levels frequently characterize the individual stages of lineage commitment in lymphocytes (Bettini and Kersh, 2007). Further, even within a given cell type, activation of ERK leads to the upregulation of both MKP1 and MKP3 (Dickinson and Keyse, 2006), with the consequent de-sensitization of ERK to any further stimulation of the cell. Thus, the composition of at least MKPs within a cell may well provide a phenotypic description of its activation and/or differentiation status, which then is also incorporated when defining the ERK output response.

Thus, in summary, our present delineation of an emergent motif that endows the MAPK pathway with flexible regimes for modulating signal output provides additional insights into mechanisms that facilitate information processing by the signaling machinery. At one level, these findings reveal a novel organizational principle wherein a kinase cascade is intricately coupled to a regulatory cascade of phosphatases. The resulting structural motif that links each kinase intermediate to both the iso-stage, and the upstream phosphatase ensures that signal transmission is subjected to tight scrutiny at

every step of the pathway. This allows the 'strength' of the links between the phosphates axis and the kinase cascade to also function as determinants of signal processing. As a result, even a simple proportional response system becomes endowed with the ability to generate an output that, in addition to signal duration and strength, is also sensitized to variations in phosphatase concentrations and activities. As noted earlier, such variation could potentially encapsulate differences in the phenotypic status of cells either at the level of cell type, differentiation state, or, the history of prior stimulations. It, however, remains to be seen whether such a regulatory module is also associated with the other pathways of the signaling network.

Summary

The fundamental rules governing the context-specified transmission and processing of intracellular signals have continued to remain elusive. One approach to addressing this issue has been to decipher the organizational motifs that are present in the different levels of the structural and functional hierarchy within the signaling network.

In this thesis we combined our own experimental data with prior literature to generate a mathematical model for the MAP kinase pathway (MAPK). Importantly, our model focused on elaborating the role of cellular phosphatases in regulating the systems behavior of this module. Our completed network identified a unique structural motif with several novel functional properties. Significant here was our demonstration that phosphatases also assemble into regulatory cascades, much like their kinase counterparts in the signaling machinery. This highlights a novel dimension to the topology of the signaling network. As discussed below, this assembly of a functional phosphatase axis provides an additional level of resolution by which both the nature of the stimulus, as well as the cellular context in which the signal was received, are defined by the signal output.

The alignment of a phosphatase cascade in parallel with the MAPK pathway led to extensive crosstalk between these two components. As a result, each intermediate in the MAPK pathway was placed under the regulatory control of both the co-aligned, and its immediately upstream, phosphatase. It was these regulatory links between the twin cascades that enabled the recruitment of novel modes through which signal transmission by the MAPK pathway could be carefully scrutinized. The regulatory interactions between the two cascades resulted in the generation of a novel signaling motif that was composed of a contiguous set of two square units (Fig 19 B). The first of these consisted of Raf, MEK, PP2A, and MKP3 as the vertices, whereas the second unit involved MEK, ERK, MKP3, and MKP1. Intriguingly, the linkage relationships between the corresponding vertices were also replicated. The existence of such a network motif has not been reported for any biological system to date. However, in view of its potential significance, it is likely that such a motif also regulates other pathways within the signaling network. We have termed this novel structural motif, which is formed upon stimulation of cells through the receptor, as the 'Signal Activated Motif' (SAM).

Assembly of the SAM involved two distinct input signals that, in turn, separately activated the functionally distinct components of the module. The first of these signals involved the cooperative action of PKC and RasGTP to activate Raf, thereby initiating signal flow through the MAPK cascade. The second signal, on the other hand, involved the CK2α -dependent phosphorylation of MKP3, which then conferred the dynamic properties to the phosphatase cascade, to enable it to modulate functioning of the MAPK pathway. Thus, while receptor activation initiated signal flow through the MAPK pathway on the one hand, it also embedded this pathway within a regulatory module that enabled appropriate calibration of the eventual signal output.

The regulatory function of the SAM was activated through the CK2α-dependent phosphorylation of MKP3, resulting in the segregation of MKP3 into two separate pools represented by its phosphorylated and non-phosphorylated forms. Importantly, the equilibrium established between these two pools was modulated in a dynamic manner by the strength and duration of the activating stimulus. Central to the functioning of the SAM was our demonstration that phosphorylated and non-phosphorylated MKP3 exhibit distinct substrate specificities. While phosphor-MKP3 displayed a preference for MEK (i.e. MAP2K) and the downstream phosphatase MKP1, MKP3 selectively targeted the MAPK, ERK. In other words, the SAM was associated with structural plasticity wherein the topological features were dynamically defined by the strength and duration of the activating stimulus. Integrated to this was the fact that the MAPK pathway was also sensitized to the concentration and/or activity gradient along the co-aligned phosphatase axis. As a result, transmission of signal through each intermediate in the MAPK pathway was tightly calibrated through the combined effects of the strength and duration of stimulus, as well as the relative concentrations and/or activities of the associated phosphatase. This resulted in a non-linear transmission of signal through the intermediates of the MAPK pathway, thereby providing for an expanded landscape of potential output responses that reflected not only the characteristics of the activating signal, but also the phosphatase milieu in which this pathway was embedded. Variations in phosphatase concentrations/activities often identify alterations in the phenotypic status of the cell. This could be either at the level of cell type, its differentiation state, or, even in terms of variations in the history of past stimuli. In other words, the novel regulatory motif described here enabled the MAPK pathway to process input signals in a manner that specified not only the strength and duration of stimulus, but also the phenotypic status of the cell.

Although this study focused on the regulation of signaling by the MAPK pathway it is likely that the findings have broader implications with respect to functioning of the signaling machinery. At one level, our discovery that phosphatases also assemble into regulatory cascades provides a new perspective on the molecular mechanisms that contribute towards signal processing. In addition, description of the interaction between phosphates and kinase cascades - to ensure that signal calibration integrates the properties of the stimulus with the phenotypic context of the cell - represents the delineation of a novel processing principle.

References

Albert, R. (2007). Network inference, analysis, and modeling in systems biology. Plant Cell *19*, 3327-3338.

Aldridge, B. B., Burke, J. M., Lauffenburger, D. A., and Sorger, P. K. (2006). Physicochemical modelling of cell signalling pathways. Nat Cell Biol *8*, 1195-1203.

Alon, U. (2007a). Network motifs: theory and experimental approaches. Nat Rev Genet *8*, 450-461.

Alon, U. (2007b). Simplicity in biology. Nature *446*, 497.

Altan-Bonnet, G., and Germain, R. N. (2005). Modeling T cell antigen discrimination based on feedback control of digital ERK responses. PLoS Biol *3*, e356.

Angeli, D., Ferrell, J. E., Jr., and Sontag, E. D. (2004). Detection of multistability, bifurcations, and hysteresis in a large class of biological positive-feedback systems. Proc Natl Acad Sci U S A *101*, 1822-1827.

Arnette, D., Gibson, T. B., Lawrence, M. C., January, B., Khoo, S., McGlynn, K., Vanderbilt, C. A., and Cobb, M. H. (2003). Regulation of ERK1 and ERK2 by glucose and peptide hormones in pancreatic beta cells. J Biol Chem *278*, 32517-32525.

Barabasi, A. L., and Oltvai, Z. N. (2004). Network biology: understanding the cell's functional organization. Nat Rev Genet *5*, 101-113.

Barkai, N., and Leibler, S. (1997). Robustness in simple biochemical networks. Nature *387*, 913-917.

Bauman, A. L., and Scott, J. D. (2002). Kinase- and phosphatase-anchoring proteins: harnessing the dynamic duo. Nat Cell Biol *4*, E203-206.

Behar, M., Hao, N., Dohlman, H. G., and Elston, T. C. (2008). Dose-to-duration encoding and signaling beyond saturation in intracellular signaling networks. PLoS Comput Biol *4*, e1000197.

Benes, C., Roisin, M. P., Van Tan, H., Creuzet, C., Miyazaki, J., and Fagard, R. (1998). Rapid activation and nuclear translocation of mitogen-activated protein kinases in response to physiological concentration of glucose in the MIN6 pancreatic beta cell line. J Biol Chem *273*, 15507-15513.

Bettini, M. L., and Kersh, G. J. (2007). MAP kinase phosphatase activity sets the threshold for thymocyte positive selection. Proc Natl Acad Sci U S A *104*, 16257-16262.

Bhalla, U. S., and Iyengar, R. (1999). Emergent properties of networks of biological signaling pathways. Science *283*, 381-387.

Bhalla, U. S., Ram, P. T., and Iyengar, R. (2002). MAP kinase phosphatase as a locus of flexibility in a mitogen-activated protein kinase signaling network. Science *297*, 1018-1023.

Binder, B., and Heinrich, R. (2002). Dynamic stability of signal transduction networks depending on downstream and upstream specificity of protein kinases. Mol Biol Rep *29*, 51-55.

Birtwistle, M. R., Hatakeyama, M., Yumoto, N., Ogunnaike, B. A., Hoek, J. B., and Kholodenko, B. N. (2007). Ligand-dependent responses of the ErbB signaling network: experimental and modeling analyses. Mol Syst Biol *3*, 144.

Bishop, G. A., and Hostager, B. S. (2001). B lymphocyte activation by contact-mediated interactions with T lymphocytes. Curr Opin Immunol *13*, 278-285.

Bluthgen, N., Bruggeman, F. J., Legewie, S., Herzel, H., Westerhoff, H. V., and Kholodenko, B. N. (2006). Effects of sequestration on signal transduction cascades. Febs J *273*, 895-906.

Bluthgen, N., and Herzel, H. (2003). How robust are switches in intracellular signaling cascades? J Theor Biol *225*, 293-300.

Brondello, J. M., Pouyssegur, J., and McKenzie, F. R. (1999). Reduced MAP kinase phosphatase-1 degradation after p42/p44MAPK-dependent phosphorylation. Science *286*, 2514-2517.

Castelli, M., Camps, M., Gillieron, C., Leroy, D., Arkinstall, S., Rommel, C., and Nichols, A. (2004). MAP kinase phosphatase 3 (MKP3) interacts with and is phosphorylated by protein kinase CK2alpha. J Biol Chem *279*, 44731-44739.

Chan, A. C., Desai, D. M., and Weiss, A. (1994). The role of protein tyrosine kinases and protein tyrosine phosphatases in T cell antigen receptor signal transduction. Annu Rev Immunol *12*, 555-592.

Chang, L., and Karin, M. (2001). Mammalian MAP kinase signalling cascades. Nature *410*, 37-40.

Chow, L. M., and Veillette, A. (1995). The Src and Csk families of tyrosine protein kinases in hemopoietic cells. Semin Immunol *7*, 207-226.

Cobb, M. H. (1999). MAP kinase pathways. Prog Biophys Mol Biol *71*, 479-500.

Coughlin, J. J., Stang, S. L., Dower, N. A., and Stone, J. C. (2005). RasGRP1 and RasGRP3 regulate B cell proliferation by facilitating B cell receptor-Ras signaling. J Immunol *175*, 7179-7184.

Csete, M. E., and Doyle, J. C. (2002). Reverse engineering of biological complexity. Science *295*, 1664-1669.

Cyster, J. G. (1999). Chemokines and cell migration in secondary lymphoid organs. Science *286*, 2098-2102.

Das, J., Ho, M., Zikherman, J., Govern, C., Yang, M., Weiss, A., Chakraborty, A. K., and Roose, J. P. (2009). Digital signaling and hysteresis characterize ras activation in lymphoid cells. Cell *136*, 337-351.

Davidson, E. H., Rast, J. P., Oliveri, P., Ransick, A., Calestani, C., Yuh, C. H., Minokawa, T., Amore, G., Hinman, V., Arenas-Mena, C., et al. (2002). A genomic regulatory network for development. Science *295*, 1669-1678.

de Menezes, M. A., and Barabasi, A. L. (2004). Fluctuations in network dynamics. Phys Rev Lett *92*, 028701.

DeFranco, A. L. (1997). The complexity of signaling pathways activated by the BCR. Curr Opin Immunol *9*, 296-308.

Dhillon, A. S., Hagan, S., Rath, O., and Kolch, W. (2007). MAP kinase signalling pathways in cancer. Oncogene *26*, 3279-3290.

Dickinson, R. J., Eblaghie, M. C., Keyse, S. M., and Morriss-Kay, G. M. (2002). Expression of the ERK-specific MAP kinase phosphatase PYST1/MKP3 in mouse embryos during morphogenesis and early organogenesis. Mechanisms of Development *113*, 193-196.

Dickinson, R. J., and Keyse, S. M. (2006). Diverse physiological functions for dual-specificity MAP kinase phosphatases. J Cell Sci *119*, 4607-4615.

Dong, C., Davis, R. J., and Flavell, R. A. (2002). MAP kinases in the immune response. Annu Rev Immunol *20*, 55-72.

Dougherty, M. K., Muller, J., Ritt, D. A., Zhou, M., Zhou, X. Z., Copeland, T. D., Conrads, T. P., Veenstra, T. D., Lu, K. P., and Morrison, D. K. (2005). Regulation of Raf-1 by direct feedback phosphorylation. Mol Cell *17*, 215-224.

Ebisuya, M., Kondoh, K., and Nishida, E. (2005). The duration, magnitude and compartmentalization of ERK MAP kinase activity: mechanisms for providing signaling specificity. J Cell Sci *118*, 2997-3002.

Echevarria, D., Martinez, S., Marques, S., Lucas-Teixeira, V., and Belo, J. A. (2005). Mkp3 is a negative feedback modulator of Fgf8 signaling in the mammalian isthmic organizer. Developmental Biology 277, 114-128.

Eungdamrong, N. J., and Iyengar, R. (2007). Compartment-specific feedback loop and regulated trafficking can result in sustained activation of Ras at the Golgi. Biophys J 92, 808-815.

Ferrell, J. E., Jr. (2002). Self-perpetuating states in signal transduction: positive feedback, double-negative feedback and bistability. Curr Opin Cell Biol 14, 140-148.

Ferrell, J. E., Jr., and Bhatt, R. R. (1997). Mechanistic studies of the dual phosphorylation of mitogen-activated protein kinase. J Biol Chem 272, 19008-19016.

Friedman, A., and Perrimon, N. (2006). A functional RNAi screen for regulators of receptor tyrosine kinase and ERK signalling. Nature 444, 230-234.

Frodin, M., Sekine, N., Roche, E., Filloux, C., Prentki, M., Wollheim, C. B., and Van Obberghen, E. (1995). Glucose, other secretagogues, and nerve growth factor stimulate mitogen-activated protein kinase in the insulin-secreting beta-cell line, INS-1. J Biol Chem 270, 7882-7889.

Gibson, T. B., Lawrence, M. C., Gibson, C. J., Vanderbilt, C. A., McGlynn, K., Arnette, D., Chen, W., Collins, J., Naziruddin, B., Levy, M. F., et al. (2006). Inhibition of glucose-stimulated activation of extracellular signal-regulated protein kinases 1 and 2 by epinephrine in pancreatic beta-cells. Diabetes 55, 1066-1073.

Gilbert, J. J., Stewart, A., Courtney, C. A., Fleming, M. C., Reid, P., Jackson, C. G., Wise, A., Wakelam, M. J., and Harnett, M. M. (1996). Antigen receptors on immature, but not mature, B and T cells are coupled to cytosolic phospholipase A2 activation: expression and activation of cytosolic phospholipase A2 correlate with lymphocyte maturation. J Immunol 156, 2054-2061.

Gille, H., Kortenjann, M., Thomae, O., Moomaw, C., Slaughter, C., Cobb, M. H., and Shaw, P. E. (1995). ERK phosphorylation potentiates Elk-1-mediated ternary complex formation and transactivation. Embo J 14, 951-962.

Hasler, P., and Zouali, M. (2001). B cell receptor signaling and autoimmunity. Faseb J 15, 2085-2098.

Hatakeyama, M., Kimura, S., Naka, T., Kawasaki, T., Yumoto, N., Ichikawa, M., Kim, J. H., Saito, K., Saeki, M., Shirouzu, M., et al. (2003). A computational model on the modulation of mitogen-activated protein kinase (MAPK) and Akt pathways in heregulin-induced ErbB signalling. Biochem J 373, 451-463.

Heinrich, R., Neel, B. G., and Rapoport, T. A. (2002). Mathematical models of protein kinase signal transduction. Mol Cell 9, 957-970.

Hou, P., Araujo, E., Zhao, T., Zhang, M., Massenburg, D., Veselits, M., Doyle, C., Dinner, A. R., and Clark, M. R. (2006). B cell antigen receptor signaling and internalization are mutually exclusive events. PLoS Biol 4, e200.

Huang, C. Y., and Ferrell, J. E., Jr. (1996). Ultrasensitivity in the mitogen-activated protein kinase cascade. Proc Natl Acad Sci U S A 93, 10078-10083.

Ishiai, M., Kurosaki, M., Inabe, K., Chan, A. C., Sugamura, K., and Kurosaki, T. (2000). Involvement of LAT, Gads, and Grb2 in compartmentation of SLP-76 to the plasma membrane. J Exp Med 192, 847-856.

Ishiai, M., Kurosaki, M., Pappu, R., Okawa, K., Ronko, I., Fu, C., Shibata, M., Iwamatsu, A., Chan, A. C., and Kurosaki, T. (1999). BLNK Required for Coupling Syk to PLC³2 and Rac1-JNK in B Cells. 10, 117-125.

Jain, S., and Krishna, S. (2001). A model for the emergence of cooperation, interdependence, and structure in evolving networks. Proc Natl Acad Sci U S A 98, 543-547.

Janes, K. A., Albeck, J. G., Gaudet, S., Sorger, P. K., Lauffenburger, D. A., and Yaffe, M. B. (2005). A systems model of signaling identifies a molecular basis set for cytokine-induced apoptosis. Science *310*, 1646-1653.

Jumaa, H., Hendriks, R. W., and Reth, M. (2005). B cell signaling and tumorigenesis. Annu Rev Immunol *23*, 415-445.

Kachalo, S., Zhang, R., Sontag, E., Albert, R., and DasGupta, B. (2008). NET-SYNTHESIS: a software for synthesis, inference and simplification of signal transduction networks. Bioinformatics *24*, 293-295.

Kawakami, Y., Rodriguez-Leon, J., Koth, C. M., Buscher, D., Itoh, T., Raya, A., Ng, J. K., Esteban, C. R., Takahashi, S., Henrique, D., *et al.* (2003). MKP3 mediates the cellular response to FGF8 signalling in the vertebrate limb. Nat Cell Biol *5*, 513-519.

Keyse, S. M. (2000). Protein phosphatases and the regulation of mitogen-activated protein kinase signalling. Current Opinion in Cell Biology *12*, 186-192.

Kholodenko, B. N. (2000). Negative feedback and ultrasensitivity can bring about oscillations in the mitogen-activated protein kinase cascades. Eur J Biochem *267*, 1583-1588.

Khoo, S., and Cobb, M. H. (1997). Activation of mitogen-activating protein kinase by glucose is not required for insulin secretion. Proc Natl Acad Sci U S A *94*, 5599-5604.

Khoo, S., Griffen, S. C., Xia, Y., Baer, R. J., German, M. S., and Cobb, M. H. (2003). Regulation of insulin gene transcription by ERK1 and ERK2 in pancreatic beta cells. J Biol Chem *278*, 32969-32977.

Kitano, H. (2002). Systems biology: a brief overview. Science *295*, 1662-1664.

Kitano, H. (2007). Towards a theory of biological robustness. Mol Syst Biol *3*, 137.

Klaus, G. G., Choi, M. S., Lam, E. W., Johnson-Leger, C., and Cliff, J. (1997). CD40: a pivotal receptor in the determination of life/death decisions in B lymphocytes. Int Rev Immunol *15*, 5-31.

Kolch, W. (2000). Meaningful relationships: the regulation of the Ras/Raf/MEK/ERK pathway by protein interactions. Biochem J *351 Pt 2*, 289-305.

Kolch, W., Calder, M., and Gilbert, D. (2005). When kinases meet mathematics: the systems biology of MAPK signalling. FEBS Lett *579*, 1891-1895.

Krogh, A. (2008). What are artificial neural networks? Nat Biotechnol *26*, 195-197.

Kumar, D., Dua, R., Srikanth, R., Jayaswal, S., Siddiqui, Z., and Rao, K. V. (2008). Cellular phosphatases facilitate combinatorial processing of receptor-activated signals. BMC Res Notes *1*, 81.

Kumar, D., Srikanth, R., Ahlfors, H., Lahesmaa, R., and Rao, K. V. (2007). Capturing cell-fate decisions from the molecular signatures of a receptor-dependent signaling response. Mol Syst Biol *3*, 150.

Kurosaki, T. (1999). Genetic analysis of B cell antigen receptor signaling. Annu Rev Immunol *17*, 555-592.

Kurosaki, T. (2000). Functional dissection of BCR signaling pathways. Curr Opin Immunol *12*, 276-281.

Kurosaki, T. (2002). Regulation of B cell fates by BCR signaling components. Curr Opin Immunol *14*, 341-347.

Kurosaki, T., and Tsukada, S. (2000). BLNK: connecting Syk and Btk to calcium signals. Immunity *12*, 1-5.

Latour, S., and Veillette, A. (2001). Proximal protein tyrosine kinases in immunoreceptor signaling. Curr Opin Immunol *13*, 299-306.

Lawrence, M. C., McGlynn, K., Naziruddin, B., Levy, M. F., and Cobb, M. H. (2007). Differential regulation of CHOP-10/GADD153 gene expression by MAPK signaling in pancreatic beta-cells. Proc Natl Acad Sci U S A *104*, 11518-11525.

Lawrence, M. C., McGlynn, K., Park, B. H., and Cobb, M. H. (2005). ERK1/2-dependent activation of transcription factors required for acute and chronic effects of glucose on the insulin gene promoter. J Biol Chem *280*, 26751-26759.

Levchenko, A., Bruck, J., and Sternberg, P. W. (2000). Scaffold proteins may biphasically affect the levels of mitogen-activated protein kinase signaling and reduce its threshold properties. Proc Natl Acad Sci U S A *97*, 5818-5823.

Levenson, J. M., O'Riordan, K. J., Brown, K. D., Trinh, M. A., Molfese, D. L., and Sweatt, J. D. (2004). Regulation of histone acetylation during memory formation in the hippocampus. J Biol Chem *279*, 40545-40559.

Lewis, C. M., Broussard, C., Czar, M. J., and Schwartzberg, P. L. (2001). Tec kinases: modulators of lymphocyte signaling and development. Curr Opin Immunol *13*, 317-325.

Lewis, T. S., Shapiro, P. S., and Ahn, N. G. (1998). Signal transduction through MAP kinase cascades. Adv Cancer Res *74*, 49-139.

Locasale, J. W., Shaw, A. S., and Chakraborty, A. K. (2007). Scaffold proteins confer diverse regulatory properties to protein kinase cascades. Proc Natl Acad Sci U S A *104*, 13307-13312.

Lorenz, K., Schmitt, J. P., Schmitteckert, E. M., and Lohse, M. J. (2009). A new type of ERK1/2 autophosphorylation causes cardiac hypertrophy. Nat Med *15*, 75-83.

Ma'ayan, A., Jenkins, S. L., Neves, S., Hasseldine, A., Grace, E., Dubin-Thaler, B., Eungdamrong, N. J., Weng, G., Ram, P. T., Rice, J. J., *et al.* (2005). Formation of regulatory patterns during signal propagation in a Mammalian cellular network. Science *309*, 1078-1083.

Maekawa, M., Yamamoto, T., Tanoue, T., Yuasa, Y., Chisaka, O., and Nishida, E. (2005). Requirement of the MAP kinase signaling pathways for mouse preimplantation development. Development *132*, 1773-1783.

Maillet, M., Purcell, N. H., Sargent, M. A., York, A. J., Bueno, O. F., and Molkentin, J. D. (2008). DUSP6 (MKP3) Null Mice Show Enhanced ERK1/2 Phosphorylation at Baseline and Increased Myocyte Proliferation in the Heart Affecting Disease Susceptibility. J Biol Chem *283*, 31246-31255.

Malecki, M. T. (2005). Genetics of type 2 diabetes mellitus. Diabetes Res Clin Pract *68 Suppl1*, S10-21.

Mangan, S., and Alon, U. (2003). Structure and function of the feed-forward loop network motif. Proc Natl Acad Sci U S A *100*, 11980-11985.

Mansour, S. J., Matten, W. T., Hermann, A. S., Candia, J. M., Rong, S., Fukasawa, K., Vande Woude, G. F., and Ahn, N. G. (1994). Transformation of mammalian cells by constitutively active MAP kinase kinase. Science *265*, 966-970.

Markevich, N. I., Tsyganov, M. A., Hoek, J. B., and Kholodenko, B. N. (2006). Long-range signaling by phosphoprotein waves arising from bistability in protein kinase cascades. Mol Syst Biol *2*, 61.

Milo, R., Shen-Orr, S., Itzkovitz, S., Kashtan, N., Chklovskii, D., and Alon, U. (2002). Network motifs: simple building blocks of complex networks. Science *298*, 824-827.

Moretta, A., Bottino, C., Vitale, M., Pende, D., Cantoni, C., Mingari, M. C., Biassoni, R., and Moretta, L. (2001). Activating receptors and coreceptors involved in human natural killer cell-mediated cytolysis. Annu Rev Immunol *19*, 197-223.

Neves, S. R., Tsokas, P., Sarkar, A., Grace, E. A., Rangamani, P., Taubenfeld, S. M., Alberini, C. M., Schaff, J. C., Blitzer, R. D., Moraru, II, and Iyengar, R. (2008). Cell shape and negative links in regulatory motifs together control spatial information flow in signaling networks. Cell *133*, 666-680.

Noble, W. S. (2006). What is a support vector machine? Nat Biotechnol *24*, 1565-1567.

Oh-hora, M., Johmura, S., Hashimoto, A., Hikida, M., and Kurosaki, T. (2003). Requirement for Ras guanine nucleotide releasing protein 3 in coupling phospholipase C-gamma2 to Ras in B cell receptor signaling. J Exp Med *198*, 1841-1851.

Okada, T., Maeda, A., Iwamatsu, A., Gotoh, K., and Kurosaki, T. (2000). BCAP: the tyrosine kinase substrate that connects B cell receptor to phosphoinositide 3-kinase activation. Immunity *13*, 817-827.

Orton, R. J., Sturm, O. E., Vyshemirsky, V., Calder, M., Gilbert, D. R., and Kolch, W. (2005). Computational modelling of the receptor-tyrosine-kinase-activated MAPK pathway. Biochem J *392*, 249-261.

Oyadomari, S., Koizumi, A., Takeda, K., Gotoh, T., Akira, S., Araki, E., and Mori, M. (2002). Targeted disruption of the Chop gene delays endoplasmic reticulum stress-mediated diabetes. J Clin Invest *109*, 525-532.

Pappu, R., Cheng, A. M., Li, B., Gong, Q., Chiu, C., Griffin, N., White, M., Sleckman, B. P., and Chan, A. C. (1999). Requirement for B Cell Linker Protein (BLNK) in B Cell Development. Science *286*, 1949-1954.

Qiao, L., Nachbar, R. B., Kevrekidis, I. G., and Shvartsman, S. Y. (2007). Bistability and oscillations in the Huang-Ferrell model of MAPK signaling. PLoS Comput Biol *3*, 1819-1826.

Raman, M., Chen, W., and Cobb, M. H. (2007). Differential regulation and properties of MAPKs. Oncogene *26*, 3100-3112.

Ravasz, E., Somera, A. L., Mongru, D. A., Oltvai, Z. N., and Barabasi, A. L. (2002). Hierarchical organization of modularity in metabolic networks. Science *297*, 1551-1555.

Roberts, P. J., and Der, C. J. (2007). Targeting the Raf-MEK-ERK mitogen-activated protein kinase cascade for the treatment of cancer. Oncogene *26*, 3291-3310.

Rolink, A. G., Tschopp, J., Schneider, P., and Melchers, F. (2002). BAFF is a survival and maturation factor for mouse B cells. Eur J Immunol *32*, 2004-2010.

Rolli, V., Gallwitz, M., Wossning, T., Flemming, A., Schamel, W. W., Zurn, C., and Reth, M. (2002). Amplification of B cell antigen receptor signaling by a Syk/ITAM positive feedback loop. Mol Cell *10*, 1057-1069.

Roose, J. P., Mollenauer, M., Ho, M., Kurosaki, T., and Weiss, A. (2007). Unusual interplay of two types of Ras activators, RasGRP and SOS, establishes sensitive and robust Ras activation in lymphocytes. Mol Cell Biol *27*, 2732-2745.

Santos, S. D., Verveer, P. J., and Bastiaens, P. I. (2007). Growth factor-induced MAPK network topology shapes Erk response determining PC-12 cell fate. Nat Cell Biol *9*, 324-330.

Sasagawa, S., Ozaki, Y., Fujita, K., and Kuroda, S. (2005). Prediction and validation of the distinct dynamics of transient and sustained ERK activation. Nat Cell Biol *7*, 365-373.

Schmidt, T. G., and Skerra, A. (2007). The Strep-tag system for one-step purification and high-affinity detection or capturing of proteins. Nat Protoc *2*, 1528-1535.

Segre, D., Vitkup, D., and Church, G. M. (2002). Analysis of optimality in natural and perturbed metabolic networks. Proc Natl Acad Sci U S A *99*, 15112-15117.

Singh, D. K., Kumar, D., Siddiqui, Z., Basu, S. K., Kumar, V., and Rao, K. V. (2005). The strength of receptor signaling is centrally controlled through a cooperative loop between Ca2+ and an oxidant signal. Cell *121*, 281-293.

Stelling, J., Sauer, U., Szallasi, Z., Doyle, F. J., 3rd, and Doyle, J. (2004). Robustness of cellular functions. Cell *118*, 675-685.

Sumara, G., Formentini, I., Collins, S., Sumara, I., Windak, R., Bodenmiller, B., Ramracheya, R., Caille, D., Jiang, H., Platt, K. A., *et al.* (2009). Regulation of PKD by the MAPK p38′ in Insulin Secretion and Glucose Homeostasis. *136*, 235-248.

Tamir, I., and Cambier, J. C. (1998). Antigen receptor signaling: integration of protein tyrosine kinase functions. Oncogene *17*, 1353-1364.

Tan, P. B., and Kim, S. K. (1999). Signaling specificity: the RTK/RAS/MAP kinase pathway in metazoans. Trends Genet *15*, 145-149.

Tarakhovsky, A. (1997). Antigen receptor signalling in B cells. Res Immunol *148*, 457-460.

Thakar, J., Pilione, M., Kirimanjeswara, G., Harvill, E. T., and Albert, R. (2007). Modeling systems-level regulation of host immune responses. PLoS Comput Biol *3*, e109.

Turner, H., and Kinet, J. P. (1999). Signalling through the high-affinity IgE receptor Fc epsilonRI. Nature *402*, B24-30.

Ueki, K., Matsuda, S., Tobe, K., Gotoh, Y., Tamemoto, H., Yachi, M., Akanuma, Y., Yazaki, Y., Nishida, E., and Kadowaki, T. (1994). Feedback regulation of mitogen-activated protein kinase kinase kinase activity of c-Raf-1 by insulin and phorbol ester stimulation. J Biol Chem *269*, 15756-15761.

van Oers, N. S., and Weiss, A. (1995). The Syk/ZAP-70 protein tyrosine kinase connection to antigen receptor signalling processes. Semin Immunol *7*, 227-236.

Veillette, A., Latour, S., and Davidson, D. (2002). Negative regulation of immunoreceptor signaling. Annu Rev Immunol *20*, 669-707.

Ward, Y., Wang, W., Woodhouse, E., Linnoila, I., Liotta, L., and Kelly, K. (2001). Signal pathways which promote invasion and metastasis: critical and distinct contributions of extracellular signal-regulated kinase and Ral-specific guanine exchange factor pathways. Mol Cell Biol *21*, 5958-5969.

White, M. A., Nicolette, C., Minden, A., Polverino, A., Van Aelst, L., Karin, M., and Wigler, M. H. (1995). Multiple Ras functions can contribute to mammalian cell transformation. Cell *80*, 533-541.

Widmann, C., Gibson, S., Jarpe, M. B., and Johnson, G. L. (1999). Mitogen-activated protein kinase: conservation of a three-kinase module from yeast to human. Physiol Rev *79*, 143-180.

Yang, W. C., Collette, Y., Nunes, J. A., and Olive, D. (2000). Tec kinases: a family with multiple roles in immunity. Immunity *12*, 373-382.

Zandomeni, R., Zandomeni, M. C., Shugar, D., and Weinmann, R. (1986). Casein kinase type II is involved in the inhibition by 5,6-dichloro-1- beta-D-ribofuranosylbenzimidazole of specific RNA polymerase II transcription. J Biol Chem *261*, 3414-3419.

Zebisch, A., Czernilofsky, A. P., Keri, G., Smigelskaite, J., Sill, H., and Troppmair, J. (2007). Signaling through RAS-RAF-MEK-ERK: from basics to bedside. Curr Med Chem *14*, 601-623.

Zhao, Y., and Zhang, Z.-Y. (2001). The Mechanism of Dephosphorylation of Extracellular Signal-regulated Kinase 2 by Mitogen-activated Protein Kinase Phosphatase 3. J Biol Chem *276*, 32382-32391.

Zi, Z., Zheng, Y., Rundell, A., and Klipp, E. (2008). SBML-SAT: a systems biology markup language (SBML) based sensitivity analysis tool. BMC Bioinformatics *9*, 342.

Zuber, J., Tchernitsa, O. I., Hinzmann, B., Schmitz, A. C., Grips, M., Hellriegel, M., Sers, C., Rosenthal, /
and Schafer, R. (2000). A genome-wide survey of RAS transformation targets. Nat Genet 24, 144-152.

ANNEXURE
(Supplementary Information)

S1. Model Details

1.   Abbreviations
2.   Reactions and Reaction Rates
3.   Parameters

S2. Materials and Methods

1. Abbreviations:

Sr. No.	Abbreviations	InitialAmount	Names
1	L	**0.25**	Ligand
2	BCR	0.05	B Cell Receptor
3	L:BCR	0	Ligand bound to receptor pair, Crosslinkin of BCR and subsequent activation of ITAM
4	L:BCRp	0	Mono Phosphorylated Activated BCR
5	Lyn	0.24	Src Kinase Lyn
6	L:BCRp:Lyn	0	Lyn Bound ot the Monophosphorylated Receptor
7	Lynp	0	Activated Lyn
8	SHP1	0	Membrane localized SHP1
9	Lynp:SHP1	0	SHP1 bound to Lyn
10	Li	0	Inactivated ligand
11	BCRi	0	Inactivated or Internalized BCR
12	CD22	0.18	Membrane Anchored CD22
13	CD22p	0	CD22 activated
14	SHP1c	0.014	Cytosolic SHP1
15	CD22p:SHP1c	0	Cytosolic SHP1 bound to phosphorylated CD22
16	Syk	0.2	SYK kinase
17	Lynp:Syk	0	Activated Lyn bound to Syk
18	Sykp	0	Activated SYK
19	Sykp:SHP1	0	Activated Syk bound to SHP1
20	L:BCRp:Sykp	0	SYK kinase bound to Mono phosphorylated ITAM of ligand activated BCR
21	L:BCRpp	0	Completely activated BCR, ITAM's Phosphorylated at multiple sites
22	L:BCRpp:Lyn	0	Completely activated BCR bound to the Lyn
23	BCRpro	**0.05**	BCR precursor
24	L:BCR1	0	Ligand bound to receptor as non crosslinked form; Single BCR bound to single molecule of antigen
25	Btk	0	Bruton's Tyrosine Kinase
26	Btk:Lynp	0	Bruton's Tyrosine Kinase (Btk)bound to activated Lyn
27	Btkp	0	Activated Btk
28	Btk:Sykp	0	Btk bound to activated Syk
29	BtkPase	0.04	Btk phosphatase
30	Btkp:BtkPase	0	Btk bound ot Btk phosphatase
31	CD19	0.12	Membrane bound CD19
32	Lynp:CD19	0	Activated Lynp bound to CD19
33	CD19p	0	Activated CD19
34	p85PI3K	0.134	p85 subunit of Phosphoinositol-3 kinase
35	CD19p:p85PI3K	0	CD19p bound to p85subunit of PI3K
36	p110PI3K	0.134	p110 subunit of Phosphoinositol-3 kinase
37	PI3K	0	Complete holoenzyme PI3K
38	CD19p:p85PI3K:p110PI3K	0	CD19p bound to p85subunit and p110subunit of PI3K
39	BCAP	0.2	Membrane anchored B cell adopter protein for PI3K signaling
40	Sykp:BCAP	0	Sykp bound to BCAP
41	BCAPp	0	Phosphorylated BCAP
42	BCAPp:p85PI3K	0	Phosphorylated BCAP bound to p85 subunit of PI3K
43	BCAPp:p85PI3K:p110PI3K	0	Phosphorylated BCAP bound to p85 and p110 subunit of PI3K
44	Pase1	0.02	Phosphatase for BCAP
45	BCAPp:Pase1	0	Phosphatase for BCAP bound to BCAPp
46	PIP2	**10**	PIP2

47	PIP3	0	PIP3
48	Aktc	0.0058	Cytosolic Akt
49	Aktm	0	Membrane localized Akt
50	PIP3:Aktc	0	PIP3 bound to Akt
51	PDK	0.18	PDK kinase
52	PIP3:PDK	0	PIP3 bound to PDK
53	PDKa	0	Activated PDK
54	PDKa:Aktm	0	PDK bound to membrane localized Akt
55	Aktp	0	Akt phosphorylated
56	PP2A	0.0071	Protein Phosphatase 2 A
57	Aktp:PP2A	0	Akt phosphorylated bound to PP2A
58	BLNK	0.34	B cell Linker Protein BLNK
59	Sykp:BLNK	0	Sykp bound to BLNK
60	BLNKp	0	BLNK phosphorylated
61	BLNKp:Btkp	0	BLNKp bound to Btkp
62	Grb2	1	Adapter Protein Grb2
63	BLNKp:Grb2	0	BLNKp bound to Grb2
64	Pase2	0.01	Phosphatase 2
65	BLNKp:Pase2	0	Phosphatase 2 bound to BLNK
66	SoS	0.01	Son of Sevenless exchanger protein for GDP GTP excha
67	BLNKp:Grb2:SoS	0	Complete complex for lymphocyte RasGTP exchanger
68	PLCg	0.8	Phospholipase C gamma2
69	BLNKp:Btkp:PLCg	0	BLNKp bound to Btkp and PLCg
70	PLCgp	0	Phosphorylated PLCg
71	IP3	0	IP3
72	DAG	0	Diacyl glycerol
73	Pase3	0.02	Phosphatase 3
74	PLCgp:Pase3	0	PLCgp bound to Phosphatase3
75	ip3deg	0	IP3 degradation product
76	dagdeg	0	DAG degradation product
77	PKCcyt	0.7884	Cytosolic Protein kinase C
78	PKCcyt:DAG	0	PKC bound to DAG
79	PKCm	0	Membrane localized PKC
80	RasGDP	0.0454	Ras bound with GDP
81	RasGTP	0	Ras bound with GTP
82	GEF	0.01	Guanine exchange factor
83	GEFp	0	GEF phosphorylated
84	GEFp:RasGDP	0	GEFp bound to RasGDP
85	GEF:PKCm	0	GEF bound to PKC
86	GAP	0.002	GTPase activating Protein
87	PKCm:GAP	0	PKCm bound to the GAP
88	GAPp	0	GAP phosphorylated
89	PKCm:Sykp	0	Membrane localized PKC bound to Sykp
90	Sykpp	0	Inhibited Double phosphorylated Syk
91	GAP:RasGTP	0	GAP bound to RasGTP
92	Raf	0.0885	Raf
93	Raf:RasGTP	0	Raf bound to RasGTP
94	Raf:RasGTP:PKCm	0	RafRasGTP bound to PKC
95	Rafp	0	Raf phosphorylated
96	Rafser259	0	Raf phosphorylated at inhibitory serine259
97	Raf:Aktp	0	Raf bound to Akt
98	PP1	0.4748	Protein Phosphatase 1
99	Rafser259:PP1	0	RafSer259 bound to PP1
100	Rafp:Aktp	0	Rafp bound to Aktp

101	Rafpp	0	Raf double phosphorylated
102	Rafpp:PP1	0	Rafpp bound to PP1
103	Rafp:PP2A	0	Rafp bound to PP2A
104	Btkcyt	0.126	Btk cytoplasmic
105	Sykp:PLCg	0	Sykp bound to PLCg
106	Rafp:PP1	0	Rafp bound to PP1
107	MEK	0.0886	MEK kinase
108	Rafp:MEK	0	Rafp bound to MEK
109	MEKp	0	MEK phosphorylated
110	Rafp:MEKp	0	Rafp bound to MEKp
111	MEKpp	0	MEK double phosphorylated and completely activated form
112	CK2alpha	0.12	Casein kinase 2 Alpha
113	PKCm:CK2alpha	0	Membrane localized PKC bound to Casein kinase 2 alpha
114	CK2alphap	0	CK2alpha phosphorylated
115	MKP3	0.0015	DUSP6 of MAPkinase phosphatase3
116	CK2alphap:MKP3	0	CK2alpha phoaphorylated bound to MKP3
117	MKP3p	0	phosphorylated MKP3
118	MKP3p:PP2A	0	MKP3p bound to PP2A
119	MEKpp:PP2A	0	MEKpp bound to PP2A
120	MEKp:PP2A	0	MEKp bound to PP2A
121	MEKpp:MKP3p	0	MEKpp bound to MKP3p
122	MEKp:MKP3p	0	MEKpbound to MKP3p
123	ERK	0.5674	Extracellular signal regulated Kinase
124	ERK:MEKpp	0	ERK bound to MEKpp
125	ERKp	0	ERK phsophorylated
126	ERKp:MEKpp	0	ERKp bound to MEKpp
127	ERKpp	0	ERK double phosphorylated and completely activated form
128	mkp1	0.00005	MKP1 mRNA
129	MKP1	0.0002	MAPkinase phophatase 1
130	mkp3	0.000375	MKP3 mRNA
131	mkp1ubi	0	MKP1 degradation product
132	mkp3ubi	0	MKP3 degradation product
133	ERKpp:MKP1	0	ERKpp bound to MKP1
134	MKP1p	0	MKP1 phosphorylated
135	MKP1p:MKP3p	0	MKP1p bound to MKP3p
136	MKP2	0.002	MAPkinase phophatase 2
137	ERKpp:MKP2	0	ERKpp bound to MKP2
138	ERKp:MKP2	0	ERKp bound to MKP2
139	ERKpp:MKP3	0	ERKpp Bound to MKP3
140	ERKp:MKP3	0	ERKp bound to MKP3
141	TrCmplx	1	Transcriptional complex
142	Rafp:ERKpp	0	Rafp bound to ERKpp
143	Rafser259:PP2A	0	Rafser259 bound to PP2A
144	Rafpp:PP2A	0	Rafpp bound to PP2A
145	Rafp:RasGTP	0	RafpRasGTP complex
146	L:BCRp:SHP1	0	SHP1 bound to ITAM at the first phosphorylation site
147	L:BCRpp:SHP1	0	SHP1 bound to ITAM at other site which are later phosphorylated by Syk
148	ERKp:MKP1p	0	ERKpp bound to MKP1p
149	ERKpp:MKP1p	0	ERKp bound to MKP1p
150	MKP1:ERKpp	0	MKP1 bound to ERKpp
151	MKP1:ERKp	0	MKP1 bound to ERKp
152	TF	0.05	Trancription Factor
153	ERKpp:TF	0	ERKpp bound to TF
154	TFa	0	Transcription Factor activated

155	NT	**1**	Nucleotide representing DNA
156	TFa:NT	0	TFa bound to the DNA(Representing active transcription)
157	MKP3x	0	ERK mediated MKP3's phophorylated form prone to ubiquitination
158	MKP3:ERKpp	0	ERKpp bound to MKP3 where ERK is acting as an enzyme

All concentrations are in micromoles.

Initial amount in bold represents buffered/constant amount throughout the simulation

Lignad Unit conversion => 25 micro gram/ml ~= 0.05 micro moles
Concentrations of Raf, MEK, ERK, MKP1, PP2A, PP1, Akt,MKP2, RasGDP(total) are experimentally estimated. Rest of the concentrations are Estimated to best fit.

2. Reaction scheme and Reaction Rates:

	Reaction	Reaction Rate
1	L + BCR <-> [L:BCR1]	kon_1*L*BCR - koff_1*[L:BCR1]
2	[L:BCR] -> [L:BCRp]	kf_2*[L:BCR]/(0.25 + [L:BCR])
3	[L:BCRp] + Lyn <-> [L:BCRp:Lyn]	kon_3*[L:BCRp]*Lyn - koff_3*[L:BCRp:Lyn]
4	[L:BCRp:Lyn] -> [L:BCRp] + Lynp	kcat_4*[L:BCRp:Lyn]
5	Lynp + SHP1 <-> [Lynp:SHP1]	kon_5*Lynp*SHP1 - koff_5*[Lynp:SHP1]
6	[Lynp:SHP1] -> Lyn + SHP1	kcat_6*[Lynp:SHP1]
7	Lynp + CD22 -> Lynp + CD22p	vm_7*Lynp*CD22/(km_7+CD22)
8	CD22p + SHP1c <-> [CD22p:SHP1c]	kf_8*CD22p*SHP1c - kb_8*[CD22p:SHP1c]
9	[CD22p:SHP1c] -> CD22p + SHP1	kcat_9*[CD22p:SHP1c]
10	SHP1 -> SHP1c	kf_10*SHP1
11	CD22p -> CD22	kf_11*CD22p
12	Lynp + Syk <-> [Lynp:Syk]	kf_12*Lynp*Syk - kb_12*[Lynp:Syk]
13	[Lynp:Syk] -> Lynp + Sykp	kcat_13*[Lynp:Syk]
14	Sykp + SHP1 <-> [Sykp:SHP1]	kf_14*Sykp*SHP1 - kb_14*[Sykp:SHP1]
15	[Sykp:SHP1] -> Syk + SHP1	kcat_15*[Sykp:SHP1]
16	[L:BCRp] + Sykp <-> [L:BCRp:Sykp]	kf_16*[L:BCRp]*Sykp - kb_16*[L:BCRp:Sykp]
17	[L:BCRp:Sykp] -> [L:BCRpp] + Sykp	kcat_17*[L:BCRp:Sykp]
18	[L:BCRpp] + Lyn <-> [L:BCRpp:Lyn]	kf_18*[L:BCRpp]*Lyn - kb_18*[L:BCRpp:Lyn]
19	[L:BCRpp:Lyn] -> [L:BCRpp] + Lynp	kcat_19*[L:BCRpp:Lyn]
20	BCRpro -> BCR	kf_20*BCRpro
21	BCR -> BCRi	kf_21*BCR
22	2 [L:BCR1] <-> [L:BCR]	kon_22*[L:BCR1]^2 - koff_22*[L:BCR]
23	[L:BCR] -> BCRi + Li	kf_23*[L:BCR]
24	Btk + Lynp <-> [Btk:Lynp]	kf_24*Btk*Lynp - kb_24*[Btk:Lynp]
25	[Btk:Lynp] -> Btkp + Lynp	kcat_25*[Btk:Lynp]
26	Btk + Sykp <-> [Btk:Sykp]	kf_26*Btk*Sykp - kb_26*[Btk:Sykp]
27	[Btk:Sykp] -> Btkp + Sykp	kcat_27*[Btk:Sykp]
28	Btkp + BtkPase <-> [Btkp:BtkPase]	kf_28*Btkp*BtkPase - kb_28*[Btkp:BtkPase]
29	[Btkp:BtkPase] -> Btk + BtkPase	kcat_29*[Btkp:BtkPase]
30	Lynp + CD19 <-> [Lynp:CD19]	kf_30*Lynp*CD19 - kb_30*[Lynp:CD19]
31	[Lynp:CD19] -> Lynp + CD19p	kcat_31*[Lynp:CD19]
32	CD19p + p85PI3K <-> [CD19p:p85PI3K]	kf_32*CD19p*p85PI3K - kb_32*[CD19p:p85PI3K]
33	[CD19p:p85PI3K] + p110PI3K <-> [CD19p:p85PI3K:p110PI3K]	kf_33*[CD19p:p85PI3K]*p110PI3K - kb_33*[CD19p:p85PI3K:p110PI3K]
34	[CD19p:p85PI3K:p110PI3K] -> CD19p + PI3K	kcat_34*[CD19p:p85PI3K:p110PI3K]
35	Sykp + BCAP <-> [Sykp:BCAP]	kf_35*Sykp*BCAP - kb_36*[Sykp:BCAP]
36	[Sykp:BCAP] -> Sykp + BCAPp	kcat_36*[Sykp:BCAP]
37	BCAPp + p85PI3K <-> [BCAPp:p85PI3K]	kf_37*BCAPp*p85PI3K - kb_37*[BCAPp:p85PI3K]
38	[BCAPp:p85PI3K] + p110PI3K <-> [BCAPp:p85PI3K:p110PI3K]	kf_38*[BCAPp:p85PI3K]*p110PI3K - kb_38*[BCAPp:p85PI3K:p110PI3K]
39	[BCAPp:p85PI3K:p110PI3K] -> BCAPp + PI3K	kcat_39*[BCAPp:p85PI3K:p110PI3K]
40	BCAPp + Pase1 <-> [BCAPp:Pase1]	kf_40*BCAPp*Pase1 - kb_40*[BCAPp:Pase1]
41	[BCAPp:Pase1] -> BCAP + Pase1	kcat_41*[BCAPp:Pase1]
42	CD19p -> CD19	kf_42*CD19p
43	PI3K -> p85PI3K + p110PI3K	kf_43*PI3K
44	PIP2 + PI3K -> PIP3 + PI3K	vm_44 * PIP2 * PI3K/(km_44 + PIP2)
45	PIP3 -> PIP2	vm_45*PIP3/(km_45+PIP3)
46	PIP3 + Akte <-> [PIP3:Akte]	kf_46*PIP3*Akte - kb_46*[PIP3:Akte]
47	[PIP3:Akte] <-> Aktm	kf_47*[PIP3:Akte] - kb_47*Aktm
48	PIP3 + PDK <-> [PIP3:PDK]	kf_48*PIP3*PDK - kb_48*[PIP3:PDK]
49	[PIP3:PDK] -> PDKa	kf_49*[PIP3:PDK]
50	PDKa -> PDK + PIP3	kf_50*PDKa

51	PDKa + Aktm <-> [PDKa:Aktm]	kf_51*PDKa*Aktm - kb_51*[PDKa:Aktm]
52	[PDKa:Aktm] -> PDKa + Aktp	kcat_52*[PDKa:Aktm]
53	Aktp + PP2A <-> [Aktp:PP2A]	kf_53*Aktp*PP2A - kb_53*[Aktp:PP2A]
54	[Aktp:PP2A] -> Aktm + PP2A	kcat_54*[Aktp:PP2A]
55	Sykp + BLNK <-> [Sykp:BLNK]	kf_55*Sykp*BLNK - kb_55*[Sykp:BLNK]
56	[Sykp:BLNK] -> Sykp + BLNKp	kcat_56*[Sykp:BLNK]
57	BLNKp + Btkp <-> [BLNKp:Btkp]	kf_57*BLNKp*Btkp - kb_57*[BLNKp:Btkp]
58	BLNKp + Grb2 <-> [BLNKp:Grb2]	kf_58*BLNKp*Grb2 - kb_58*[BLNKp:Grb2]
59	BLNKp + Pase2 <-> [BLNKp:Pase2]	kf_59*BLNKp*Pase2 - kb_59*[BLNKp:Pase2]
60	[BLNKp:Pase2] -> BLNK + Pase2	kcat_60*[BLNKp:Pase2]
61	[BLNKp:Grb2] + SoS <-> [BLNKp:Grb2:SoS]	kf_61*[BLNKp:Grb2]*SoS - kb_61*[BLNKp:Grb2:SoS]
62	[BLNKp:Btkp] + PLCg <-> [BLNKp:Btkp:PLCg]	kf_62*[BLNKp:Btkp]*PLCg - kb_62*[BLNKp:Btkp:PLCg]
63	[BLNKp:Btkp:PLCg] -> [BLNKp:Btkp] + PLCgp	kcat_63*[BLNKp:Btkp:PLCg]
64	PLCgp + Pase3 <-> [PLCgp:Pase3]	kf_64*PLCgp*Pase3 - kb_64*[PLCgp:Pase3]
65	[PLCgp:Pase3] -> PLCg + Pase3	kcat_65*[PLCgp:Pase3]
66	IP3 -> ip3deg	kdeg_66*IP3
67	DAG -> dagdeg	kdeg_67*DAG
68	PLCgp + PIP2 -> PLCgp + IP3 + DAG	vm_68 * PIP2 * PLCgp/(km_68 +PIP2)
69	PKCcyt + DAG <-> [PKCcyt:DAG]	kf_69*PKCcyt*DAG - kb_69*[PKCcyt:DAG]
70	[PKCcyt:DAG] <-> PKCm	kf_70*[PKCcyt:DAG] - kb_70*PKCm
71	RasGTP -> RasGDP	kf_71*RasGTP
72	GEFp + RasGDP <-> [GEFp:RasGDP]	kf_72*GEFp*RasGDP - kb_72*[GEFp:RasGDP]
73	[GEFp:RasGDP] -> GEFp + RasGTP	kcat_73*[GEFp:RasGDP]
74	GEF + PKCm <-> [GEF:PKCm]	kf_74*GEF*PKCm - kb_74*[GEF:PKCm]
75	[GEF:PKCm] -> GEFp + PKCm	kcat_75*[GEF:PKCm]
76	PKCm + GAP <-> [PKCm:GAP]	kf_76*PKCm*GAP - kb_76*[PKCm:GAP]
77	[PKCm:GAP] -> PKCm + GAPp	kcat_77*[PKCm:GAP]
78	GEFp -> GEF	kf_78*GEFp
79	GAPp -> GAP	kf_79*GAPp
80	PKCm + Sykp <-> [PKCm:Sykp]	kf_80*PKCm*Sykp - kb_80*[PKCm:Sykp]
81	[PKCm:Sykp] -> PKCm + Sykpp	kcat_81*[PKCm:Sykp]
82	Sykpp -> Sykp	kf_82*Sykpp
83	GAP + RasGTP <-> [GAP:RasGTP]	kf_83*GAP*RasGTP - kb_83*[GAP:RasGTP]
84	[GAP:RasGTP] -> GAP + RasGDP	kcat_84*[GAP:RasGTP]
85	Raf + RasGTP <-> [Raf:RasGTP]	kf_85*Raf*RasGTP - kb_85*[Raf:RasGTP]
86	[Raf:RasGTP] + PKCm <-> [Raf:RasGTP:PKCm]	kf_86*[Raf:RasGTP]*PKCm - kb_86*[Raf:RasGTP:PKCm]
87	[Raf:RasGTP:PKCm] -> [Rafp:RasGTP] + PKCm	kcat_87*[Raf:RasGTP:PKCm]
88	Raf + Aktp <-> [Raf:Aktp]	kf_88*Raf*Aktp - kb_88*[Raf:Aktp]
89	[Raf:Aktp] -> Rafser259 + Aktp	kcat_89*[Raf:Aktp]
90	Rafser259 + PP1 <-> [Rafser259:PP1]	kf_90*Rafser259*PP1 - kb_90*[Rafser259:PP1]
91	[Rafser259:PP1] -> Raf + PP1	kcat_91*[Rafser259:PP1]
92	Rafp + Aktp <-> [Rafp:Aktp]	kf_92*Rafp*Aktp - kb_92*[Rafp:Aktp]
93	[Rafp:Aktp] -> Rafpp + Aktp	kcat_93*[Rafp:Aktp]
94	Rafpp + PP1 <-> [Rafpp:PP1]	kf_94*Rafpp*PP1 - kb_94*[Rafpp:PP1]
95	[Rafpp:PP1] -> Rafp + PP1	kcat_95*[Rafpp:PP1]
96	Rafp + PP2A <-> [Rafp:PP2A]	kf_96*Rafp*PP2A - kb_96*[Rafp:PP2A]
97	[Rafp:PP2A] -> Raf + PP2A	kcat_97*[Rafp:PP2A]
98	Btkcyt + PIP3 <-> Btk	kf_98*Btkcyt*PIP3 - kb_98*Btk
99	Sykp + PLCg <-> [Sykp:PLCg]	kf_99*Sykp*PLCg - kb_99*[Sykp:PLCg]
100	[Sykp:PLCg] -> Sykp + PLCgp	kcat_100*[Sykp:PLCg]
101	Rafp + PP1 <-> [Rafp:PP1]	kf_101*Rafp*PP1 - kb_101*[Rafp:PP1]
102	[Rafp:PP1] -> Raf + PP1	kcat_102*[Rafp:PP1]
103	Rafp + MEK <-> [Rafp:MEK]	kf_103*Rafp*MEK - kb_103*[Rafp:MEK]
104	[Rafp:MEK] -> Rafp + MEKp	kcat_104*[Rafp:MEK]

105	Rafp + MEKp <-> [Rafp:MEKp]	kf_105*Rafp*MEKp - kb_105*[Rafp:MEKp]
106	[Rafp:MEKp] -> Rafp + MEKpp	kcat_106*[Rafp:MEKp]
107	PKCm + CK2alpha <-> [PKCm:CK2alpha]	kf_107*PKCm*CK2alpha - kb_107*[PKCm:CK2alpha]
108	[PKCm:CK2alpha] -> PKCm + CK2alphap	kcat_108*[PKCm:CK2alpha]
109	CK2alphap -> CK2alpha	kf_109 * CK2alphap * PP2A/(0.05 + CK2alphap)
110	CK2alphap + MKP3 <-> [CK2alphap:MKP3]	kf_110*CK2alphap*MKP3 - kb_110*[CK2alphap:MKP3]
111	[CK2alphap:MKP3] -> CK2alphap + MKP3p	kcat_111*[CK2alphap:MKP3]
112	MKP3p + PP2A <-> [MKP3p:PP2A]	kf_112*MKP3p*PP2A - kb_112*[MKP3p:PP2A]
113	[MKP3p:PP2A] -> MKP3 + PP2A	kcat_113*[MKP3p:PP2A]
114	MEKpp + PP2A <-> [MEKpp:PP2A]	kf_114*MEKpp*PP2A - kb_114*[MEKpp:PP2A]
115	[MEKpp:PP2A] -> MEKp + PP2A	kcat_115*[MEKpp:PP2A]
116	MEKp + PP2A <-> [MEKp:PP2A]	kf_116*MEKp*PP2A - kb_116*[MEKp:PP2A]
117	[MEKp:PP2A] -> MEK + PP2A	kcat_117*[MEKp:PP2A]
118	MEKpp + MKP3p <-> [MEKpp:MKP3p]	kf_118*MEKpp*MKP3p - kb_118*[MEKpp:MKP3p]
119	[MEKpp:MKP3p] -> MEKp + MKP3p	kcat_119*[MEKpp:MKP3p]
120	MEKp + MKP3p <-> [MEKp:MKP3p]	kf_120*MEKp*MKP3p - kb_120*[MEKp:MKP3p]
121	[MEKp:MKP3p] -> MEK + MKP3p	kcat_21*[MEKp:MKP3p]
122	ERK + MEKpp <-> [ERK:MEKpp]	kf_122*ERK*MEKpp - kb_122*[ERK:MEKpp]
123	[ERK:MEKpp] -> ERKp + MEKpp	kcat_123*[ERK:MEKpp]
124	ERKp + MEKpp <-> [ERKp:MEKpp]	kf_124*ERKp*MEKpp - kb_124*[ERKp:MEKpp]
125	[ERKp:MEKpp] -> ERKpp + MEKpp	kcat_125*[ERKp:MEKpp]
126	mkp1 <-> MKP1	kf_126*mkp1 - kb_126*MKP1
127	mkp3 <-> MKP3	kf_127*mkp3 - kb_127*MKP3
128	MKP1 -> mkp1ubi	kf_128*MKP1
129	MKP3 -> mkp3ubi	kf_129*MKP3
130	ERKpp + MKP1 <-> [ERKpp:MKP1]	kf_130*ERKpp*MKP1 - kb_130*[ERKpp:MKP1]
131	[ERKpp:MKP1] -> ERKpp + MKP1p	kcat_131*[ERKpp:MKP1]
132	MKP1p + MKP3p <-> [MKP1p:MKP3p]	kf_132*MKP1p*MKP3p - kb_132*[MKP1p:MKP3p]
133	[MKP1p:MKP3p] -> MKP1 + MKP3p	kcat_133*[MKP1p:MKP3p]
134	ERKpp + MKP2 <-> [ERKpp:MKP2]	kf_134*ERKpp*MKP2 - kb_134*[ERKpp:MKP2]
135	[ERKpp:MKP2] -> ERKp + MKP2	kcat_135*[ERKpp:MKP2]
136	ERKp + MKP2 <-> [ERKp:MKP2]	kf_136*ERKp*MKP2 - kb_136*[ERKp:MKP2]
137	[ERKp:MKP2] -> ERK + MKP2	kcat_137*[ERKp:MKP2]
138	ERKpp + MKP3 <-> [ERKpp:MKP3p]	kf_138*ERKpp*MKP3 - kb_138*[ERKpp:MKP3p]
139	[ERKpp:MKP3p] -> ERKp + MKP3	kcat_139*[ERKpp:MKP3p]
140	ERKp + MKP3 <-> [ERKp:MKP3p]	kf_140*ERKp*MKP3 - kb_140*[ERKp:MKP3p]
141	[ERKp:MKP3p] -> ERK + MKP3	kcat_141*[ERKp:MKP3p]
142	TrCmplx -> mkp1	kf_142*TrCmplx
143	TrCmplx -> mkp3	kf_143*TrCmplx
144	Rafp + ERKpp <-> [Rafp:ERKpp]	kf_144*Rafp*ERKpp - kb_144*[Rafp:ERKpp]
145	[Rafp:ERKpp] -> Rafpp + ERKpp	kcat_145*[Rafp:ERKpp]
146	Rafser259 + PP2A <-> [Rafser259:PP2A]	kf_146*Rafser259*PP2A - kb_147*[Rafser259:PP2A]
147	[Rafser259:PP2A] -> Raf + PP2A	kcat_147*[Rafser259:PP2A]
148	[Rafp:RasGTP] -> Rafp + RasGTP	kf_148*[Rafp:RasGTP]
149	[L:BCR1] + BCR <-> [L:BCR]	kf_149*[L:BCR1]*BCR - kb_149*[L:BCR]
150	[L:BCRp] + SHP1 <-> [L:BCRp:SHP1]	kf_150*[L:BCRp]*SHP1 - kb_150*[L:BCRp:SHP1]
151	[L:BCRp:SHP1] -> [L:BCR] + SHP1	kcat_151*[L:BCRp:SHP1]
152	[L:BCRpp] + SHP1 <-> [L:BCRpp:SHP1]	kf_152*[L:BCRpp]*SHP1 - kb_152*[L:BCRpp:SHP1]
153	[L:BCRpp:SHP1] -> [L:BCRp] + SHP1	kcat_153*[L:BCRpp:SHP1]
154	[BLNKp:Grb2:SoS] + RasGDP -> [BLNKp:Grb2:SoS] + RasGTP	vm_154*RasGDP*[BLNKp:Grb2:SoS]/(km_154+RasGDP)
155	ERKpp + MKP1p <-> [ERKpp:MKP1p]	kf_155*ERKpp*MKP1p - kb_155*[ERKpp:MKP1p]
156	[ERKpp:MKP1p] -> ERKp + MKP1p	kcat_156*[ERKpp:MKP1p]
157	ERKp + MKP1p <-> [ERKp:MKP1p]	kf_157*ERKp*MKP1p - kb_157*[ERKp:MKP1p]
158	[ERKp:MKP1p] -> ERK + MKP1p	kcat_158*[ERKp:MKP1p]

159	ERKpp + MKP1 <-> [MKP1:ERKpp]	kf_159*ERKpp*MKP1 - kb_159*[MKP1:ERKpp]
160	[MKP1:ERKpp] -> MKP1 + ERKp	kcat_160*[MKP1:ERKpp]
161	ERKp + MKP1 <-> [MKP1:ERKp]	kf_161*ERKp*MKP1 - kb_161*[MKP1:ERKp]
162	[MKP1:ERKp] -> MKP1 + ERK	kcat_162*[MKP1:ERKp]
163	ERKpp + TF <-> [ERKpp:TF]	kf_163*ERKpp*TF - kb_163*[ERKpp:TF]
164	[ERKpp:TF] -> ERKpp + TFa	kcat_164*[ERKpp:TF]
165	TFa + NT <-> [TFa:NT]	kf_165*TFa*NT - kb_165*[TFa:NT]
166	TFa -> TF	kf_166*TFa
167	NT -> mkp1	trnsc_167*NT* [TFa:NT]
168	NT -> mkp3	trnsc_168* NT * [TFa:NT]
169	PKCm -> PKCcyt	kf_169*PKCm
170	MKP3 + ERKpp <-> [MKP3:ERKpp]	kf_170*MKP3*ERKpp - kb_170*[MKP3:ERKpp]
171	[MKP3:ERKpp] -> MKP3x + ERKpp	kcat_171*[MKP3:ERKpp]
172	MKP3x -> mkp3xubi	kf_172*MKP3x

3. Parameter Details:

Sr. No.	Parameter	Scope (Reaction)	Value
1	kon_1	L + BCR <-> [L:BCR1]	50
2	koff_1	L + BCR <-> [L:BCR1]	10
3	kf_2	[L:BCR] -> [L:BCRp]	0.99
4	kon_3	[L:BCRp] + Lyn <-> [L:BCRp:Lyn]	0.8857
5	koff_3	[L:BCRp] + Lyn <-> [L:BCRp:Lyn]	0.8766
6	kcat_4	[L:BCRp:Lyn] -> [L:BCRp] + Lynp	0.515
7	kon_5	Lynp + SHP1 <-> [Lynp:SHP1]	7
8	koff_5	Lynp + SHP1 <-> [Lynp:SHP1]	7.9716
9	kcat_6	[Lynp:SHP1] -> Lyn + SHP1	2
10	km_7	Lynp + CD22 -> Lynp + CD22p	1.933
11	vm_7	Lynp + CD22 -> Lynp + CD22p	5.4291
12	kf_8	CD22p + SHP1c <-> [CD22p:SHP1c]	0.7532
13	kb_8	CD22p + SHP1c <-> [CD22p:SHP1c]	1.201
14	kcat_9	[CD22p:SHP1c] -> CD22p + SHP1	0.9426
15	kf_10	SHP1 -> SHP1c	0.01
16	kf_11	CD22p -> CD22	0.0943
17	kb_12	Lynp + Syk <-> [Lynp:Syk]	8.7948
18	kf_12	Lynp + Syk <-> [Lynp:Syk]	0.448
19	kcat_13	[Lynp:Syk] -> Lynp + Sykp	21.56515
20	kf_14	Sykp + SHP1 <-> [Sykp:SHP1]	20
21	kb_14	Sykp + SHP1 <-> [Sykp:SHP1]	3.6
22	kcat_15	[Sykp:SHP1] -> Syk + SHP1	0.9
23	kf_16	[L:BCRp] + Sykp <-> [L:BCRp:Sykp]	0.3143
24	kb_16	[L:BCRp] + Sykp <-> [L:BCRp:Sykp]	1.2092
25	kcat_17	[L:BCRp:Sykp] -> [L:BCRpp] + Sykp	0.3023
26	kf_18	[L:BCRpp] + Lyn <-> [L:BCRpp:Lyn]	0.899
27	kb_18	[L:BCRpp] + Lyn <-> [L:BCRpp:Lyn]	0.8766
28	kcat_19	[L:BCRpp:Lyn] -> [L:BCRpp] + Lynp	0.6915
29	kf_20	BCRpro -> BCR	1.5E-06
30	kf_21	BCR -> BCRi	1.5E-06
31	kon_22	2 [L:BCR1] <-> [L:BCR]	10
32	koff_22	2 [L:BCR1] <-> [L:BCR]	5
33	kf_23	[L:BCR] -> BCRi + Li	0.0067
34	kf_24	Btk + Lynp <-> [Btk:Lynp]	0.645
35	kb_24	Btk + Lynp <-> [Btk:Lynp]	4
36	kcat_25	[Btk:Lynp] -> Btkp + Lynp	1
37	kf_26	Btk + Sykp <-> [Btk:Sykp]	2.4
38	kb_26	Btk + Sykp <-> [Btk:Sykp]	4
39	kcat_27	[Btk:Sykp] -> Btkp + Sykp	4
40	kf_28	Btkp + BtkPase <-> [Btkp:BtkPase]	12
41	kb_28	Btkp + BtkPase <-> [Btkp:BtkPase]	16
42	kcat_29	[Btkp:BtkPase] -> Btk + BtkPase	4
43	kf_30	Lynp + CD19 <-> [Lynp:CD19]	1.2245
44	kb_30	Lynp + CD19 <-> [Lynp:CD19]	12
45	kcat_31	[Lynp:CD19] -> Lynp + CD19p	3
46	kf_32	CD19p + p85PI3K <-> [CD19p:p85PI3K]	0.00345
47	kb_32	CD19p + p85PI3K <-> [CD19p:p85PI3K]	1.064
48	kf_33	[CD19p:p85PI3K] + p110PI3K <-> [CD19p:p85PI3K:p110PI3K]	0.2
49	kb_33	[CD19p:p85PI3K] + p110PI3K <-> [CD19p:p85PI3K:p110PI3K]	4
50	kcat_34	[CD19p:p85PI3K:p110PI3K] -> CD19p + PI3K	1
51	kf_35	Sykp + BCAP <-> [Sykp:BCAP]	4.8699

52	kb_36	Sykp + BCAP <-> [Sykp:BCAP]	14
53	kcat_36	[Sykp:BCAP] -> Sykp + BCAPp	3.5
54	kf_37	BCAPp + p85PI3K <-> [BCAPp:p85PI3K]	0.5
55	kb_37	BCAPp + p85PI3K <-> [BCAPp:p85PI3K]	3
56	kf_38	[BCAPp:p85PI3K] + p110PI3K <-> [BCAPp:p85PI3K:p110PI3K]	22
57	kb_38	[BCAPp:p85PI3K] + p110PI3K <-> [BCAPp:p85PI3K:p110PI3K]	24
58	kcat_39	[BCAPp:p85PI3K:p110PI3K] -> BCAPp + PI3K	6
59	kf_40	BCAPp + Pase1 <-> [BCAPp:Pase1]	22
60	kb_40	BCAPp + Pase1 <-> [BCAPp:Pase1]	8
61	kcat_41	[BCAPp:Pase1] -> BCAP + Pase1	2
62	kf_42	CD19p -> CD19	0.1
63	kf_43	PI3K -> p85PI3K + p110PI3K	0.251829
64	km_44	PIP2 + PI3K -> PIP3 + PI3K	0.00391
65	vm_44	PIP2 + PI3K -> PIP3 + PI3K	1.69
66	km_45	PIP3 -> PIP2	0.092
67	vm_45	PIP3 -> PIP2	1.7
68	kf_46	PIP3 + Aktc <-> [PIP3:Aktc]	6
69	kb_46	PIP3 + Aktc <-> [PIP3:Aktc]	12
70	kf_47	[PIP3:Aktc] <-> Aktm	3
71	kb_47	[PIP3:Aktc] <-> Aktm	0.3
72	kf_48	PIP3 + PDK <-> [PIP3:PDK]	2.0408
73	kb_48	PIP3 + PDK <-> [PIP3:PDK]	4.2
74	kf_49	[PIP3:PDK] -> PDKa	3.5261
75	kf_50	PDKa -> PDK + PIP3	0.9597
76	kf_51	PDKa + Aktm <-> [PDKa:Aktm]	1200
77	kb_51	PDKa + Aktm <-> [PDKa:Aktm]	4
78	kcat_52	[PDKa:Aktm] -> PDKa + Aktp	1
79	kf_53	Aktp + PP2A <-> [Aktp:PP2A]	12
80	kb_53	Aktp + PP2A <-> [Aktp:PP2A]	0.65
81	kcat_54	[Aktp:PP2A] -> Aktm + PP2A	2
82	kf_55	Sykp + BLNK <-> [Sykp:BLNK]	2.4
83	kb_55	Sykp + BLNK <-> [Sykp:BLNK]	4
84	kcat_56	[Sykp:BLNK] -> Sykp + BLNKp	1
85	kf_57	BLNKp + Btkp <-> [BLNKp:Btkp]	2.723833
86	kb_57	BLNKp + Btkp <-> [BLNKp:Btkp]	1.8372
87	kf_58	BLNKp + Grb2 <-> [BLNKp:Grb2]	1
88	kb_58	BLNKp + Grb2 <-> [BLNKp:Grb2]	0.05
89	kf_59	BLNKp + Pase2 <-> [BLNKp:Pase2]	222
90	kb_59	BLNKp + Pase2 <-> [BLNKp:Pase2]	3.68
91	kcat_60	[BLNKp:Pase2] -> BLNK + Pase2	0.926
92	kf_61	[BLNKp:Grb2] + SoS <-> [BLNKp:Grb2:SoS]	0.05
93	kb_61	[BLNKp:Grb2] + SoS <-> [BLNKp:Grb2:SoS]	1
94	kf_62	[BLNKp:Btkp] + PLCg <-> [BLNKp:Btkp:PLCg]	200
95	kb_62	[BLNKp:Btkp] + PLCg <-> [BLNKp:Btkp:PLCg]	0.6333
96	kcat_63	[BLNKp:Btkp:PLCg] -> [BLNKp:Btkp] + PLCgp	4
97	kf_64	PLCgp + Pase3 <-> [PLCgp:Pase3]	52
98	kb_64	PLCgp + Pase3 <-> [PLCgp:Pase3]	0.54
99	kcat_65	[PLCgp:Pase3] -> PLCg + Pase3	4
100	kdeg_66	IP3 -> ip3deg	0.021
101	kdeg_67	DAG -> dagdeg	0.0225
102	km_68	PLCgp + PIP2 -> PLCgp + IP3 + DAG	0.05
103	vm_68	PLCgp + PIP2 -> PLCgp + IP3 + DAG	0.48
104	kf_69	PKCcyt + DAG <-> [PKCcyt:DAG]	0.45
105	kb_69	PKCcyt + DAG <-> [PKCcyt:DAG]	0.226

106	kf_70	[PKCcyt:DAG] <-> PKCm	9.9
107	kb_70	[PKCcyt:DAG] <-> PKCm	0.005
108	kf_71	RasGTP -> RasGDP	0.25
109	kf_72	GEFp + RasGDP <-> [GEFp:RasGDP]	0.08
110	kb_72	GEFp + RasGDP <-> [GEFp:RasGDP]	0.033
111	kcat_73	[GEFp:RasGDP] -> GEFp + RasGTP	0.2
112	kf_74	GEF + PKCm <-> [GEF:PKCm]	1.5
113	kb_74	GEF + PKCm <-> [GEF:PKCm]	16
114	kcat_75	[GEF:PKCm] -> GEFp + PKCm	4
115	kf_76	PKCm + GAP <-> [PKCm:GAP]	1.3125
116	kb_76	PKCm + GAP <-> [PKCm:GAP]	100
117	kcat_77	[PKCm:GAP] -> PKCm + GAPp	25
118	kf_78	GEFp -> GEF	0.1
119	kf_79	GAPp -> GAP	0.1
120	kf_80	PKCm + Sykp <-> [PKCm:Sykp]	0.25
121	kb_80	PKCm + Sykp <-> [PKCm:Sykp]	3.92
122	kcat_81	[PKCm:Sykp] -> PKCm + Sykpp	0.98
123	kf_82	Sykpp -> Sykp	0.041
124	kf_83	GAP + RasGTP <-> [GAP:RasGTP]	2.1666
125	kb_83	GAP + RasGTP <-> [GAP:RasGTP]	1
126	kcat_84	[GAP:RasGTP] -> GAP + RasGDP	10
127	kf_85	Raf + RasGTP <-> [Raf:RasGTP]	100
128	kb_85	Raf + RasGTP <-> [Raf:RasGTP]	2
129	kf_86	[Raf:RasGTP] + PKCm <-> [Raf:RasGTP:PKCm]	8
130	kb_86	[Raf:RasGTP] + PKCm <-> [Raf:RasGTP:PKCm]	0.0444
131	kcat_87	[Raf:RasGTP:PKCm] -> [Rafp:RasGTP] + PKCm	4
132	kf_88	Raf + Aktp <-> [Raf:Aktp]	2.5
133	kb_88	Raf + Aktp <-> [Raf:Aktp]	4
134	kcat_89	[Raf:Aktp] -> Rafser259 + Aktp	1
135	kf_90	Rafser259 + PP1 <-> [Rafser259:PP1]	12.85
136	kb_90	Rafser259 + PP1 <-> [Rafser259:PP1]	9
137	kcat_91	[Rafser259:PP1] -> Raf + PP1	3
138	kf_92	Rafp + Aktp <-> [Rafp:Aktp]	0.89
139	kb_92	Rafp + Aktp <-> [Rafp:Aktp]	2
140	kcat_93	[Rafp:Aktp] -> Rafpp + Aktp	0.5
141	kf_94	Rafpp + PP1 <-> [Rafpp:PP1]	9.88
142	kb_94	Rafpp + PP1 <-> [Rafpp:PP1]	13.6
143	kcat_95	[Rafpp:PP1] -> Rafp + PP1	3.4
144	kf_96	Rafp + PP2A <-> [Rafp:PP2A]	2.2
145	kb_96	Rafp + PP2A <-> [Rafp:PP2A]	16
146	kcat_97	[Rafp:PP2A] -> Raf + PP2A	4
147	kf_98	Btkcyt + PIP3 <-> Btk	90
148	kb_98	Btkcyt + PIP3 <-> Btk	0.00034
149	kf_99	Sykp + PLCg <-> [Sykp:PLCg]	10
150	kb_99	Sykp + PLCg <-> [Sykp:PLCg]	16
151	kcat_100	[Sykp:PLCg] -> Sykp + PLCgp	4
152	kf_101	Rafp + PP1 <-> [Rafp:PP1]	3
153	kb_101	Rafp + PP1 <-> [Rafp:PP1]	4
154	kcat_102	[Rafp:PP1] -> Raf + PP1	4
155	kf_103	Rafp + MEK <-> [Rafp:MEK]	6.8
156	kb_103	Rafp + MEK <-> [Rafp:MEK]	9.62
157	kcat_104	[Rafp:MEK] -> Rafp + MEKp	2.405
158	kf_105	Rafp + MEKp <-> [Rafp:MEKp]	6.8
159	kb_105	Rafp + MEKp <-> [Rafp:MEKp]	9.62

160	kcat_106	[Rafp:MEKp] -> Rafp + MEKpp	2.405
161	kf_107	PKCm + CK2alpha <-> [PKCm:CK2alpha]	2
162	kb_107	PKCm + CK2alpha <-> [PKCm:CK2alpha]	8
163	kcat_108	[PKCm:CK2alpha] -> PKCm + CK2alphap	2.667
164	kf_109	CK2alphap -> CK2alpha	0.333
165	kf_110	CK2alphap + MKP3 <-> [CK2alphap:MKP3]	1
166	kb_110	CK2alphap + MKP3 <-> [CK2alphap:MKP3]	4.64
167	kcat_111	[CK2alphap:MKP3] -> CK2alphap + MKP3p	1.16
168	kf_112	MKP3p + PP2A <-> [MKP3p:PP2A]	15
169	kb_112	MKP3p + PP2A <-> [MKP3p:PP2A]	16
170	kcat_113	[MKP3p:PP2A] -> MKP3 + PP2A	4
171	kf_114	MEKpp + PP2A <-> [MEKpp:PP2A]	1.31
172	kb_114	MEKpp + PP2A <-> [MEKpp:PP2A]	4
173	kcat_115	[MEKpp:PP2A] -> MEKp + PP2A	1
174	kf_116	MEKp + PP2A <-> [MEKp:PP2A]	1.31
175	kb_116	MEKp + PP2A <-> [MEKp:PP2A]	4
176	kcat_117	[MEKp:PP2A] -> MEK + PP2A	1
177	kf_118	MEKpp + MKP3p <-> [MEKpp:MKP3p]	26
178	kb_118	MEKpp + MKP3p <-> [MEKpp:MKP3p]	64
179	kcat_119	[MEKpp:MKP3p] -> MEKp + MKP3p	16
180	kf_120	MEKp + MKP3p <-> [MEKp:MKP3p]	26
181	kb_120	MEKp + MKP3p <-> [MEKp:MKP3p]	64
182	kcat_21	[MEKp:MKP3p] -> MEK + MKP3p	16
183	kf_122	ERK + MEKpp <-> [ERK:MEKpp]	1.6
184	kb_122	ERK + MEKpp <-> [ERK:MEKpp]	1
185	kcat_123	[ERK:MEKpp] -> ERKp + MEKpp	0.25
186	kf_124	ERKp + MEKpp <-> [ERKp:MEKpp]	1.6
187	kb_124	ERKp + MEKpp <-> [ERKp:MEKpp]	1
188	kcat_125	[ERKp:MEKpp] -> ERKpp + MEKpp	0.25
189	kf_126	mkp1 <-> MKP1	0.0004
190	kb_126	mkp1 <-> MKP1	0.0001
191	kf_127	mkp3 <-> MKP3	0.0004
192	kb_127	mkp3 <-> MKP3	0.0001
193	kf_128	MKP1 -> mkp1ubi	3.7E-16
194	kf_129	MKP3 -> mkp3ubi	3.7E-16
195	kf_130	ERKpp + MKP1 <-> [ERKpp:MKP1]	0.30101
196	kb_130	ERKpp + MKP1 <-> [ERKpp:MKP1]	4.44
197	kcat_131	[ERKpp:MKP1] -> ERKpp + MKP1p	2.2
198	kb_132	MKP1p + MKP3p <-> [MKP1p:MKP3p]	108
199	kf_132	MKP1p + MKP3p <-> [MKP1p:MKP3p]	141
200	kcat_133	[MKP1p:MKP3p] -> MKP1 + MKP3p	27
201	kf_134	ERKpp + MKP2 <-> [ERKpp:MKP2]	76
202	kb_134	ERKpp + MKP2 <-> [ERKpp:MKP2]	4
203	kcat_135	[ERKpp:MKP2] -> ERKp + MKP2	1
204	kf_136	ERKp + MKP2 <-> [ERKp:MKP2]	76
205	kb_136	ERKp + MKP2 <-> [ERKp:MKP2]	4
206	kcat_137	[ERKp:MKP2] -> ERK + MKP2	1
207	kf_138	ERKpp + MKP3 <-> [ERKpp:MKP3p]	1
208	kb_138	ERKpp + MKP3 <-> [ERKpp:MKP3p]	0.25
209	kcat_139	[ERKpp:MKP3p] -> ERKp + MKP3	9
210	kf_140	ERKp + MKP3 <-> [ERKp:MKP3p]	1
211	kb_140	ERKp + MKP3 <-> [ERKp:MKP3p]	0.25
212	kcat_141	[ERKp:MKP3p] -> ERK + MKP3	9
213	kf_142	TrCmplx -> mkp1	1E-18

214	kf_143	TrCmplx -> mkp3	1E-18
215	kf_144	Rafp + ERKpp <-> [Rafp:ERKpp]	0.05
216	kb_144	Rafp + ERKpp <-> [Rafp:ERKpp]	2
217	kcat_145	[Rafp:ERKpp] -> Rafpp + ERKpp	0.5
218	kf_146	Rafser259 + PP2A <-> [Rafser259:PP2A]	2.25
219	kb_147	Rafser259 + PP2A <-> [Rafser259:PP2A]	8
220	kcat_147	[Rafser259:PP2A] -> Raf + PP2A	4
221	kf_148	[Rafp:RasGTP] -> Rafp + RasGTP	1
222	kf_149	[L:BCR1] + BCR <-> [L:BCR]	10
223	kb_149	[L:BCR1] + BCR <-> [L:BCR]	2
224	kf_150	[L:BCRp] + SHP1 <-> [L:BCRp:SHP1]	83
225	kb_150	[L:BCRp] + SHP1 <-> [L:BCRp:SHP1]	2.77
226	kcat_151	[L:BCRp:SHP1] -> [L:BCR] + SHP1	1
227	kf_152	[L:BCRpp] + SHP1 <-> [L:BCRpp:SHP1]	240
228	kb_152	[L:BCRpp] + SHP1 <-> [L:BCRpp:SHP1]	2
229	kcat_153	[L:BCRpp:SHP1] -> [L:BCRp] + SHP1	1
230	km_154	[BLNKp:Grb2:SoS] + RasGDP -> [BLNKp:Grb2:SoS] + RasGTP	0.050505
231	vm_154	[BLNKp:Grb2:SoS] + RasGDP -> [BLNKp:Grb2:SoS] + RasGTP	22
232	kf_155	ERKpp + MKP1p <-> [ERKpp:MKP1p]	450
233	kb_155	ERKpp + MKP1p <-> [ERKpp:MKP1p]	600
234	kcat_156	[ERKpp:MKP1p] -> ERKp + MKP1p	150
235	kf_157	ERKp + MKP1p <-> [ERKp:MKP1p]	450
236	kb_157	ERKp + MKP1p <-> [ERKp:MKP1p]	600
237	kcat_158	[ERKp:MKP1p] -> ERK + MKP1p	150
238	kf_159	ERKpp + MKP1 <-> [MKP1:ERKpp]	30
239	kb_159	ERKpp + MKP1 <-> [MKP1:ERKpp]	600
240	kcat_160	[MKP1:ERKpp] -> MKP1 + ERKp	150
241	kf_161	ERKp + MKP1 <-> [MKP1:ERKp]	30
242	kb_161	ERKp + MKP1 <-> [MKP1:ERKp]	600
243	kcat_162	[MKP1:ERKp] -> MKP1 + ERK	150
244	kf_163	ERKpp + TF <-> [ERKpp:TF]	4
245	kb_163	ERKpp + TF <-> [ERKpp:TF]	0.000335
246	kcat_164	[ERKpp:TF] -> ERKpp + TFa	1
247	kf_165	TFa + NT <-> [TFa:NT]	0.0001
248	kb_165	TFa + NT <-> [TFa:NT]	0.0002
249	kf_166	TFa -> TF	1E-25
250	trnsc_167	NT -> mkp1	2E-07
251	trnsc_168	NT -> mkp3	0.000002
252	kf_169	PKCm -> PKCcyt	0.1
253	kf_170	MKP3 + ERKpp <-> [MKP3:ERKpp]	0.0034
254	kb_170	MKP3 + ERKpp <-> [MKP3:ERKpp]	1
255	kcat_171	[MKP3:ERKpp] -> MKP3x + ERKpp	0.25
256	kf_172	MKP3x -> mkp3xubi	1.5E-15

Units of
rate
Constants   kf * => micromoles sec^-1(for second order reactions), minromoles^-1sec^-1(for first order reactions)

kb* => sec^{-1}

kcat* => sec^{-1}

km* => micromoles

vm* => sec^{-1}

Model building and numerical simulations:

A complete description of model building and details of the reaction scheme and parameters including rate equations for each of the reactions is provided in the Supplementary data S1A (Description of model) and S1B (Model content, parameters, reaction and their rates, initial conditions). All reactions were converted into molecule-molecule interactions defining either binding interactions, or catalytic reactions. We have used Simbiology2.2 (Mathworks) on MATLAB7.5 as a platform for implementing the model and for carrying out numerical simulations. All calculations except for that of restimulation experiments were done using ode15s, which is a solver for stiff differential equations and DAE. It uses the variable order method based on numerical differentiation formula for stiff differential equations. Restimulation experiments were done using Sundials solver CVODE provided with Simbiology. Parameters were either taken from literature, scaled up if required or estimated. Estimation of unknown parameters was done either by iteratively fitting to the experimental constraints, or by using local optimization with *lsqnonlin*, *lsqcurvefit* (wherever experimental data was available for immediate readout). Sensitivity analysis of the complete model was done by using SBML_SAT (Zi et al., 2008)., a freely available SBML-based MATLAB toolbox available at (http://sysbio.molgen.mpg.de/SBML-SAT/).Complete model building was carried out with Simbiology2.2 with MATLAB7.5 on hpxw4400 workstation (Intel core 2 duo 2.13GHz) running Red Hat Enterprise Linux WS-4.

Stimulation of cells and detection of phosphoproteins

A20 cells (1×10^7/ml) were stimulated with the $F(ab)_2$ fragment of goat anti-mouse IgG at a final concentration of 25 µg/ml in RPMI for a period of up to 30 min (Singh et al., 2005). At appropriate times, aliquots of cells were collected, centrifuged, and the cell pellets stored in liquid nitrogen. When required, cells were lysed, the detergent-soluble proteins resolved by SDS–PAGE, and specific proteins and phosphoproteins detected (and quantified) by Western blot using the procedure and antibodies as previously described (Kumar et al., 2007).

Co-Immunoprecipitation:

Lysates were prepared from 2×10^7 cells/group/time point in a buffer containing a cocktail of protease and phosphatase inhibitors as previously described (Singh et al., 2005). Lysates were pre-cleared with protein A-agarose and then incubated with appropriate antibody (0.6 – 1 mg, at 4°C for 2h), after which the immune-complexes were precipitated with protein A-sepharose. The immunoprecipitates were identified by immunoblotting with specific antibodies (Santa Cruz Biotech).

Over-expression of MKP3 in A20 cells.

MKP3 was over-expressed as a Strep-tag II fusion protein in A20 cells (Schmidt and Skerra, 2007). For this the cDNA was cloned into the pEXPR-IBA103 vector and then transfected into cells by electroporation. Subsequent selection for neomycin resistance over a 4-week period yielded stably-transfected cells. A Western blot analysis revealed that these cells expressed about 2-fold higher levels of MKP3 when compared to un-transfected A20 cells.

1. **Virendra K. Chaudhri**, Dhiraj Kumar, Manjari Misra and Kanury V.S. Rao[*] . Integration of a phosphatase cascade with the MAPKinase pathway provides for a novel signal processing function *(Communicated)*